Chapter 1

General Introduction

In this chapter the metabolite alpha-ketoglutarate is first presented in the context of the metabolic cycle in which it is involved. Its effect, after oral administration, on bone mineralization and amino acids synthesis is then reported as well as its role in collagen synthesis. Collagen is a major component of the skin and this tissue will be briefly characterized in higher vertebrates and teleosts. In addition, collagen is extremely important in mineralization of hard tissue such as bone and also scales in teleosts. The regulation of mineralization by hyper- and hypocalcaemic factors in higher vertebrates and teleosts are described and the potential of teleost scales as a biological model is highlighted.

1.1 Alpha-ketoglutarate

Alpha-ketoglutarate (AKG) is an intermediate metabolite in the tricarboxylic acid cycle (TCA, Krebs` cycle or citric acid cycle) (figure 1.1). It is part of the aerobic processing of glucose, which is the source of most of the ATP generated in the cell. The TCA cycle is the final common pathway for the oxidation of fuel molecules, like carbohydrates and fatty acids and also amino acids when necessary.

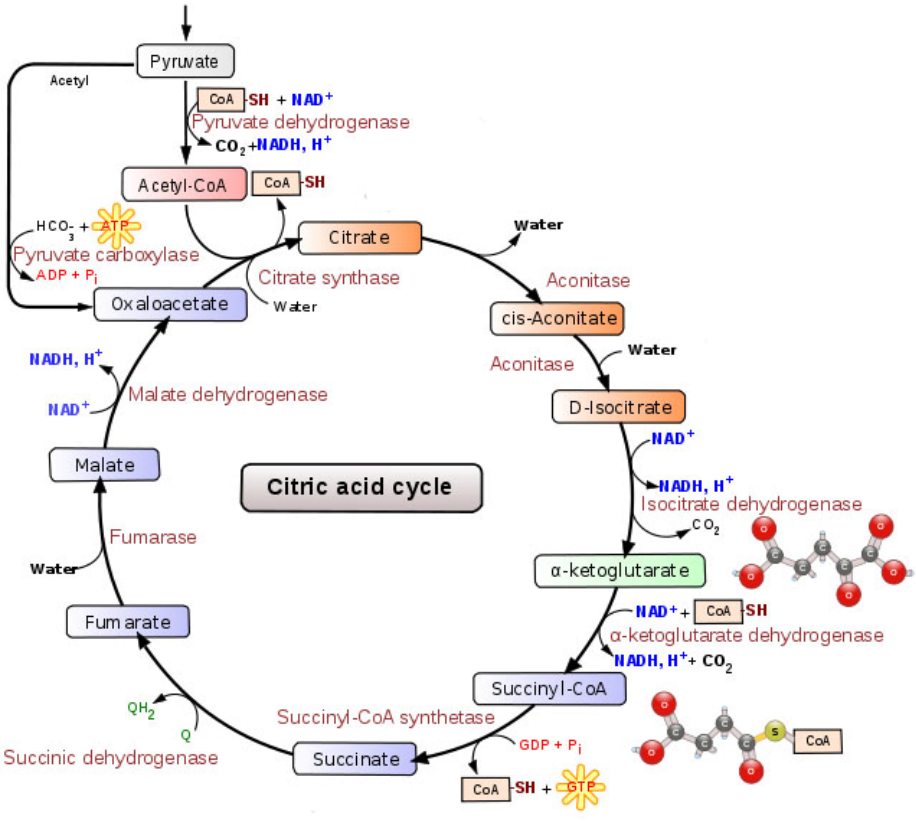

Figure 1. 1 – Diagram representing the tricarboxylic acid cycle. The citric acid cycle oxidizes two carbon units, producing two molecules of CO_2, one molecule of GTP and high-energy electrons in the form of NADH e $FADH_2$ (Berg *et al.* 2002). Alpha-ketoglutarate is in green. Words in brown correspond to enzymes in the cycle. Taken from: http//z.about.com /d/chemistry/1/0/F/m/citricacidcycle.jpg.

Most of these molecules enter the cycle as acetyl coenzyme A and, through a sequential series of oxidations and reductions are utilised and converted into one molecule of GTP (guanosine 5-triphosphate) and two molecules of NADH (reduced nicotinamide adenine dinucleotide) and $FADH_2$ (reduced flavin adenine dinucleotide) that are high electron donors for the subsequent electron-transport chain. The TCA cycle, in conjunction with oxidative phosphorylation, provides most of the energy used by aerobic cells. It is highly efficient because a limited number of molecules can generate large amounts of NADH and $FADH_2$ (Berg *et al.* 2002). The rate of the TCA cycle is tightly adjusted to meet the cell's need for ATP (adenosine triphosphate). Levels of alpha-ketoglutarate are tightly controlled by the enzymes isocitrate dehydrogenase and alpha-ketoglutarate dehydrogenase. Alpha-ketoglutarate is continuously recycled (Berg *et al.* 2002) and determines the final rate of the citric acid cycle (Son *et al.* 2007).

1.2 Alpha-ketoglutarate supplementation

In addition to its role in the TCA cycle, AKG is also involved in the synthesis of amino acids. Its derivatives glutamine and glutamate are immediately converted to carbon dioxide during their passage across the gut epithelium. In order to stimulate the synthesis of amino acids AKG has to be administrated as a pure dietary supplement (Harrison & Pierzynowski 2008). Several studies have addressed the role of alpha-ketoglutarate in the metabolism of higher vertebrates such as rats (Bienko *et al.* 2002), turkeys (Tatara *et al.* 2005; Tatara *et al.* 2004), piglets (Kowalik *et al.* 2005) and lambs (Harrison *et al.* 2004). The positive influence of AKG supplementation in humans has also been demonstrated. Relatively few studies have been directed at understanding AKG metabolism in fish and in a single study on Atlantic salmon AKG reduced urea emission after 17β-oestradiol induced vitellogenin synthesis (Olin *et al.* 1992). During glutamate oxidation, the first step is the transamination by several enzymes or deamination by glutamate dehydrogenase (GDH), all of which are expressed in the gastrointestinal tract. During transamination by branched-chain amino acid transferase (BCAT) glutamate donates an amino moiety to a branched-chain alpha-keto acid, forming alpha-ketoglutarate. For this reason, AKG could serve as a metabolic fuel for the cell, sparing glutamate and glutamine carbon (Lambert *et al.* 2006). It was demonstrated in a pig model that AKG, when given orally, was only partly converted to CO_2 as compared to glutamine/glutamate, 100% of which was metabolized in its first passage across the intestine

(Rutten *et al.* 2005). In humans with chronic renal failure, AKG supplementation improves bone metabolism and renal function. These studies reflect important aspects of AKG metabolism which may justify its use in nutrition and human and animal health.

1.3 Alpha-ketoglutarate and synthesis of collagen

Collagen is the main constituent of the dermis and is responsible for most of the structural resistance of the skin (Seeley *et al.* 2001). It is a long fibrous structural protein that constitutes approximately one third of the total protein in the body (Colgravea *et al.* 2008), is synthesized by fibroblasts and is the major component of many tissues. It is composed of three polypeptide chains with a triple helix arrangement and each collagen α chain is characterized by a unique repeating amino acid structure, Gly-X-Y, where Y is often proline. Hydroxyproline is essential for the formation of the collagen triple helix (Taşkiran *et al.* 1999). It has been reported that alpha-ketoglutarate is involved in collagen metabolism through a variety of mechanisms and these were described in detail by Son *et al.* (2007). In figure 1.2 a schematic representation of the role of AKG in collagen production is presented.

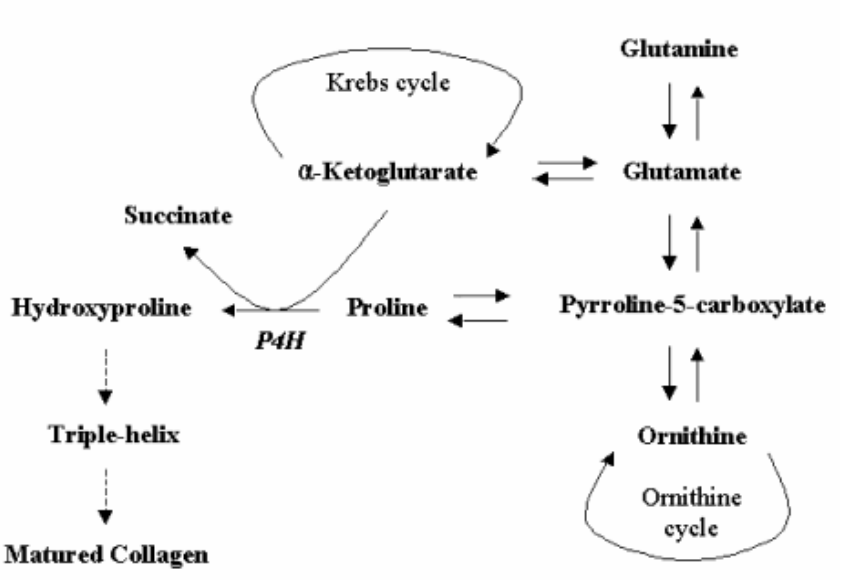

Figure 1. 2 – Schematic representation of the role of alpha-ketoglutarate in collagen production. Taken from Son *et al.* (2007).

AKG is a cofactor of prolyl-4-hydroxylase (P4H). P4H is located in the endoplasmic reticulum (ER) and catalyzes the formation of 4-hydroxyproline, which is essential for the

formation of the triple helix of the collagen molecule. The other way by which AKG contributes to collagen synthesis is by increasing the pool of proline residues *via* glutamate. Proline is a primary substrate for collagen metabolism and is generated through the conversion of pyrroline 5-carboxylate (P5C), which is an intermediate in the interconversion of proline, ornithine and glutamate (Son *et al.* 2007). Prolidase is a key enzyme in proline recycling, and is stimulated by the P5C-pathway. Under normal circumstances the P5C-pathway is a minor contributor to the proline pool for collagen synthesis but gains importance in the recycling of products from collagen degradation. While studying the enteral AKG administration in young pigs, Lamber *et al*. (2006) demonstrated that AKG was immediately converted to proline in the intestinal wall. Several studies have reported increased plasma levels of proline after oral but not systemic AKG administration together with enhancement of trabecullar collagen synthesis and bone formation in turkeys (Tatara *et al.* 2005; Tatara *et al.* 2004), piglets (Kowalik *et al.* 2005) and lambs (Harrison *et al.* 2004). Considering that collagen is the platform for bone mineralization, Harrison and Pierzynowski (2008) postulated that AKG has an anabolic effect on bone synthesis and is therefore an important factor for improving bone mineralization in osteoporosis patients. Considering that AKG was more effective in counteracting the loss of trabecular bone than that of cortical bone also lends support to the view that AKG acts by promoting collagen synthesis.

1.4 The skin

Skin is the major sensory organ in the body. Its structure, organisation and composition has attracted researchers for a long time. In humans, the integument functions as a barrier against external agents, it participates in the regulation of body temperature and excretion of salts, water, small amounts of urea and ammonia, and is essential for the production of vitamin D (Seeley *et al.* 2001). In humans it is composed of three typical layers (figure 1.3): the epidermis, dermis and hypodermis, all of them with higher complexity than in fish.

Numerous studies exist from a molecular perspective in avian and mammalian models of skin and appendage development, feathers and hairs, but only limited data is available for fish skin. In teleosts the integument is the primary barrier against the environment, allowing normal internal physiological function (Roberts 2001). The skin separates the interior of the animal from the aquatic environment, maintains the body shape, improves hydrodynamics and houses sensory organs, like mucus glands which produce antifungal and antibacterial

substances, club cells responsible for the production of alarm substances and sensory cells, like the neuromasts of the lateral line system.

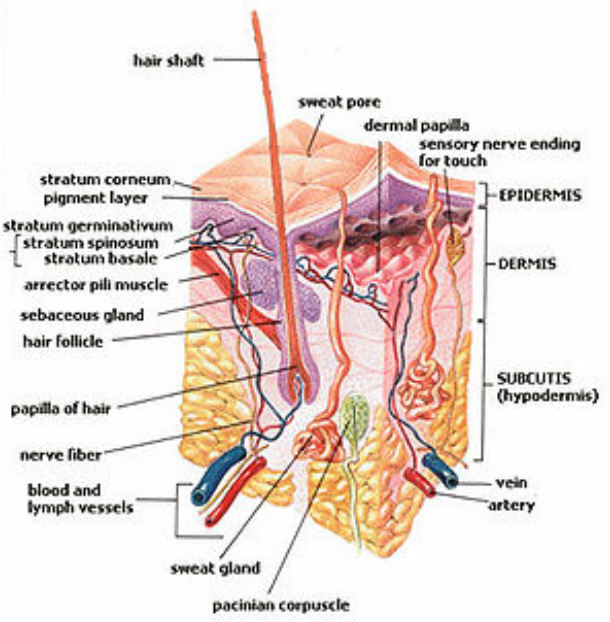

Figure 1. 3 – Different layers of human skin. The image illustrates the complexity of the human skin, with several appendages and accessory glands. Taken from http://upload.wikimedia.org/wikipedia/commons/thumb/3/34/Skin.jpg/300px-Skin.jpg.

Skin in fish is composed of the same three layers as in higher vertebrates, epidermis, dermis and hypodermis, but the structural organization is considerably different. One main difference is the keratinisation, which is uncommon in teleosts but the rule in terrestrial vertebrates. The function of keratin, a tough and insoluble protein, is to provide rigidity and protection against impacts and water loss. In terrestrial vertebrates, keratinisation occurs in the stratum corneum of the epidermis, in feathers, hairs, claws, nails, hooves and horns. In adult teleosts keratinisation occurs only in specific sites that are subject to abrasion, such as adhesive organs, lips and pads, and the epidermal surface of some amphibious species which inhabit aquatic and terrestrial environments (Guellec *et al.* 2004; Seeley *et al.* 2001). While studying skin development during the metamorphosis of Atlantic halibut Campinho *et al.* (2007) demonstrated that the larval supra basal and basal cells of the thin epidermis expressed keratin type I before metamorphosis. At the climax and after metamorphosis keratin is down regulated, and this process is related to the increase in thyroxine (T4) levels. In contrast to terrestrial vertebrates which are covered by an outer layer of dead keratinised cells, the epidermis of teleosts is comprised of living cells (Guellec *et al.* 2004). In fish, the dermis is

highly vascularised since the skin is also an accessory respiratory surface. It is composed of a collagenous matrix which contains fibroblasts, nerves, pigment cells and scales.

1.5 Teleosts scales

In most fish species, the dermis contains well differentiated elasmoid scales. Scales are thin and flexible structures imbricated in the superficial dermis below the epidermis and are located inside individual scale pockets. They are composed of collagen fibrils arranged in a plywood-like structure that confers their transparency and mechanical resistance. Cellular elements are osteoblasts (or scleroblasts) which are responsible for extracellular matrix (ECM) deposition and mineralization on the upper side and osteoclasts responsible for turnover and remodelling on the lower side (Bereiter-Hahn & Zylberberg 1993; Sire *et al.* 1990; Witten *et al.* 2001). Scales are neural-crest derivatives that form through epidermal-dermal interactions, cell proliferation and differentiation.

The presence of scales in fish skin is related to the protective functions of the vertebrate integument (Mugiya 1980). Despite being a protective barrier, almost all fish lose their scales during their lifetime and the shed scales are immediately replaced by regeneration. Regenerating scales (Bereiter-Hahn & Zylberberg 1993; Sire & Akimenko 2004) grow and mineralize very quickly and require in a short timescale a large quantity of calcium which is unlike the gradual accumulation which occurs during normal ontogeny. The development of an elasmoid scale has been described in detail for zebrafish and five phases have been distinguished (figure 1.4): early morphogenesis, late morphogenesis, early differentiation, late differentiation and epidermis folding. During these five steps, the anterior region of the scale progressively withdraws from the epidermis surface and sinks into the dermal stroma, becoming overlapped (Huysseune & Sire 1998; Sire & Akimenko 2004).

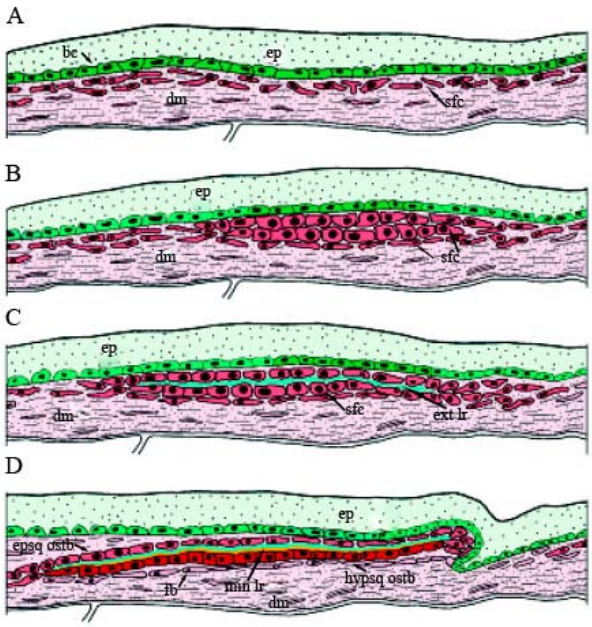

Figure 1. 4 – Scale formation in the zebrafish *Danio rerio*. **A**: Fibroblasts in the dermis accumulate along the basal layer of the epidermis. **B**: The scale papilla differentiates in well defined regions of the dermis. **C**: The first external layer is deposited between two layers of the papilla. **D**: The external layer starts to extend, contributing to the enlargement of the scale, the basal layer starts to mineralize in the inner surface of the scale and the folding of the epidermis along the posterior margin of the scale starts to develop. Ep: epidermis, dm: dermis, bc: base cells, epsq ostb: episquamal osteoblasts, ext lr: external layer, fb: fibroblasts, hypsq ostb: hyposquamal osteoblasts, min lr: mineralized layer, sfc: scale forming cells. Taken from Sire and Akimenko (2004).

1.6 Collagen in teleosts skin and scales

The comparison between fish and tetrapod collagen sequences indicates that the main characteristics of collagens were conserved during vertebrate evolution. Several genes encoding collagens have been identified in fish: type I, type II, type V/XI and type XVIII (Guellec *et al.* 2004). In skin and intramuscular connective tissue type I and type V are the major and minor collagens, respectively (Guellec & Zylberberg 1998; Yata *et al.* 2001; Zylberberg *et al.* 1992). Onozato and Watanabe (1979) were the first to demonstrate that the lamellae of the fibrillary plate of the goldfish *Carassius auratus* contain sheet-like structures (figure 1.5) composed of collagen fibers and organic matrix which set the pattern for the deposition of calcium phosphate crystals. In human bone the natural affinity of the collagen fibers for the calcium salts causes their precipitation (Guyton & Hall 2006). The matrix region in elasmoid scales contains materials serving as nucleation sites for hydroxyapatite crystals. Collagen type III is associated with collagen type I in other vertebrate lineages but has not been identified in teleosts yet. Besides the classical collagen type Iα1 and Iα2 chains which

assemble as a heterodimer $(\alpha1)2\alpha_2$, fish skin collagen type I also has a third chain, α3, leading to an α1, α2, α3 heterotrimer (Guellec *et al.* 2004).

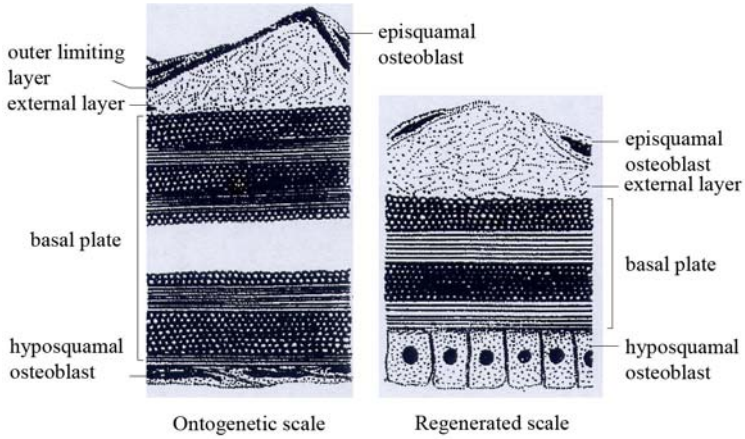

Figure 1. 5 – Diagram of ontogenetic and regenerated scales of *Poecilia reticulata* (Actinopterygii, Cyprinodontiformes) showing different layers of the elasmoid scale in teleosts. The outer limiting layer does not contain collagen fibrils and does not exist in the newly regenerating scale. In the basal plate the collagen fibrils are organized in superimposed plies forming a plywood pattern. Hyposquamal osteoblasts are flat cells in the ontogenetic scale and prismatic in the regenerating one. Taken from Bereiter-Hahn and Zylberberg (1993).

Two kinds of collagen fibrils can be found in elasmoid scales: thin (about 30 nm in diameter) fibrils present in the external layer, responsible for the resistance to plastic deformity, and thick (about 100 nm in diameter) fibrils in the basal plate, densely packed and superimposed forming the typical plywood structure responsible for the resistance to high stress (Guellec & Zylberberg 1998). It remains to be established if and how modifications in collagen synthesis influence scale characteristics and their role as a reservoir of readily mobilized calcium.

1.7 Characteristics of bone tissue in higher vertebrates and teleosts

Bone is a supportive skeletal tissue impregnated by hydroxyapatite (calcium and phosphate salts) and type I collagen (ColIα1) is the major extracellular matrix component both in higher vertebrates and teleosts. It is deposited by bone-forming cells, the osteoblasts and modelled, remodelled and/or removed by mono- and multinucleated osteoclasts, the bone-resorptive cells. Besides supporting the body, bone protects internal organs and is the site of attachment of ligaments and muscles (Hall & Witten 2007). The three major non-collagenous proteins in bone are the osteopontin, osteonectin (or SPARC) and osteocalcin. Osteopontin, or Secreted Phosphoprotein 1 (SPP1), is a sialoprotein ubiquitously expressed in adult mammalian

organisms (Kerr *et al.* 1991) and in calcified and partially calcified tissues but not soft tissues in teleost (Fonseca *et al.* 2007). It is involved in cell adhesion and bone mineralization and remodelling (Zhang *et al.* 1990). Osteonectin is a calcium-binding glycoprotein that participates in processes that involve substantial changes in extracellular matrix structure, like bone remodelling, cell turnover and tissue repair. It plays an important role in bone and cartilage mineralization (Pacifici *et al.* 1990), is a terminal marker of osteoblasts differentiation (Jundt *et al.* 1987) and serves as a link between collagen and hydroxyapatite (Termine *et al.* 1981). In an *in vitro* bioassay with sea bream scales, where osteonectin is highly expressed, osteonectin was down regulated by parathyroid hormone-related protein (PTHrP) (Redruello *et al.* 2005). Osteocalcin is an osteoblast-specific protein associated with bone formation and turnover and a marker of osteogenic maturation (Nakamura *et al.* 2009). It can be synthesised and secreted in the general circulation as a pre-pro-hormone (Harada & Rodan 2003). Despite being produced by osteoblasts, an additional role in the regulation of energy metabolism as been proposed for osteocalcin (Lee *et al.* 2007), suggesting a link between bone and metabolic processes.

Bone tissue in higher vertebrates is composed of an organic matrix that is greatly strengthened by deposits of calcium salts, mainly calcium and phosphate, to which magnesium, sodium, potassium and carbonate ions are also conjugated. Osteoblasts secrete collagen molecules and proteoglycans and become trapped in the matrix. Calcium salts (such as $CaHPO_4 \cdot 2H_2O$ and $Ca_3(PO_4)_2 \cdot 3\ H_2O$) then starts to precipitate, forming the osteoid. Through a process of substitution and addition of atoms in this osteoid tissue, crystals of hydroxyapatite form over a period of days or weeks into the finished product (figure 1.6).

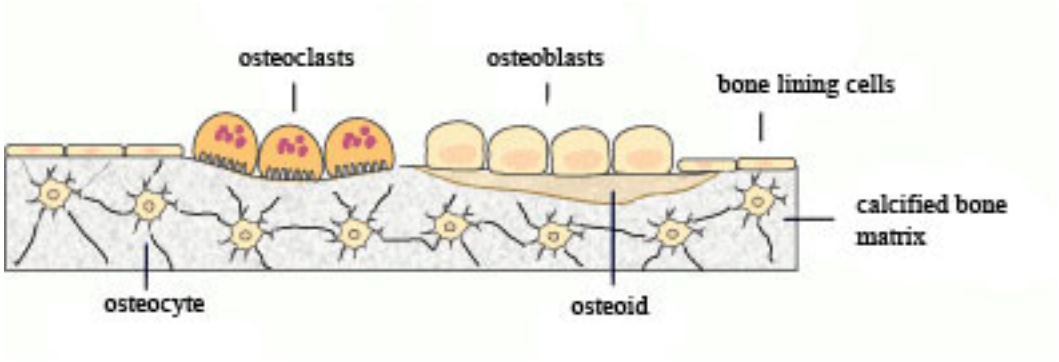

Figure 1. 6 – General structure of the bone in higher vertebrates. Osteoblasts are the cells involved in bone formation and osteoclasts are responsible for bone modelling. Osteocytes are osteoblasts that became entrapped in bone matrix during the process of mineralization and the osteoid is the first mineralized tissue composed of collagen fibers and proteoglycans. Taken from www.iofbonehealth.org/osteofound/cache/img/1c.

The entrapped osteoblasts are called osteocytes (figure 1.6), and they communicate with each other and with the circulatory system through a system of small blood vessels, the osteocytic membrane system. Most species of modern bony fish (higher Actinopterygii) have acellular bone – anosteocytic bone (Witten 1997). The bone in fish lacks osteocytes and so far no proof of its involvement in calcium metabolism under normal conditions has been demonstrated. Osteoblasts, which never became entrapped in bone matrix, and osteoclasts are present at the bone and scales surface and are involved in its deposition and remodelling. Anosteocytic bone is a regular bony tissue with a chemical composition that generally does not differ from the bone of other vertebrates. In common, with higher vertebrates, putative lining cells have been described in *Oreochromis niloticus* bones (Witten 1997). Some species from the lower Actinopterygii have cellular bone, which does contain osteocytes in its matrix (Kranenbarg *et al.* 2005).

1.8 Calcium balance and mineral turnover in higher vertebrates

In mammals, bone is the major calcium reservoir and calcium balance is promptly regulated through the feedback mechanisms of parathyroid hormone (PTH) secreted by the parathyroid gland and calcitonin (CT) secreted from the parafollicular thyroid C cells. In normal humans, plasma calcium ranges between 2.2 and 2.5 mmol/L (www.endotext.org/female/female14/female14_2.htm) and when it drops slightly below normal, PTH is released from the parathyroid gland and stimulates a range of processes to increase plasma calcium including osteolysis and osteoclasts activity to reabsorb calcium salts and bone, in this preferential order. In osteolysis, osteoblasts and osteocytes function to cause calcium and phosphate salts reabsorption but not the fibrous and gel matrix of bones. The task of osteoclasts is to absorb bone and not merely calcium phosphate salts and this is achieved by the action of proteolytic enzymes and release of acids, like citric acid and lactic acid. The enzymes digest or dissolve the organic matrix of the bone, and the acids cause the dissolution of bone salts. Osteoclasts engulf minute particles of bone matrix and crystals by fagocytosis, which are eventually dissolved and the products released into the blood. When plasma calcium is above the normal range CT, a hypocalcaemic factor in mammals, is released and inverts osteolysis, in favour of calcium and phosphate deposition and inhibits osteoclasts activity restablishing calcium equilibrium in plasma (Guyton & Hall 2006). In addition, to the

bone and parathyroid gland, calcium homeostasis in mammals also involves the kidneys and intestine, where calcium absorption and excretion is tightly regulated (Guyton & Hall 2006).

1.9 Calcium balance and mineral turnover in teleosts

Fish like mammals maintain their circulating calcium levels within controlled limits, although the systems involved in this regulation are not totally clarified and differ substantially from mammals. Terrestrial vertebrates obtain their calcium from the diet, absorbing it through the intestinal wall, while fish obtain their calcium from the diet and also from the water, a readily available source of calcium. Water exposed epithelia such as the gills, skin, scales, and the intestine are a fundamental part of the uptake and excretion process (Rotllant *et al.* 2005). Freshwater species drink very little water, so virtually all the calcium comes from the diet and is absorbed in the intestine. The uptake of calcium by the gills is extremely important. In contrast, marine species drink a high volume of water to compensate for renal and branchial osmotic water loss (Roberts 2001).

Teleosts possess two hormones with hypocalcaemic action, stanniocalcin (STC) and CT. STC is produced in the corpuscles of Stannius in the kidney. The main targets for STC are the entry routes of calcium: the gills and intestines, where it acts by preventing calcium entry (Ishibashi & Imai 2002). CT is secreted from the ultimobranchial body and although there is controversy surrounding the action of CT in fish (Mukherjee *et al.* 2004), some authors showed it suppressed TRAP activity in an *in vitro* bioassay with scales from goldfish and nibbler fish and suggested it may protect scales from excess degradation during vitellogenesis (Suzuki *et al.* 2000).

Fish possess a hypercalcaemic factor distinct from, but related to PTH in higher vertebrates, parathyroid hormone-related protein (PTHrP) (Flanagan *et al.* 2000). Fish do not have a parathyroid gland, a functional gland first appeared in amphibians, but they do possess PTH, although its importance as a hypercalcemic factor is unresolved (Canario *et al.* 2006). In fish, PTHrP is present in high concentrations in the pituitary gland (Rotllant *et al.* 2003) and its hypercalcaemic role in calcium metabolism was shown when administration of (1-38) PTHrP N-terminal region increased whole body calcium uptake and a decreased calcium efflux in sea bream larvae (Guerreiro *et al.* 2001). Since then, several studies of this hypercalcaemic factor exist in fish, revealing that different tissues express PTH receptors that bind PTHrP and that besides PTH receptor 1 (PTH1R) which is also present in terrestrial vertebrates, fish also have

a PTH3R that activates the adenylate cyclase/protein kinase A intracellular signalling pathway. Fuentes *et al.* (2005) demonstrated that PTHrP stimulates calcium transport in the sea bream intestine and Rotllant *et al.* (2005) showed that calcium mobilization from fish scales is mediated via PTH1R and activated the cAMP/AC (cyclic adenosine monophosphate/adenylyl cyclase) intracellular signalling pathway, providing further evidence of the hypercalcaemic action of PTHrP in teleosts.

1.10 Studies on calcium mobilization from fish scales and bone

The skeleton of teleost fish encloses 99% of the calcium in the body, distributed between the two potential reservoirs of bones and scales. Witten (1997) using histological and enzyme histochemical observations demonstrated that in *Oreochromis niloticus* osteoblasts and osteoclasts are present at the bone surface. Despite such studies, mineral homeostasis through bone turnover as occur in terrestrial vertebrates has not been demonstrated in teleosts yet.
In teleosts calcium is mobilized from scales in periods of high calcium demand, such as during vitellogenesis and spawning and also after treatment with 17β-oestradiol (E_2) (Persson *et al.* 1995). In mammals, estradiol inhibits osteoclasts activity in bones, while in teleosts it has the opposite effect and stimulates calcium absorption. Persson *et al.* (1999) showed that tartrate-resistant acid phosphatase (TRAP), an enzyme that characterizes the osteoclasts of higher vertebrates, can also be used to characterize teleost osteoclasts and its activity in rainbow trout *Oncorhynchus mykiss* scales is higher after E_2 treatment. Three different estrogen receptors (ERα, ERβa and ERβb) are expressed in sea bream and Mozambique tilapia scales (Pinto *et al.* 2009) and ERs are also found in goldfish scales (Yoshikubo *et al.* 2005) in putative osteoclast-like cells supporting the notion that E_2 directly induces calcium mobilization from fish scales. All these studies suggest the scales are an important calcium reservoir in teleosts.

1.11 The sea bream skin and scales as a model

Teleosts scale formation is well studied at the tissue and cellular level, but molecular data on scale development are still limited (Monnot *et al.* 1999), probably because the skin of fish is very specialised and because scales form late in ontogeny. According to Sire and Akimenko (2004), the late development of scales appears to be a disadvantage for studies of their

development but offers the possibility of studying the squamation pattern and scale development. This becomes even more relevant when considering that several genes known to be involved in the control of organogenesis are expressed during scale development. Developmental processes such as epidermal-dermal interactions, cell proliferation and differentiation can be easily studied during scale formation since they occur in larger animals (late larval phases) compared to embryos and their development occurs over a relatively short period of time.

OBJECTIVES

In the present thesis, the skin, scales and scale regeneration of gilthead sea bream were studied after oral administration of alpha-ketoglutarate a key metabolite of the citric acid cycle and also important for collagen synthesis. The study characterised the morphological modifications which accompanied scale and skin regeneration and also the modifications in the transcription of target genes previously shown to be important in scale formation. The specific objectives of the thesis were:

1. To describe the morphology of sea bream intact and regenerated skin and scales after oral administration of AKG.
2. To characterize by immunohistochemical and *in situ* hybridization techniques the intact and regenerated skin and scales after oral administration of AKG.
3. To evaluate the expression of collagen type I and SPP1 in sea bream skin.

Chapter 2

General Materials and Methods

The present chapter describes the general methods common to various parts of the practical work. The specific methods and/or conditions relevant to the work reported in each of the subsequent chapters will be included as a short methods section which will follow the introduction and precede the results.

2.1 Experimental animals and set up

Adult sea bream (*Sparus aurata* L.) were purchased from a commercial supplier (Viveiros Vilanova, Lda., Vila Nova de Milfontes, Portugal) who reared the fish in aquaculture ponds. Fish were transferred and maintained in Ramalhete's Marine Station (University of Algarve, Faro, Portugal) in a flow through sea water system under natural annual conditions of water temperature, photoperiod and salinity. Fish were fed at 3% of the total weight (kg) of fish in the tank once daily in the morning at 10h30min with commercial ration (Diasoja). For the experiments, 20 adult fish were transferred and maintained in three 500 L tanks with an open circuit of sea water and constant aeration at 20 ºC. In order to administer the treatment it was necessary to adapt the fish to fresh food (commercial frozen clams) instead of dried ration and this was done over one week, during which fish were fed every morning 2% of their body weight in clams coated with a few drops of cod liver oil (Maialab, Lda., Portugal) which served to mask the flavour of the treatment during the experiment and to supply an abundant source of cholecalciferol. Fish adapted readily to the new diet. The experiments described comply with the ethical guidelines of the Animal Behaviour Society (The Association for the Study of Animal Behaviour – ASAB) and Animal Behaviour Society (ABS) and National legislation.

Three experimental groups were considered: Treated group – 7 sea bream treated daily with 0.1 g/kg alpha-ketoglutarate (AKG) (1 pill = 1000 mg AKG, 280 mg Calcium, chewable tablets, batch nº CK775, Gramineer International AB, Sweden); Placebo group – 6 sea bream treated daily with 140 mg of calcium pills (Calcium 600, Wyeth; 1 pill = 600 mg calcium – tribasic calcium phosphate, 125 I.U. cholecalciferol, batch nº 8FC001) and the Control group – 7 sea bream fed daily with clams only. The food was freshly prepared every morning immediately before feeding the fish. Clams were chopped up, the number of pills necessary to administer the appropriate dose was determined and cut into smaller pieces and inserted into the clams. Clams were pulverised with cod liver oil and the food fed manually over half an

hour ensuring all fish ate and no food remained at the bottom of the tank. The experiment took place over 14 days, between May 27th and June 9th 2008. Fish were anesthetised on day 0 to determine weight (kg), standard length (cm) and for scale removal from the left side of the body, which was done by gently shaving the scales with forceps in order to minimise injury of the dermis and an inflammatory reaction. Fish were allowed to recover in a tank with flowing salt water and reintroduced into the experimental tanks.

2.2 Tissue sampling and processing

The adult sea bream from the three experimental groups were anesthetised with 2-phenoxy-ethanol (Sigma-Aldrich, Madrid, Spain), weighed and standard length measured (appendix I) and 1 ml of blood was collected from the caudal region using sterile syringes treated with heparin (appendix II), immediately transferred to 1.5 ml polypropylene tubes (Eppendorf) and kept on ice until centrifugation for 5 minutes at 13 000 rpm in order to separate the plasma from all blood cells. Plasma was transferred to new tubes, immediately frozen in liquid nitrogen and kept at -80 ºC until use. Dissection was carried out in aseptic conditions, maintaining all instruments used in 95% ethanol throughout the process. Two blood vessels, the aorta and the kidney artery were collected from all fish and preserved at 4 ºC in a saline solution (appendix II) for elasticity analysis.

For histology, skin with regenerated scales, skin with intact scales and skin without scales were collected and fixed in fresh 4% PFA pH 7.4 (appendix II) overnight at 4 ºC, washed three times for 10 minutes with sterile 1× PBS (appendix II) and kept in 70% ethanol at 4 ºC until use. Skin with regenerated scales was sampled from the left side of the fish in a 2x4 cm^2 area starting at the level of the dorsal fin; skin with intact scales was collected in the same way but on the right side of the fish and skin without scales was collected on this same side after gently shaving off the scales with forceps. Tissues were decalcified for 24 h in 0.5 M EDTA pH 8 (appendix II) at 4 ^{o}C, washed three times for 20 minutes with sterile DEPC treated water (appendix II) and prepared for paraffin embedding in an automated tissue processor (Leica TP1020, Leica®) by dehydration in an ascending series of ethanol (70%, 95% and 100%), cleared in xylene, xylene-paraffin (1:1, in volume) and embedded in low melting point paraffin wax Histosec (Merck, VWR, Portugal; for details see appendix III) with a Miles Scientific console (Thermal Console, Dispensing Console and Cryo Console,

Tissue-Tek, Miles Scientific). Serial 5 µm longitudinal/transverse sections were cut using a microtome (LeicaRM2125RT, Leica®) with disposable stainless steel low profile blades (Sakura, Labometer, Portugal) and mounted on 3-aminopropyltriethoxysilane (APES; Sigma-Aldrich, Madrid, Spain) coated slides (appendix III).
For RNA extraction, a skin sample (with regenerated, intact and no scales) of 1x1 cm^2 was also collected, frozen in liquid nitrogen and kept at -80 ºC until use.

2.3 General Histology

All staining procedures described subsequently were carried out with sections which had been dewaxed and rehydrated. This was done by immersing for fifteen minutes in two xylene baths and then in a graded series of ethanol baths (100%, 95% and 70%) for 5 minutes each. The rehydration process was completed by a final immersion in distilled water for five minutes.

2.3.1 Haematoxylin-eosin staining

Haematoxylin-eosin staining is a basic histological procedure that allows the morphological identification of cells and tissues. With this staining procedure, negatively charged nuclei stain purple and the basic cytoplasm stains pink.
After hydration, every 5^{th} slide of sectioned material were immersed in Harris haematoxylin solution (appendix II) for 5 minutes, blued in running tap water, rapidly rinsed in distilled water, immersed in an aqueous solution of eosin Y (appendix II) for 3 minutes and rinsed in distilled water with a few drops of acetic acid. To obtain definitive preparations, tissue sections were dehydrated through an ascending series of ethanol and cleared with xylene (Pronalab, VWR, Potugal), as described in appendix III.

2.3.2 Masson's trichrome staining

This method relies upon two similar acid dyes to provide a differential visualization of tissue elements. The following trichrome staining was done according to the protocol described by Witten and Hall (2003). Deparaffinized sections were stained for 10 minutes with Mayer's acid haematoxylin (Sigma-Aldrich, Madrid, Spain), exposed to running tap water for 10 minutes and rinsed in distilled water. Sections were then stained with freshly prepared

Xylidine ponceau for 2 minutes (appendix II), rinsed in distilled water, treated for 4 minutes with 1% phosphomolybdic acid (appendix II), rinsed again and stained with light green for 90 seconds (appendix II). The excess dye was cleaned from the slides, which were then rapidly passed through an ascending ethanol series (50%, 70%, 90% and 100%), cleared and mounted in DPX (BioChemika, Sigma-Aldrich, Madrid, Spain), as described in appendix III. With this staining procedure mineralized tissue such as scales and bone is stained red while non-mineralized connective tissue is stained green. Stained sections were analyzed using a microscope (Leica DM2000) coupled to a digital camera (Leica DFC480) and linked to a computer for digital image analyses.

2.3.3 Picro-sirius birefringence for collagen

The Sirius red staining for collagen exploits the enhancement by sirius red of the birefringence of collagen fibres, which is largely due to co-aligned molecules of type I collagen. Birefringence or double-refraction is the decomposition of a ray of light in two components. The resulting rays become polarized and travel at different velocities. This happens in all anisotropic crystals (http://www.olympusmicro.com/primer/lightandcolor/birefringence.html). According to (Junqueira & Carneiro 2005) the birefringence is highly specific for collagen and is commonly used in the diagnosis of altered collagen pathologies in hard and soft tissues.

Deparaffinized and hydrated sections were stained for 8 minutes with Weigert's haematoxylin; washed 10 minutes in running tap water followed by a 1 hour immersion in 0.1% picro-sirius red solution (appendix II). Slides were washed in two changes of acidified water (appendix II), dehydrated in 3 changes of 100% ethanol, cleared and mounted in DPX (Fluka), as described in appendix III. In bright-field microscopy collagen is red on a pale yellow background. Nuclei should be black, but may often be grey or brown. When examined with polarized light the larger collagen fibres – normally collagen type I, are bright yellow or orange, and the thinner ones, including reticular fibres, are green (Pearse 1985). Stained sections were analyzed under polarized light using a microscope (Olympus BH2) coupled to a digital camera (JVC TK-1280E) used to registry the images.

2.3.4 Demonstration of TRAP in sea bream scales

An enzyme histochemical procedure was used to demonstrate the presence of Tartrate-resistant acid phosphatase (TRAP) in sea bream scales. TRAP is an enzyme commonly used as an indicator of osteoclasts activity and it is involved in resorption of bone. The method of (Witten *et al.* 2001) was followed. Hydrated tissue sections were immersed in a pre-incubation solution (appendix II) containing 0.1M acetate buffer and 0.5M di-sodium tartrate (Sigma-Aldrich, Madrid, Spain) pH 5.5 for 30 minutes at 20 ºC. Afterwards sections were immersed in the developing solution (appendix II) containing napthol AS-TR phosphate (N-AS-TR-P, Sigma-Aldrich, Madrid, Spain) as the substrate and hexazotized pararosaniline (PRS, Sigma-Aldrich, Madrid, Spain; appendix II) for 40 minutes at 20 ºC. Subsequently, sections were rinsed in demineralised water and counterstained with haematoxylin for 1 minute, blued in running tap water, rinsed in distilled water, dried at 40 ºC and mounted with DPX (Fluka). Stained sections were analyzed using a microscope (Leica DM2000) coupled to a digital camera (Leica DFC480) and linked to a computer for digital image analyses.

2.4 Immunohistochemistry

Immunohistochemistry techniques allow the visualization of specific antigens in the tissue through interaction with specific antibodies marked with a fluorescent dye, enzyme, radioactive element or colloidal gold (http://www.ihcworld.com/introduction.htm). As this method involves a specific antibody-antigen reaction it provides more information than enzymatic staining procedures that identify a limited number of proteins and tissue structures. There are several direct methods which use one antibody directly identified with a reporter molecule. Alternatively an indirect method in which the primary antibody is not labelled is used and is coupled to the use of a secondary antibody that binds to the constant fraction of the first antibody.

In the present work, a 3-step indirect method was used to visualize the presence of Proliferating Cell Nuclear Antigene (PCNA, a marker of cells in proliferation), osteonectin (a marker of bone) and p63 (a keratinocyte stem cells marker) in sea bream skin (with regenerated, intact and no scales). This 3-step method uses the high affinity that streptavidin (a tetrameric high molecular weight protein) has for biotin (vitamin B_7) in order to detect the

biotinylated secondary antibody bound to the primary antibody. Streptavidin is conjugated to peroxidase, which produces a brown coloured precipitate when 3,3'- diaminobenzidine (DAB) is oxidized, revealing the distribution of the target antigen.

During rehydration (section 2.3) of tissue sections slides were immersed for 5 minutes in a 50% ethanol bath before the final hydration with distilled water. In some cases (see chapter 4), it was necessary to conduct heat induced epitope retrieval (HIER) by heating the sections in 0.1M Sodium Citrate pH 6 in the microwave at maximum power for several pulses of 30 seconds, refilling the coplin with the buffer when necessary. This step allowed the recovery of the specific antigen that may have become masked by the protein cross-linking induced during tissue fixation. Endogenous tissue peroxidase was inactivated from rehydrated skin and scales sections in a solution of 20% methanol (Merck, VWR, Portugal) in PBST containing 3% H_2O_2 (appendix II) for 20 minutes. Sections were washed twice for 2 minutes in PBST and blocked for 1 hour with 4% sheep serum (Sigma-Aldrich, Madrid, Spain) in Tris-Carrageenan Triton X100 (TCT, appendix II). The vegetal protein carrageenan binds non-specifically to proteins in the tissue and blocks non-specific interactions in subsequent incubations with the specific antisera. Non-specific interactions lead to a higher background and to a dramatic dilution of the primary and secondary antibodies. Also, the 0.5% detergent Triton X100 extracts some proteins from the cellular membranes and improves the accessibility of the antigen to the antibodies. After blocking, sections were rinsed twice for 2 minutes in PBST and incubated with a dilution of the primary antibody in TCT. Sections were incubated overnight with the primary antibody at 4 ºC. Sections were washed twice for 5 minutes in PBST and incubated with a 1/200 dilution of the secondary antibody in PBST for 1 hour at room temperature. Excess antibody was removed by washing sections twice in 0.15M PBS pH 7.2 (appendix II) and sections then incubated with the complex Streptavidin – horseradish peroxidase conjugate (GE Healthcare UK Limited) 1/400 in 0.15M PBS pH 7.2 for 45 minutes before preparing sections for colour development by washing them in 0.15M PBS pH 7.2 (2x 5 minutes). Sections were incubated with a DAB and peroxidase substrate solution (0.05% DAB, 0.015% H_2O_2 in 0.15M PBS pH 7.2, appendix II) for 10 minutes at room temperature and the reaction was stopped by rinsing sections in 0.15M PBS pH 7.2, followed by distilled water before dehydrating, clearing and mounting in DPX (appendix III). Control reactions in which the primary or secondary antibodies were omitted from the staining procedure were also performed. Stained sections were analyzed using a microscope

(Leica DM2000) coupled to a digital camera (Leica DFC480) and linked to a computer for digital image analyses.

2.5 mRNA tissue distribution by *in situ* hybridization

In situ hybridization allows the visualization of specific nucleic acid sequences in morphologically preserved tissues. In the present study, non-radioactive digoxigenin (DIG)-labelled cRNA (riboprobes) probes were used to favour the formation of tighter hybrids (RNA:RNA), which would allow a higher stringency in post-hybridization washes and the absence of competing reactions that occur in the case of double-stranded DNA probes, which re-anneal in addition to binding to target mRNA (Darby & Hewitson 2006; Science 1996).

2.5.1 Riboprobe synthesis

A cDNA encoding for part of Col1α1 (801 bp) was ligated into the pGem-T Easy vector (Promega, VWR, Portugal; appendix IV, figure 1) and a cDNA encoding part of osteonectin (400 bp) was ligated in pBluescript SK(-) (Stratagene; appendix IV, figure 2). Both clones were generously conceded by Doctor Dulce Estêvão, Centre of Marine Sciences (CCMAR), Comparative and Molecular Endocrinology Group, University of Algarve, Portugal.

2.5.1.1 Competent cells transformation

Competent bacteria (*Escherichia coli*) maintained at -80 ºC were thawed on ice for 5 minutes, gently mixed with 1 µl of each recombinant plasmid and kept on ice for 30 minutes until a heat shock was applied (42 ºC for 45 seconds) in order to fragilize the bacteria cellular wall and membrane and allow the entrance and incorporation of the plasmid DNA in the cell. The putative transformed bacteria were plated out on LB/Amp/X-gal/IPTG (appendix II) agar and incubated overnight (≈ 14 to 16 hours) at 37 ºC. Plates were then placed a 4 ºC for a few hours to permit colour intensification of bacterial colonies before selecting colonies for plasmid extraction. To isolate the bacterial colonies that contained the recombinant plasmid from a mixture of non-recombinant plasmid containing cells a blue/white screening was performed. When the cloned sequence is inserted into the vector's multiple cloning site (MCS) it disrupts the *lacZ* region which encodes for the β-galactosidase gene. The X-gal

present in the culture medium is the substrate for this enzyme: when the enzyme is active it degrades X-gal producing a blue precipitate – Lac^+ colonies; when it is not active, X-gal is not degraded and the colonies are white – Lac^- colonies (Hartl & Jones 1999). Following these principals, two small and isolated white colonies were selected from each culture plate and grown in duplicate in LB broth (appendix II) with Ampicilin and incubated overnight (≈ 14 to 16 hours) in an orbital shaker (Gallenkamp) at 250 rpm at 37 ºC.

2.5.1.2 Plasmidic DNA extraction

The plasmidic DNA was extracted from the bacteria by alkaline lysis. Liquid cultures of bacteria were centrifuged at 10 000 rpm for 3 minutes and the supernatant was discarded. To destabilize the cell membrane and inhibit DNases, cells were resuspended in 200 µl of GTE (appendix II) and incubated with 5 µl RNase (10 mg/ml) for 10 minutes at room temperature. Cell lysis was promoted by incubation for 5 minutes on ice with 400 µl of a fresh solution of 0.2M NaOH and 1% SDS (appendix II); followed by another 45 minutes incubation on ice with 300 µl of 3M KAc pH 5.2 (appendix II) to renature plasmid DNA and promote the precipitation of cell debris. After a 10 minutes centrifugation at 10 000 rpm, the supernatant containing the plasmid DNA was removed to a new tube containing 1 ml of cold 100% ethanol and incubated for 1 h at -80 ºC and centrifuged 20 minutes at 13 000 rpm to collect the precipitate which formed. The DNA pellet was rinsed twice with 500 µl of cold 100% ethanol at 13 000 rpm for 10 minutes, dried at room temperature for 20 minutes and resuspended in 50 µl of MilliQ filtered water. To verify the quality of the miniprep, 1 µl was run on a 1% agarose gel (appendix III).

2.5.1.3 Preparation of template DNA – linearization and purification

The plasmid DNA containing the fragments of interest was linearized at 37 ºC for 2 h with the restriction enzyme that would originate the anti-sense probe. A reaction volume of 20 µl was used, containing 2 – 5 µl of plasmid DNA, 0.25 U/µl of restriction enzyme and 1x enzyme buffer. The reaction products were extracted with phenol pH 8 in order to eliminate contaminants which could inhibit downstream applications. The reaction volume was adjusted to 100 µl with MilliQ filtered water and 100 µl of phenol was added and thoroughly mixed. The solution was incubated for 35 minutes at room temperature and then centrifuged

(MiniSpin, Eppendorf) at 13 000 rpm for 5 minutes. The upper phase was removed, its volume measured and the linear DNA was precipitated overnight at -20 ºC by adding 1/10 volume of 3M NaAc pH 5.2 (appendix II) and 2.5x volumes of cold ethanol 100%. The recovery of the pure linear plasmid DNA was attained by centrifuging the samples at 13 000 rpm for 20 minutes, and then washing and centrifuging the pellets 2x 10 minutes with cold 75% ethanol. The pellets were allowed to dry at room temperature and then resuspended in 20 µl of MilliQ filtered water. The DNA linearization reaction was evaluated by fractioning the reaction products on a 1% agarose gel (appendix III).

2.5.1.4 *In vitro* transcription

In vitro transcription with the pure linear DNA was carried out with 1 U/µl of the appropriate RNA polymerase in 1x transcription buffer with 1 µl of Digoxigenin – RNA labelling mix (Roche Diagnostics, Mannheim, Germany), for 2 h at 37º C. The reactions were stopped with 2 µl of 0.2M EDTA pH 8. The riboprobes were purified by lithium precipitation, resuspended in 25 µl of MilliQ filtered water and its purity and concentration was determined by fractioning the reaction products on a 1% agarose gel (appendix III).

2.5.2 *In situ* hybridization

Tissue sections were dewaxed, rehydrated, incubated for 10 minutes in phosphate-Tween buffer (PTW, appendix II) at room temperature and pre-hybridized at 56 ºC for 2 h with hybridization solution containing 50% formamide, 4× SSC, 1 mg/ml torula RNA, 0.1 mg/ml heparin, 1×Denhardt's and 0.04% CHAPS (appendix II). For the hybridization, tissues were covered with 2 µl probe/ 100 µl of hybridization solution and left to incubate overnight at 56 ºC in a humidified box. As a negative control the riboprobes were excluded from the hybridizations and hybridization solution was used instead. To remove non-specifically bound probes, stringency washes were carried out at 56 ºC for 2x 5 minutes with 2× SSC (appendix II) and 5 minutes with 1× SSC. Tissue sections were then washed at room temperature for 2x 5 minutes with 2× SSC/0.12% CHAPS (appendix II), followed by a 5 minutes wash with 2× SSC/PTW (1:1, v/v; appendix II) and finally with PTW for 5 minutes. The blocking step was performed by incubation in 2% blocking reagent (Roche Diagnostics, Mannheim, Germany; appendix II) with 10% heat inactivated sheep serum (Sigma-Aldrich, Madrid, Spain) for 2 h at

room temperature. Detection of hybridized probes was carried out with 1/600 anti-Digoxigenin – Alkaline Phosphatase (AP) Fab fragments (Roche Diagnostics, Mannheim, Germany) in 1% blocking reagent (Roche Diagnostics, Mannheim, Germany; appendix II), overnight at 4 ºC.

Colour development was carried out with a solution of two chromogens: 4-nitroblue tetrazolium chloride (NBT) and 5-bromo-4-chloro-3-indolylphosphate (BCIP; both chromogens from Roche Diagnostics, Mannheim, Germany) in developing buffer (appendix II) at 37 ºC for 6 h. The reaction was stopped by rinsing sections for 5 minutes in 1× PBS and then fixed for 15 minutes in 4% PFA (appendix II) at room temperature then washed 2x 5 min with 1× PBS and tissue sections mounted with pre-warmed glycerol-gelatine (BioChemika, Sigma-Aldrich, Madrid, Spain). Analysis of sections was carried out using a microscope (Leica DM2000) coupled to a digital camera (Leica DFC480) linked to a computer for digital image analysis.

2.6 Plasma parameters

It has been shown that enteral feeding of AKG supplements increases circulating plasma levels such as insulin, growth hormone and the insulin-like growth factor IGF-I (Jeevanandam & Petersen 1999; Moukarzel *et al.* 1994). Moreover, studies in rats (Bienko *et al.* 2002), pigs (Kowalik *et al.* 2005; Tatara *et al.* 2007), turkeys (Tatara *et al.* 2004; Tatara *et al.* 2004) and sheep (Harrison *et al.* 2004) have shown a positive effect of AKG on skeletal homeostasis. To determine the possible effect of treatments not only on plasma composition but also to evaluate the physiological condition of the experimental animals, a set of plasma parameters were determined. These were two hormones, cortisol and estradiol, and two ions, calcium and phosphorus. Plasma binding proteins were heat denaturated for 1 h at 80 ºC, which allowed the measurement of plasma hormones without extraction (Donohue & Sgoutas 1975; Foster & Dunn 1974).

2.6.1 Determination of plasma calcium

The total calcium in sea bream plasma (diluted 1/40 in 0.01M PBS pH 7.6, appendix II) from the three experimental groups was determined with the kit Calcium – o-C v/v (o-cresolphtalein, v/v, colorimetric; Spinreact ref. 1001061, Spain). In this method, a purple

colour complex forms when calcium reacts with o-cresolphtalein in alkaline medium. The intensity of the colour formed is proportional to the calcium concentration of the sample.
A standard curve was prepared by dilution of a 10 mmol/L Calcium Chloride stock ($CaCl_2 \cdot 2H_2O$ Fw=147) in MilliQ filtered water in order to obtain the following calcium concentrations: 0, 0.3125, 0.625, 1.25, 2.5, 3.75, 3.75, 5 and 7.5 mmol/L (with linearity between 0 – 5 mmol/L). The assay was run on a 96-well microplate: 2.5 µl of each standard and denatured plasma sample were pipetted in duplicate to the plate and mixed with 250 µl of working reagent added to each well. The working reagent is a 1:1 mixture (v/v) of 500 mmol/L ethanolamine buffer and the chromogen solution (0.62 mmol/L o-cresolphtalein, 69 mmol/L 8-hydroxyquinolein). After 10 minutes incubation at room temperature (15-25 ºC) the absorbance at 570 nm was determined using a microplate reader (Benchmark BioRad Microplate Reader). Calcium concentrations in the samples were determined using the formula: [Calcium] mmol/L = (ABS – b) / a, where *ABS* is the duplicate mean of the plasma sample absorbance at 570 nm, *b* is 0.0311 and *a* is 0.1802 given by the standard curve's regression line ($R^2 = 0.9901$).

2.6.2 Determination of plasma phosphorus

The phosphorus in sea bream plasma (diluted 1/20 in 0.01M PBS pH 7.6, appendix II) from the three experimental groups was determined with a colourimetric method using the kit Phosphorus – UV (Phosphomolybdate, uv; Spinreact ref. 1001155, Spain). This method allows the direct determination of inorganic phosphate as the intensity of the colour formed in the test is proportional to the inorganic phosphorus concentration in the sample.
A standard curve was prepared by dilution of a 10 mmol/L Phosphorus stock ($Na_2HPO_4 \cdot NaH_2PO_4$) in MilliQ filtered water in order to have the following phosphorus concentrations: 0, 0.3125, 0.625, 1.25, 2.5, 3.75, 3.75, 5 and 7.5 mmol/L (with linearity between 0 – 7.5 mmol/L). The assay was run on a 96-well microplate: 2.5 µl of each standard and denatured plasma sample were pipetted in duplicate to the plate and mixed with 250 µl of working reagent added to each well. Working reagent is directly supplied by the manufacturer and consists in 0.40 mmol/L ammonium molybdate, 210 mmol/L sulphuric acid and detergents. After 10 minutes incubation at room temperature (15-25 ºC) the absorbance at 340 nm was determined using a microplate reader (Benchmark BioRad Microplate Reader). Inorganic phosphorus concentration in the samples was determined according to the formula:

[Phosphorus] mmol/L = (ABS – b) / a, where *ABS* is the duplicate mean of the plasma sample absorbance at 340 nm, *b* is 0.528 and *a* is 0.1435 given by the standard curve's regression line ($R^2 = 0.9711$).

2.6.3 Radioimmunoassays for Cortisol and Estradiol

Radioimmunoassay is a competition assay between a known amount of labelled hormone and an unknown amount of cold hormone by a limiting amount of antibody, followed by the separation of the free from the bound fraction (Chard 1973). It is a very sensitive technique and was first described by Yallow and Berson in 1960. It was considered a major break through in endocrinology because it allowed the measurement of minute amounts of antigene without the need of a bioassay. The formation of the hormone-antibody complex is regulated by the law of Mass Action H + Ab $\Leftrightarrow$ H:Ab, according to which, in equilibrium conditions:

$$\frac{[H:Ab]}{[H]\cdot[Ab]} = K$$

where [H] is the molar concentration of free hormone, [Ab] the concentration of free antibody, [H:Ab] the concentration of the hormone-antibody complex and *K* is the antibodies affinity constant. The sensitivity of the radioimmunoassay depends almost entirely on the *K* value of the antibody (Chard 1973, 1990).

One disadvantage of the radioimmunoassay (RIA) is that it gives no measure of biological activity of the hormones: it uses a small proportion of the molecule which represent its antigenic site and does not necessarily correspond to that responsible for biological activity (Chard 1973). For this reason it is essential to characterise the specificity for the hormone of the RIA in order to establish if it gives a biologically relevant measurement. The method used in the present work offers the advantage that tracer, antibody and buffer are added in a single step, reducing errors introduced by pipetting (Donohue & Sgoutas 1975).

Preliminary assays were done to determine the appropriate tracer and antibody concentration for both hormones measured, cortisol (F) and estradiol (E). Titration of the tracers was optimized so that 100 µl of tracer solution in gelatine buffer (appendix II) would have 1500 cpm. The titre of both antibodies was defined as the dilution at which 50% of the titrated tracer was bound to the antibody. The F assay was done with a 1/40 dilution (in 0.01M PBS pH 7.6, appendix II) of the denatured plasma samples, with a 1/50 dilution of Cortisol

20CR50 (Agrisera) antibody and [1,2,6,7-^{3}H]Cortisol (TRK407 Specific activity 50-90 Ci/mmol, Amersham Biosciences, GE Healthcare UK Limited) as the tracer. The E assay was done with a 1/20 dilution (in 0.01M PBS pH 7.6, appendix II) of the denatured plasma samples, with a 1/10 dilution of E RD1-40 E2 (Research Diagnostics, USA) antibody and [2,4,6,7,16,17-^{3}H] estradiol (TRK587 Specific activity 154 Ci/mmol, Amersham Biosciences, GE Healthcare UK Limited) as the tracer.

A set of standards was prepared for each hormone ranging from 0.5 to 500 ng/ml prepared from a stock solution of 0.5 mg /ml in ethanol. Both radioimmunoassays were run in duplicate in gelatine buffer with a total assay volume of 200 µl containing 100 µl of standard dilution or diluted plasma sample and 100 µl of the antibody and tracer solution. The competition between cold and labelled hormone for the respective antibodies was allowed to occur overnight at 4 ºC in order to reach equilibrium. Separation of the free hormone from the total bound hormone was carried out with 250 µl of a dextran coated activated charcoal suspension (appendix II) for 12 minutes at 4 ºC, followed by a centrifugation at 2000 rpm for 12 minutes at 4 ºC. Activated charcoal was added to all tubes except total counts tube, where 250 µl of gelatine buffer were added instead. Supernatants containing the antibody bound [^{3}H]-hormone were decanted into scintillation vials (Sarstedt 73.680 HD-PE) where 4 ml of liquid scintillant EcoLite™ (+) (MP Biomedicals, Madrid, Spain) were added. Luminescence measurements were converted to cpm using a LS 6000 IC Beckman beta-counter.

2.6.4 Plasma transaminases enzymatic assays

The analysis of plasma transaminases was performed by Dr. Toni Ibarz i Vals, Department of Physiology, Universitat de Barcelona, Spain. Plasma aspartate-aminotransferase (AST; EC.2.6.1.1) and alanine-aminotransferase (ALT; EC 2.6.1.2) activities were determined using the method of Gallardo *et al.* (2003). In these assays, enzyme activities were coupled, through the action of malic dehydrogenase (MDH), to the oxidation of NADH, which was measured spectrophotometrically at 340 nm. Alpha-ketoglutarate and aspartate or alanine was used as substrates for AST or ALT, respectively. Enzyme activities are expressed as IU per ml of plasma.

2.7 Sea bream aorta elasticity

The analysis of the sea bream aorta elastic recoil was performed by Dr. Adrian Paul Harrison, Associate Professor at the Department of Animal & Veterinary Basic Sciences (IBHV), Faculty of Life Sciences at Copenhagen University, Denmark. The elastic recoil of the kidney artery has not been analysed yet. In physiology, the elastic recoil of a tissue is a measure of its inherent resistance to change in shape, and the tendency of the same tissue to revert to its original shape once deformed (http://medical-dictionary.thefreedictionary.com/elastic+recoil).

2.7.1 Aorta preparation

A dissected portion of the sea bream abdominal aorta was carefully cleaned to remove adhering tissues. The aorta pieces ranged from 2.5-9.0 mm in length with a diameter at rest of approx.1 mm (1.1-2.1 mm), and each piece was then securely attached at one end to a force transducer and at the other to a metal pin on a mounting block, as described in Harrison and Flatman (1999) and Harrison *et al.* (1997). The weight of the aorta pieces ranged from 6 to 20 mg. Aorta sections were immersed into oxygenated and thermostatically controlled chambers (37 ^{o}C), having an internal depth and diameter of 5.5 and 3.2 cm, respectively, and holding 44 ml of phosphate buffered saline (0.15 M PBS pH 7.4) consisting of 136.91 mM NaCl, 2.68 mM KCl, 8.08 mM Na_2HPO_4 and 1.66 mM NaH_2PO_4. Force was measured using a FTO3 force displacement transducer (Grass Instrument, West Warwick, RI) connected to a home-built bridge amplifier, which was interfaced with an 8S PowerLab A/D Converter (ADInstruments, Chalgrove, Oxfordshire, UK). The transducer had a functional range of 0-0.05 kg, with a reliable force of 2 mg, equivalent to 0.004% of the functional range. The PowerLab 8S A/D converter was connected to an iBook G4 running Chart v.5.4 Software (AD Instruments, Australia). The data recording was at a sampling speed of 40 000 data samples per second (40 KHz) and the input impedance of the amplifier was 200 M differential.

2.7.2 Force measurements

Aorta sections were suspended vertically, and in duplicate. The recorded signal was adjusted to zero for un-tensioned aorta sections with the aid of an offset dial mounted on the pre-

amplifier unit. Each aorta section was then exposed to a step-wise increase in tension (approx. 0.09 N or 10 g), measured using the FT03 Grass Force transducer. The aorta sections were then allowed to relax totally before being exposed to repeat step-wise increases in tension two more times, in close succession. Aorta sections were subsequently removed and weighed. Immediately after a step-wise increase in tension, the recording trace was seen to fall very slightly as the aorta tissue exerted a degree of elastic recoil. This fall in the recording trace was measured over time using the Average Slope calculation which is available in Chart v.5.4 Software (AD Instruments, Australia). Average Slope (g ms^{-1}) is a time derivative of the data points in a trace selection and is calculated from the least-square line of best fit.

2.7.3 Elastic recoil calculations

It was assumed that the tension in the wall of the aorta sections was equivalent to that recorded by the force transducer as the result of a manual stretch. The fall in the recording trace that was seen immediately after a step-wise increase in tension was then measured as a degree of elastic recoil in the aorta sections. The measurement of Average Slope (g ms^{-1}) obtained for each aorta sample was subsequently converted into Newtons (N ms^{-1}) before being adjusted for sample weight to give a final elastic recoil value in N ms^{-1} mg^{-1} wet wt.

2.7.4 Statistical analyses

Data are presented as the mean ± SEM. The results were analyzed by one-way ANOVA using StatGraphics 4.1 Plus (StatPoint, Inc., USA) and were tested for Gaussian Normal Distribution. Data were found to be normally distributed and to have equal variance. A difference of $P < 0.05$ between means was considered to be significant.

2.8 Analysis of gene expression

Osteopontin (SPP1) was one of the genes analysed in the present work. It was chosen based on a previous work with sea bream scale regeneration where it was described as having modified expression during regeneration. The gene alpha-1 collagen type I (Col1α1) was chosen because of its relevance in the process of mineralization. The gene chosen for normalization and correction for individual variation was ribosomal 18S and the method

chosen to study these genes was the real–time quantitative polymerase chain reaction (RT-qPCR).

In PCR any sequence of nucleic acids can be amplified in a temperature cyclic process to generate a large number of identical copies that can readily be analysed. The amount of PCR product is measured at the end point of amplification. As an analytical technique, quantification of the product is not accurate because the final amount of product does not reflect the initial copy number of the target: it will be the same between different samples, independent of initial copy number. This problem was overcome in 1992 by the development of real-time PCR by Higuchi *et al*. (Higuchi *et al.* 1992). In real-time PCR the kinetics of the amplification reaction can be studied by monitoring the fluorescence of dyes or probes introduced into the reaction: these dyes are incorporated into the PCR product in each round of amplification, the gain in fluorescence is registered and is directly proportional to DNA concentration. The cycle at which the product fluorescence becomes higher than the background is called the threshold cycle (C_T) and it is used to calculate the amount of template present in the experimental samples at the beginning of the reaction using a standard curve. The higher the initial copy number of the template, the lower the C_T (Kubista *et al.* 2006; Sigma-Aldrich 2008; Wong & Medrano 2005). Several fluorescence reporters can be used to label qPCR products: labelled probes or DNA binding dyes. The former, like hydrolysis probes (Taqman) or molecular beacons, are sequence specific and can be used in multiplex assays, but are also more expensive and require extensive optimization. The latter, like SYBR®Green, emit fluorescence when bound to double–stranded DNA (dsDNA), are not sequence-specific and require a dissociation curve analysis to discriminate false positives. The SYBR®Green chemistry was the one chosen in the present work not only because it is economical but also because it is the most flexible since it uses conventional primers and can be used to detect different genes in independent assays (Sigma-Aldrich 2008; Wong & Medrano 2005).

2.8.1 Total RNA extraction

Total RNA extraction was done with the Sigma-Aldrich's TRI Reagent, which is an effective method for isolating RNA molecules of all types from 0.1 to 15 kb in length. This product is a mixture of guanidine thiocyanate and phenol in a mono-phase solution which effectively

dissolves DNA, RNA and protein on homogenization or lysis of tissue sample. After adding chloroform and centrifuging, the mixture separates into 3 phases: an aqueous phase containing the RNA, the interphase containing DNA and an organic phase containing proteins; each component can be isolated after separating the phases.

The RNA extraction was done according to the manufacturer's instructions. The sea bream skin and scales samples (with the regenerated, intact and no scales) collected from the three experimental groups and preserved at –80 ºC were weighted on a digital balance (Shimadzu AUX120), sliced into small pieces and immediately homogenized in a sterile 3 ml glass tissue grinder (FisherScientific, Lab+, Portugal) with 1 ml of TRI Reagent (Sigma-Aldrich, Madrid, Spain). After being transferred into 2 ml polypropylene tubes, all samples were allowed to stand for 5 minutes at room temperature to ensure complete dissociation of nucleoprotein complexes before adding 0.2 ml of chloroform (Merck, VWR, Portugal). Samples were shaken vigorously for 15 seconds, allowed to stand for 15 minutes at room temperature and centrifuged at 12 000 rpm for 15 minutes at 4 ºC to separate the resulting mixture into the 3 phases mentioned above. The colorless upper aqueous phase containing the RNA was transferred to 1.5 ml tubes into which 0.5 ml of isopropanol (Sigma-Aldrich, Madrid, Spain) was added and mixed. The samples were incubated for 5 minutes at room temperature and then at -20 ºC for approximately 3 h in order to ensure maximum RNA precipitation before being centrifuged at 12 000 rpm for 10 minutes at 4 ºC. The supernatant was removed and the RNA pellets were washed with 1 ml of 75% DEPC ethanol, vortexed and centrifuged again at 12 000 rpm for 5 minutes at 4 ºC. After removing the supernatant, the RNA pellets were air-dried for 15 minutes and resuspended in 100 µl of DEPC treated MilliQ® water (appendix II). The quality of the extracted total RNA was evaluated by electrophoresis on 1.5 % agarose gel (appendix III) stained with ethidium bromide. The concentration of RNA extracts was evaluated with a GeneQuant spectrophotometer (Amersham Bioscience, Lisbon, Portugal) and its purity was assessed using the ratio 260/280. Samples were utilised for analysis when the ratio 260/280 was > 1.7. The level of protein contamination and the purity of each extract were also determined.

2.8.2 RNA purification

Total RNA extracts were treated with the Ambion DNA-*free*™ (Bioportugal, Lisboa, Portugal) to eliminate genomic DNA contamination. RNA extracts (4 µg) were treated with 0.1 U/µl of rDNAse I in 0.1x volume of DNAse buffer for 30 minutes at 37 ºC in a reaction volume of 20 µl, according to the manufacturer's instructions. The enzyme was inactivated by vortexing the reaction with 0.1x volume of DNAse inactivation reagent. The solution was then centrifuged at 10 000 rpm for 1.5 minutes at 4 ºC and the DNA-free RNA transferred to a new tube.

The treatment of RNA extracts with DNAse can lead to some RNA lost, so it was necessary to repeat quantification of treated RNA before proceeding with the cDNA synthesis. A Quant-iT™ RNA Assay Kit 5 – 100 ng (Invitrogen, Barcelona, Spain) and a Qubit™ fluorometer were used for this purpose. The fluorophore used in this kit has high affinity for RNA and becomes fluorescent upon binding to it. The kit reagents stored at 4 ºC were allowed to reach room temperature and a 1/200 working solution of Quant-iT™ RNA reagent in RNA buffer was prepared. For each sample, 1 µl of RNA was diluted in 199 µl of working solution, vortexed 2–3 seconds and incubated at room temperature for 2 minutes. The RNA concentration was determined with the Qubit fluorometer by reading the fluorescence at 260 nm.

2.8.3 cDNA synthesis

RNA transcript quantification was carried out on complementary DNA (cDNA) generated by reverse-transcription of the RNA using an RNA-dependent DNA polimerase from a retrovirus. One problem with cDNA synthesis is that not all RNAs are reversed-transcribed with the same efficiency. This problem can be minimized by priming the reaction at random starting positions on the RNA.

First strand cDNA synthesis was performed using the Moloney Murine Leukemia Virus Reverse Transcriptase (MMLV-RT) procedure in a reaction volume of 20 µl containing: 500 ng of RNA, 0.5 mM dNTPs, 200 ng of random hexamers primers, 100 U of MMLV-RT and 20 U of RNAsin. First, a 13 µl solution containing 500 ng of DNAse treated RNA, 1 µl of 10 mM dNTPs and 1 µl of random hexamers primers p(dN)6 (200 ng/µl; GE Healthcare, UK) was heated for 5 minutes at 65 ºC to eliminate any secondary structure that could interfere

with the annealing step and promote the annealing of the random hexamers. Afterwards, a 7 µl mixture containing 0.5 µl of MMLV-RT, 0.5 µl of RNAsin® Plus RNase Inhibitor, 4 µl of 5x RT buffer (50 mM Tris-HCl, 75 mM KCl, 3 mM MgCl2, 10 mM DTT) and 2 µl of MilliQ water were added, all reagents from Promega (VWR, Portugal). The reverse transcription reaction took place in a Robocycler Gradient 40 well Hot Top thermocycler (Stratagene) for 10 minutes at 20 ºC and 50 minutes at 42 ºC and was stopped by heating 5 minutes at 72 ºC. A total of 57 individual reactions were done with sea bream skin samples (regenerated, intact and no scales): 21 for the Control group, 21 for the AKG group and 15 for the Placebo group. As a negative control for the reactions to confirm there was no genomic DNA contamination –RT controls were performed. For this, the reverse transcriptase enzyme was omitted from the reaction and was substituted with water.

The efficiency of cDNA synthesis was evaluated by running an amplification protocol using the reference gene 18S ribosomal RNA. A 25 µl reaction containing 1 µl of cDNA (diluted 1/10), 1.5 mM $MgCl_2$, 0.1 mM dNTPs, 2.5 pmol/µl forward primer (5'-TCAAGAACGAAAGTCGGAGG-3'), 2.5 pmol/µl reverse primer (5'-GGACATCTAAGGGCATCACA-3'), 0.5 U EuroTaq Taq DNA polimerase (EuroCLone, Italy) was run on a MyCycler thermocycler (BioRad Laboratories) with the following program: 2 minutes at 95 ºC, 25 cycles of 45 seconds at 95 ºC, 30 seconds at 59 ºC and 45 seconds at 72 ºC, followed by a final step of 5 minutes at 72 ºC to inactivate the enzyme. The reaction products were fractioned on a 1.5 % agarose gel (appendix III) stained with ethidium bromide to determine its quality.

2.8.4 Cloning of genes of interest

2.8.4.1 Database search and semi-quantitative PCR

The nucleic acid sequences of the genes of interest were obtained through database search (http://www.ncbi.nlm.nih.gov/). The data base and the respective accession number are shown in table 2.1.

Table 2. 1 - Name of the gene, accession number and database where it is localised.

Gene	Data base	Accession number
ColIα1	Genbank	DQ324363.1
SPP1	Genbank	AY651247.1

Primers for fragment amplification and cloning were designed in Primer Premier 5 (Premier Biosoft, Palo Alto, California) software and their sequence is shown in table 2.2. Semi-quantitative PCR was used to confirm the quality of synthesised cDNA and the transcript abundance of the two target genes in experimental samples before qPCR.

Table 2. 2– Primers name, sequence, amplified fragment size (base pares) and temperature of annealing for semi-quantitative PCR.

Primer name	Primer sequence	Fragment size (bp)	T_a (ºC)
Sa_ColIα1 Fw	CAAGAACCCCGCCAGAACCTGCCGC	462	60
Sa_ColIα1 Rv	AAGCGACTGTTGCCCTCGGCTCTGA		
Sa_SPP1 Fw	TTTTCGTTCTGCTCTTTGC	642	57
Sa_SPP1 Rv	CCATCTTCTTTCCTGTGCC		
Sa_18S Fw	TCAAGAACGAAAGTCGGAGG	500	59
Sa_18S Rv	GGACATCTAAGGGCATCACA		

Preliminary experiments were run to optimize the number of cycles and the annealing temperatures of the ColIα1 and SPP1 primers. The composition of the PCR reaction mix is described in table 2.3 and the thermocycle was performed in a MJ Research PTC-100 thermocycler (GMI, Inc., USA) with the following programme: 1 minute at 95 ºC, 30 cycles of 30 seconds at 95 ºC, 1 minute at the respective annealing temperature (table 2.2), 30 seconds at 72 ºC for elongation and 1 minute at 72 ºC to finalise the reaction. Negative controls without sample cDNA and the –RT control were also tested. PCR products were analyzed on a 1.5 % ethidium bromide agarose gel.

Table 2. 3 – Semi-quantitative PCR mix conditions.

PCR mix	Concentration (V_{final} = 25 µl)
$MgCl_2$ (50mM)	2 mM
Reaction buffer (10x)	1x
Fw primer (25 pmol/µl)	0.5 pmol/µl
Rw primer (25 pmol/µl)	0.5 pmol/µl
dNTPs (10mM)	0.2 mM
cDNA	1 µl
Taq (5 U/µl)	0.02 U/µl

2.8.4.2 Confirmation of fragment identity

To confirm the identity of the amplified PCR products they were sequenced before proceeding for downstream applications. The amplified fragments were purified with the kit Illustra GFX™ PCR DNA and Gel Band Purification Kit (Amersham Biosciences, GE Healthcare UK Limited) and then inserted into the cloning vector pGem-T Easy (Promega). Cloning of the fragments into the vector was done with 3 µl of purified PCR product with 0.3 µl of pGem-T Easy vector and 0.15 U/µl of T4 DNA ligase (Promega). The mix was incubated overnight at 4 ºC and competent *E. coli* transfected. In order to obtain the minipreps with the cloned PCR fragments, the method described in sections 2.5.1.1 and 2.5.1.2 was followed. Purified recombinant plasmids were sequenced with primers which initiated from the 5' and 3' of the insert of interest (CCMAR, University of Algarve, Portugal). To confirm the identity of the cloned fragments the obtained sequences were compared to those in the database using blastn (http://blast.ncbi.nlm.nih.gov/Blast.cgi?PROGRAM=blastn&BLAST_PROGRAMS=megaBlast&PAGE_TYPE=BlastSearch&SHOW_DEFAULTS=on&LINK_LOC=blasthome) followed by an alignment with the sequences used to design the primers (table 2.1) (http://blast.ncbi.nlm.nih.gov/Blast.cgi?PAGE_TYPE=BlastSearch&PROG_DEF=blastn&BLAST_PROG_DEF=megaBlast&SHOW_DEFAULTS=on&BLAST_SPEC=blast2seq&LINK_LOC). The chromatogram was also analysed in BioEdit (Hall 1999) to confirm the quality of the sequencing reaction and insert. These confirmation steps are necessary to ensure the specificity of the primers for the target template in the PCR reaction.

2.8.5 qPCR Primer Design

The sequences of the cloned fragments were used to design the primers for qPCR in Beacon Designer 7 (Premier Biosoft, Palo Alto, California) software followed by evaluation of false priming sites in Primer Premier 5 (Premier BioSoft, Palo Alto, California) software. qPCR primer design was carried out based on the following criteria: amplicons should ideally be between 50–150 bp in length to allow not only faster and more efficient reactions and increased consistency of results but also because short amplicons have a limited capability to fold. The amplicons defined by the pairs of primers were positioned inside the previous cloned fragments. Problems with the secondary structure of the template and the primers were also avoided by taking the following aspects into consideration: avoid runs of Gs longer than

3 bases that could fold template into a tetraplex structure and hinder primers from annealing and prevent complete product extension by the polymerase; avoid inverted repeats in primers or sequence complementarity at the 3' ends which could form primer-dimers or runs of Gs or Cs could cause the polymerase slippage. Primers were designed to have a melting temperature (T_m) higher than the T_m of any of the predicted template secondary structures (Kubista *et al.* 2006; Nolan *et al.* 2006; Sigma-Aldrich 2008). Primer name and sequence for qPCR are presented in table 2.4.

Table 2. 4 – Primers name, sequence and amplified fragment size (base pairs) for qPCR.

Primer name	Primer sequence	Fragment size (bp)
Sa_ColIα1 Fw	AGACCTGCGTATCCCCAACTC	110
Sa_ColIα1 Rv	GCCACCGTTCATAGCCTCTCC	
Sa_SPP1 Fw	AGGTTGCTGACAGTTCTGAGAG	130
Sa_SPP1 Rv	GCGGCTGCTGCTACAATG	
Sa_18S Fw	CGATCAGATACCGTCGTAGTTC	86
Sa_18S Rv	CCCTTCCGTCAATTCCTTTA	

2.8.6 qPCR pre-run tests

Before proceeding to the qPCR analyses, a number of optimization tests were performed to calibrate and standardize the assays. Tests aim to optimize the annealing temperature for each pair of primers, the cDNA dilution of the samples and also the standards in order to obtain valid and reproducible results with maximum specificity and sensitivity. Ideal primer concentrations for qPCR assays had already been optimized in previous studies.

The first step in qPCR optimization is the definition of the annealing temperature (T_a). Three different temperatures were tested for each pair of primers (based on the information from Beacon Designer 7 and Primer Premier 5): 55, 57 and 59 ºC. A test cDNA sample was used for this purpose. Each gene was tested on a 20 µl reaction volume containing 2 µl of cDNA, 10 µl of Power SYBR®Green PCR master mix (Applied Biosystems, UK) and 0.5 µl of forward and reverse primers (10 pmol/µl). In the no-template control, water was used instead of sample cDNA. The PCR reaction took place in a sealed 96-well PCR plate (Applied Biosystems, UK) in a StepOnePlus thermocycler (Applied Biosystems, UK) with the following programme: 10 minutes at 95 ºC to activate the Taq DNA polymerase, followed by 55 cycles of 30 seconds at 95 ºC to denature template cDNA, a 20 seconds annealing step at

the test temperatures and 30 seconds at 72 ºC for elongation. Fluorescence was measured at the end of each cycle, after the elongation step.

Since SYBR Green binding dye is a non-specific dye that detects any dsDNA, it is important to verify that only the desired product is being amplified (Sigma-Aldrich 2008). For this quality control, a melt-curve of the obtained product was done by heating the PCR product for 15 seconds at 95 ºC and, after 10 seconds at 60 ºC, temperature was gradually raised up to 95 ºC again, measuring fluorescence continuously every 0.5 ºC to detect any non specific products. The melting temperature (T_m) is defined as the characteristic temperature at which the two strands of dsDNA separate from each other releasing the fluorescent dye, providing accurate T_m data for every single amplified product. DNA melting temperature depends on both its size and nucleotide composition. The product of the amplified target can easily be distinguished from the shorter primer dimers and other small amplification artefacts because these melt at lower temperatures (Kubista *et al.* 2006; Nolan *et al.* 2006). The amplification plots and respective melt curves for the target genes can be found in figure 2.1, the assay represented is the optimization of the annealing temperature.

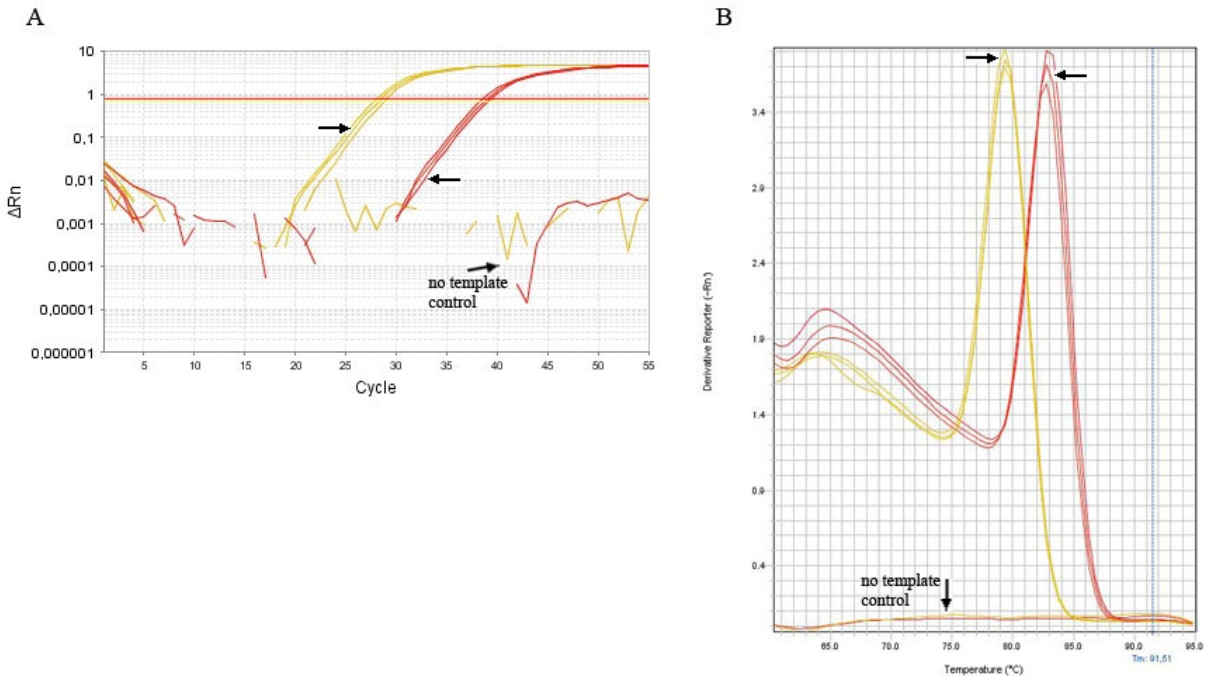

Figure 2. 1 – qPCR optimization of annealing temperatures for Collα1 (in yellow) and SPP1 (in red). Panel A shows three logarithmic amplification curves for each gene at the three different annealing temperatures. The horizontal lines represent the threshold for each gene. The no-template control had no amplification. Arrows point the curves where the amplification was more efficient (57 ºC for both genes). Panel B shows the melt curves correspondent to amplification curves in panel A. When T_m is reached, fluorescence drops abruptly because the dye is released. The melt curve showed that only one specific product was being amplified with each pair of primers.

1 µl of the obtained PCR products were fractionated on a 1.5 % agarose gel stained with ethidium bromide and the rest was purified and sequenced to confirm fragment identity (section 2.8.4.2). The optimal annealing temperature chosen for each gene was selected to give the maximum fluorescence at the lowest cycle number and a very specific melt curve.

2.8.7 Preparation of standard curve

There are different strategies to quantify samples in qPCR assays. These can be absolute quantifications or relative quantifications. In absolute quantifications a standard curve relating the C_T values with initial amounts of RNA or cDNA is produced, allowing the determination of targets in samples based on their C_T values. It is assumed that the amplification efficiency is the same in both standards and samples. In relative quantifications, sample gene expression is based on either a reference sample or a calibrator, minimising potential variation in sample preparation and handling. The quantification of target and calibrator can be done in one assay or in separate assays, depending on the level of precision required for the reaction.
In the present work, a relative quantification using the relative standard curve method (ΔC_T) was used to determine the amount of target copy number in the samples. With this method, the same sample is analysed for both the target and the reference gene and it requires the construction of two standard curves: one for the target gene and another for the reference gene (Sigma-Aldrich 2008; Wong & Medrano 2005). As the PCR efficiency in not the same in all qPCRs, the amplification efficiencies of both target and reference template are measured and a correction factor is determined to normalise the results. A ratio between the amount of target template and the reference template is then established for the same sample, a process that minimizes potential variations in sample preparation and handling, as the uncertainty of the RT reaction or differences in the amount of cDNA loaded for each sample in the assay are compensated. According to Wong and Medrano (2005), this is also the simplest method of quantification because it requires no preparation of exogenous standards, no quantification of internal controls and is not based on complex mathematics.

To verify that the recombinant plasmid containing the target template (section 2.8.4.2) behaved in a similar way to cDNA, they had to be linearized and purified. A restriction map of each cloned insert was done with BioEdit (Hall 1999) and a restriction enzyme chosen that would not cut the insert. Isolated recombinant plasmid DNA was digested at 37 ºC for 2 h in a

reaction volume of 20 µl containing 10 µl of plasmid DNA, 0.25 U/µl *Nco*I for SPP1 or 0.25 U/ µl of *Sal*I for ColIα1 and 1x enzyme buffer (Promega, VWR, Portugal). A 1.5 % agarose gel stained with ethidium bromide was used to confirm the efficiency of the linearization reaction. The linear plasmid DNA were immediately purified with the kit Illustra GFX™ PCR DNA and Gel Band Purification Kit (Amersham Biosciences, GE Healthcare UK Limited), resuspended in 50 µl of MilliQ filtered water and then quantified with the kit Quant-iT™ dsDNA BR (Invitrogen, Barcelona, Spain) in a Qubit™ fluorometer. The kit reagents stored at 4 ºC were allowed to reach room temperature and a 1/200 working solution of Quant-iT™ dsDNA BR reagent in DNA buffer was prepared. 1 µl of each linearized plasmid was diluted in 199 µl of working solution, vortexed 2–3 seconds and incubated at room temperature for 2 minutes. The DNA concentration was determined with the Qubit fluorometer by reading the fluorescence at 280 nm. Knowing the concentration of the linear DNA in the minipreps, a 10-fold dilution series was designed to extend past both the highest and the lowest expected concentration of template in the experimental samples. A first standard solution was prepared in order to have a concentration of 0.5 ng/µl; starting from this one, another 7 standards were prepared so that the working dynamic range of the assay would be: 1 ng, 100 pg, 10 pg, 1 pg, 100 fg, 10 fg, 1 fg and 100 ag. An example of a tested standard curve for SPP1 can be seen in figure 2.2.

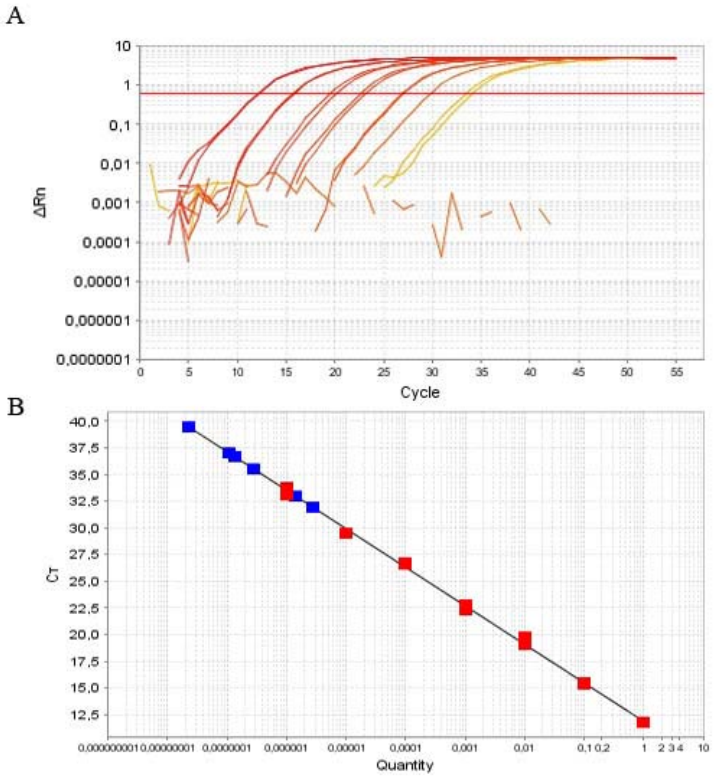

Figure 2. 2 – qPCR standard curve optimization for SPP1 gene and 5-fold test sample cDNA dilutions. Panel A shows the amplification plot of serial SPP1 standards ranging from 1 ng to 10 ag. Panel B represents the respective standard curve with the tested cDNA dilutions.

2.8.8 Preparation of cDNA dilutions

As mentioned above, the quantification of the targets in the cDNA samples is done in reference to a standard curve. So in order to assure that all the samples fit in the range of standards used and that all samples can be quantified in the same assay, a curve using serial dilutions of the test cDNA sample was also prepared. A serial 5-fold dilution series of test cDNA sample in MilliQ filtered water was tested for each pair of primers to have an idea of the amount of target represented in the samples. The cDNA dilutions tested were: 1:5, 1:25, 1:125, 1:625, 1:3125 and 1:15325. The qPCR conditions were the same as in section 2.8.6, with the chosen T_a temperatures. An example of target SPP1 quantified in this serial dilution can be seen in figure 2.2. Depending on the level of expression of the gene, the range of standards and the cDNA dilution to use can vary: if it is a highly expressed gene there is no need to use the most diluted standards; if it is a low expressed gene the cDNA can not be too diluted and the most diluted standards have to be included in the curve.

2.8.9 qPCR

After optimizing all parameters the qPCR was established and applied to the experimental samples. The optimal temperatures of annealing and cDNA dilutions used to quantify the two target genes plus one reference gene can be seen in table 2.5. Primers sequence is shown in table 2.4. qPCR mix conditions and thermo cycling were the same described in section 2.8.6.

Table 2. 5 – Optimized qPCR mix conditions, cDNA dilution and T_a for each pair of primers used.

Target gene	**ColIα1**	**SPP1**	**18S**
cDNA dilution	1:10	1:2	1:10
PCR mix	Concentration (V_{final} = 20 µl)		
Power SYBR® Green PCR master mix (2x) (Applied Biosystems, UK)	1x		
Fw primer (10 pmol/µl)	0.1 pmol/µl		
Rw primer (10 pmol/µl)	0.1 pmol/µl		
cDNA	2 µl		
T_a (ºC)	57	57	60

2.8.10 Data processing

Data from qPCR assays was acquired with the Applied Biosystems StepOne™ Real-Time PCR Software v2.0 (Applied Biosystems, UK).

2.8.11 Normalization

A reference gene has to be stably expressed independent of experimental treatment, for this reason it has to be validated for each experimental set-up. Process of normalization involves reporting the ratios of mRNA concentrations of the genes of interest to those of the reference gene (Bustin *et al.* 2009; Nolan *et al.* 2006). Ribosomal 18S was chosen and validated for the present experiment. Results are presented as relative expression of the gene given by the ratio quantity of target gene/quantity of reference gene.

2.8.12 Statistics

Differences between groups were analysed by One-way ANOVA or t-test in SigmaStat 3.1 software. Results are presented as mean ± SEM unless otherwise stated. A difference of $P < 0.05$ between means was considered to be significant.

Chapter 3

Morphological Characterization of sea bream skin and scales after oral administration of alpha-ketoglutarate (AKG)

3.1 INTRODUCTION

Alpha-ketoglutarate (AKG) is a key intermediate metabolite in the tricarboxylic acid cycle, where it determines the cycle's final rate. Outside the cycle it is also involved in amino acids metabolism. When glutamate is transaminated by BCAT it donates an amino moiety to an alpha-keto acid, forming alpha-ketoglutarate (Berg *et al.* 2002). AKG is a co-factor in the synthesis 4-hydroxyproline, which is essential for the formation of the collagen triple helix. AKG can also influence collagen synthesis by increasing the pool of proline residues *via* glutamate (Son *et al.* 2007) and this has already been demonstrated in young pigs after oral administration of AKG (Lambert *et al.* 2006). In several studies directed at understanding the role of AKG on long bone mineralization, AKG was more effective in counteracting the loss of trabecullar bone than that of cortical bone, lending support to the idea that AKG acts by promoting collagen synthesis (Harrison & Pierzynowski 2008).

Scales are thin and flexible structures imbricated in the superficial dermis below the epidermis and are located inside individual scale pockets. The presence of scales in fish skin is related to the protective functions of vertebrate integument (Mugiya 1980). Despite being a protective barrier, almost all fish lose scales during their life time and the shed scales are immediately replaced by regenerating ones. Regenerating scales grow and mineralize very quickly, which means that they need a larger quantity of calcium than those which develop during ontogeny (Bereiter-Hahn & Zylberberg 1993). Collagen type I is the major form of collagen and one of the most abundant proteins in fish skin and scales, and is normally associated with the less abundant collagen type V (Guellec & Zylberberg 1998; Yata *et al.* 2001; Zylberberg *et al.* 1992). Collagen I fibrils determine the deposition and arrangement of the calcium phosphate crystals during scale mineralization and are responsible for the plywood-like structure typical of elasmoid scales (Bereiter-Hahn & Zylberberg 1993; Sire & Akimenko 2004; Sire *et al.* 1990). The connective tissue of the dermis in the skin, also has collagen as a major component and it is responsible by the integrity and resistance of the integument (Seeley *et al.* 2001).

The present work aims at the morphological characterization of regenerated sea bream skin and scales after oral administration of alpha-ketoglutarate. Plasma levels of cortisol and estradiol were determined, as well as the levels of calcium and phosphorus in order to evaluate the physiological conditions of the experimental fish after the experimental trial. The plasma levels of two transaminases, alanine-aminotransferase (ALT) and aspartate-

aminotransferase (AST) were also determined. Tissue morphology was characterized using basic histological techniques: Masson's trichrome that allows the distinction between mineralized and non-mineralized tissue and picro sirius red staining which permits identification of different types of collagen under polarized light.

3.2 MATERIALS AND METHODS

3.2.1 Experimental animals and set up

Twenty adult sea bream (*Sparus aurata* L.) acquired from Viveiros Vila Nova (Vila Nova de Milfontes, Portugal) were divided and maintained in three 500 L conic tanks and acclimated to fresh food (commercial frozen clams) during one week (section 2.1). During this period fish were fed every morning 2% of their body weight in clams, coated with a few drops of cod liver oil. Once adapted to the fresh food, the clams were used as the vehicle to apply the desired treatments. Three experimental groups were considered, corresponding to each tank: the AKG treated group, the Placebo and the Control group – section 2.1 for details. Experiments took place over 14 days: on day 0, fish were anesthetised not only to confirm their weight (kg) and standard length (cm) but also for scale removal from the left side of the body. All fish were sampled by the end of the experiment.

3.2.2 Tissue sampling and processing

At day 14 post start of experiment, the sea bream from the 3 experimental groups were anesthetised, weighted and measured (appendix I), and a blood sample collected from the caudal peduncle which was blotted dry to avoid contamination of samples with sea water (section 2.2). The blood was immediately centrifuged for 5 minutes at 13 000 rpm to separate the plasma, which was then frozen in liquid nitrogen. Subsequently, fish were decapitated to kill them and samples of skin with regenerated scales, intact scales and skin from which scale had been removed (no scales) were collected and fixed in 4% PFA pH 7.4 for histological examination.

3.2.3 Plasma parameters

Total plasma calcium from the three experimental groups was determined using colourimetric assays with the kits, Calcium – o-C v/v (o-cresolphtalein, v/v, colorimetric; Spinreact; section 2.6.1.1) and Phosphorus – UV (Phosphomolybdate, uv; Spinreact; section 2.6.1.2). The amount of circulating cortisol and estradiol was evaluated with specific RIA (section 2.6.2).
The analysis of plasma transaminases was performed by Dr. Toni Ibarz i Vals, Department of Physiology, Universitat de Barcelona, Spain. Plasma aspartate-aminotransferase (AST; EC.2.6.1.1) and alanine-aminotransferase (ALT; EC 2.6.1.2) activities were determined as described by Gallardo *et al.* (2003).

3.2.4 General histology

To characterize skin and scale morphology, the sea bream skin samples (with regenerated, intact and removed scales) fixed in 4% PFA were decalcified for 24 h in 0.5 M EDTA pH 8, embedded in Histosec and cut into 5 µm serial sections mounted on APES coated slides (section 2.2 and appendix III). A basic haematoxylin and eosin stain (section 2.3.1) was done on every 5th slide of each block to evaluate tissue integrity and afterwards Masson's trichrome staining (section 2.3.2) was applied to distinguish between mineralized and non-mineralized tissue. Collagen fibers were distinguished with pico sirius red staining and observed under polarized light (see section 2.3.3 for details).

3.2.5 Sea bream aorta elastic recoil

The elastic recoil of the aortas was determined for all experimental groups. Aortas were cleaned to remove adhering tissues, weighted (g) in length and diameter at rest and attached at one end to a force transducer and at the other end to a metal pin on a mounting block. The tissues were then vertically suspended, in duplicate, and immersed into a chamber containing 0.15M PBS pH 7.4 (section 2.7.1) at 37 ºC. Force was measured with an FTO3 Grass Force transducer connected to a bridge amplifier. The recorded signal was adjusted to zero for un-tensioned tissue and aorta sections were then exposed to a step-wise increase in tension (0.09 N or 10 g) and then allowed to relax totally before being forced again for two more times (section 2.7.2). The fall in the recording trace that was seen immediately after the increase in

tension was measured as a degree of elastic recoil in the aorta sections. Final values are presented as mean ($N \cdot ms^{-1} \cdot mg^{-1}$ wet weight) ± SEM.

3.3 RESULTS

3.3.1 Plasma parameters

The analysis of the plasma parameters in the three experimental groups are represented in figures 3.1 and 3.2. Cortisol levels varied from 14.92 – 89.91 ng/ml in the Control group, from 3.607 – 88.47 ng/ml in the AKG treated group and from 18.51 – 74.47 ng/ml in the Placebo group.

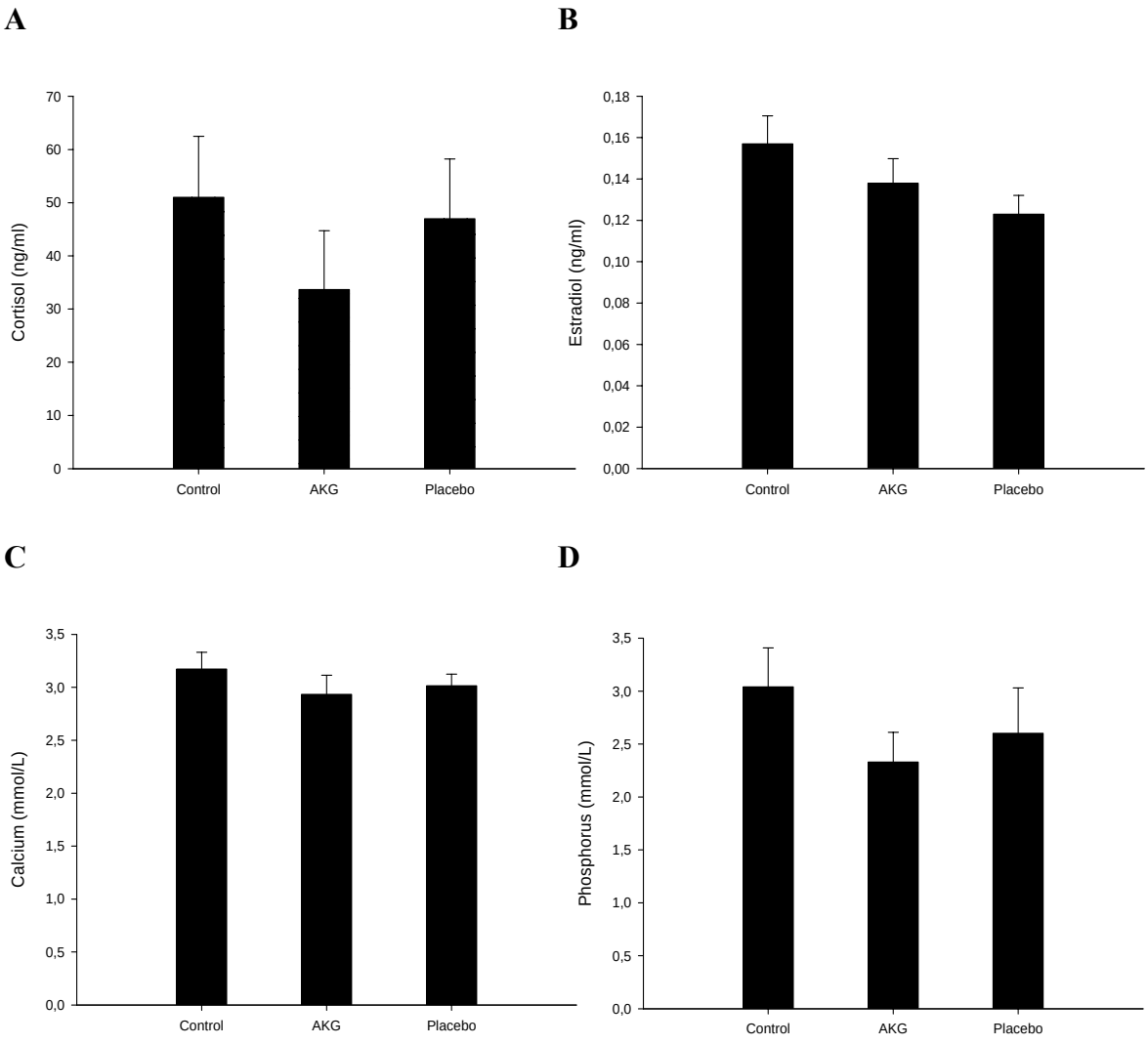

Figure 3. 1 – Plasma parameters determined for the Control (*n* = 7), AKG (*n* = 7) and Placebo (*n* = 5) groups. Results are presented as mean + SEM. **A**: Cortisol **B**: Estradiol **C**: Total calcium **D**: Phosphorus.

Estradiol levels varied from 0.115 – 0.193 ng/ml in the Control group, from 0.101 – 0.184 ng/ml in the AKG group and from 0.100 – 0.146 ng/ml in the Placebo group. The levels of the hormones cortisol and estradiol in the experimental fish were not statistically different (P = 0.516 and P = 0.181, respectively) between experimental groups and were in the normal range for adult individuals of this species.

Calcium levels varied from 2.56 – 3.92 mmol/L in the Control group, from 2.22 – 3.40 mmol/L in the AKG treated group and from 2.01 – 3.36 mmol/L in the Placebo group. The levels of phosphorus were 1.32 – 4.15 mmol/L for the Control group, 1.21 – 3.17 mmol/L in the treated group and 1.27 – 3.49 mmol/L in the Placebo group. The levels of the two ions calcium and phosphorus did not vary between experimental groups (P = 0.549 and P = 0.347, respectively) and both were in the normal range for this species.

The plasma levels of aspartate-aminotransferase (AST) and alanine-aminotransferase (ALT) in the experimental groups are represented in figure 3.2. AKG supplementation in the diet caused a significant increase in AST levels relative to the control group (P<0.05), whereas ALT activity was not modified. The transaminases activities measured were both in the normal range for sea bream.

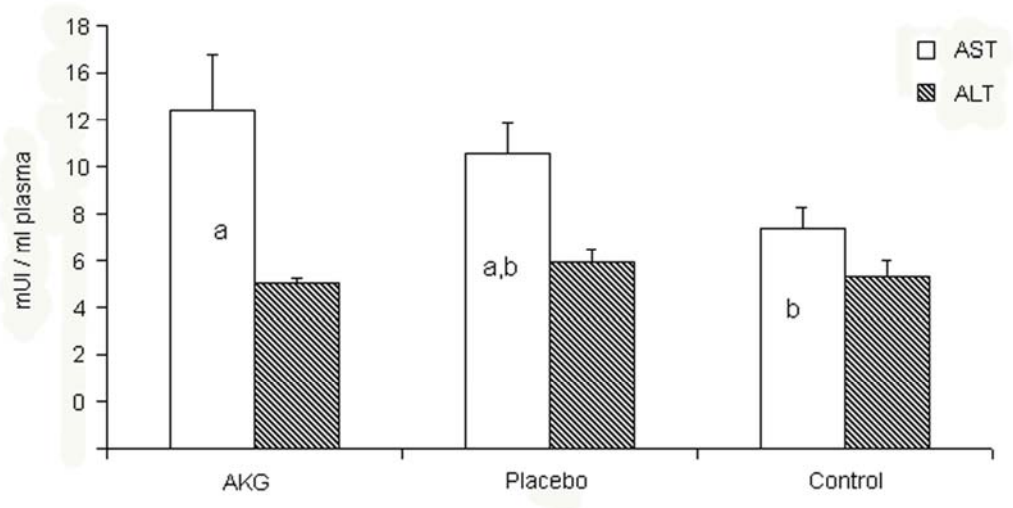

Figure 3. 2 – Transaminases in sea bream plasma samples. Plasmatic alanine-aminotransferase (ALT) and aspartate-aminotransferase (AST) from the Control (n = 7), AKG (n = 7) and Placebo (n = 5) groups. Values are shown as mean + SEM. Group differences (P<0.05) for each parameter are marked with different letters.

3.3.2 Morphology of sea bream skin

The basic structure of the intact sea bream skin and scale is represented in figure 3.3. The three layers that characterize the integument were observed: the epidermis, dermis, hypodermis and muscle. Some blood vessels could be observed in the dermis. The scale structure was as described in the literature: it was enclosed in a well defined scale pocket, with several layers of mineralized tissue forming the basal plate with its plywood-like arrangement of superimposed layers and a partially mineralized external layer where ornamentation with *circulli* could be observed.

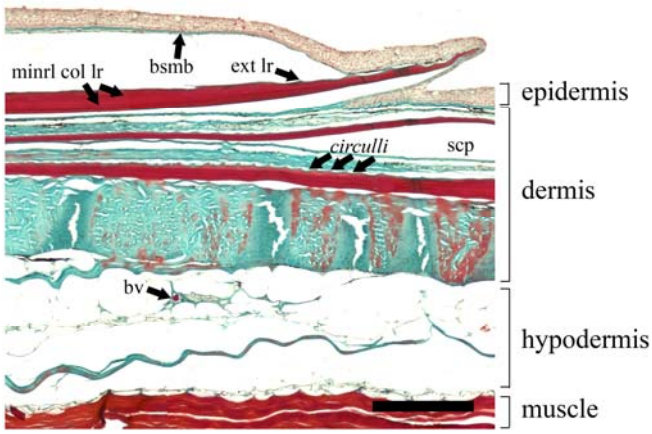

Figure 3. 3 – Transverse section of sea bream skin stained with Masson's Trichrome. The different layers that compose the integument are identified as well as some typical structures of the elasmoid scale, like the *circulli* and the superimposed collagen layers. bv: blood vessel, bsmb: basement membrane, ext lr: external layer, minrl col lr: mineralized collagen layers, scp: scale pocket. Scale bar: 200 µm.

The morphology of sea bream skin from all experimental groups is represented in figure 3.4. All pictures were taken at the longitudinal central axis of the scale. Not only the scales from unmanipulated fish and 14 days-regenerated scales are represented but also the morphology of the tissue after scale removal. The process of tissue sampling, processing and sectioning can create artefacts in the tissue which can modify the appearance of some structures. In the present case, wide scale pockets or wavy scales are artefacts common to all sea bream longitudinal and transverse skin sections. All typical skin layers were observed above the muscle: hypodermis, dermis and epidermis.

The scale in intact skin which was not manipulated in the study (original scale, figures 3.4 A, D and G) is inside an individual scale pocket, inserted in the superficial dermis and is composed of 5-7 layers of mineralized collagen sheets, as revealed by the different intensity

of staining between subsequent layers. In the posterior region of the scale, the external layer is partially mineralized. Non-mineralized *circulli* can be observed in the anterior margin of the scale, inside the scale pocket, while in the posterior margin of the scale mineralized *circulli* can be observed. In elasmoid scales, *circulli* are mineralized concentric ridges formed during scale growth that run along the margin of the scale. No *radii* (non-mineralized structures irregularly spaced along the anterior edge of the scale) were observed. Some blood vessels can be observed in the connective tissue of the dermis, above and below the scale pocket, highlighting the irrigation system of the skin. The removal of scales (figures 3.4 B, E and H) tears and damages the epidermis, the dermis and the scale pocket. The dermis and scale pocket become exposed to the ambient water and loose pieces of epidermis hang attached to the skin. No signs of inflammation were observed.

Sections of skin with regenerated scales observed 14 days after their removal (figures 3.4 C, F and I) revealed a re-established epidermis which formed a scale pocket containing a thin regenerated scale in all fish of the groups. Only 1-3 layers of mineralized collagen fibers were observed independent of the experimental treatment. An external non-mineralized matrix layer was observed above the mineralized layer of the regenerated scales, and *circulli* could already be observed in the posterior margin of the scale (figure 3.4 C). *Radii* were also not observed but folding of the epidermis could be seen. Active and cuboidal hyposquamal osteoblasts were observed in all regenerated scales and are shown in figure 3.4 F, along with elongated and less active osteoblasts. Episquamal osteoblasts were observed in some sections (images not shown). In figure 3.4 I the anchoring bundles that attach the scale to the scale pocket were evident. The thin and elongated scale pocket lining cells were not observed.

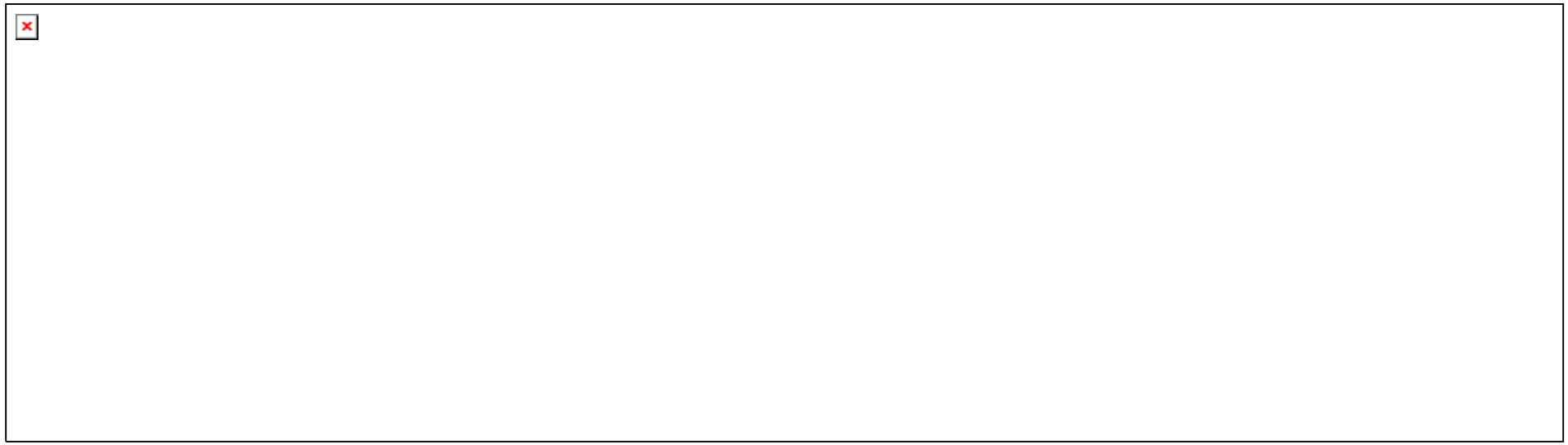

Figure 3. 4 – Longitudinal transverse sections of sea bream skin from the Control (**A-C**), AKG (**D-F**) and Placebo (**G-I**) groups, with the intact (original), missing or regenerated scales stained with Masson's Trichrome. The posterior region of the scale is orientated to the right. Tissues were partially demineralised. Connective tissue is stained green and mineralized and collagen-rich tissues are stained bright red. The three typical skin layers can be observed: the epidermis, dermis and hypodermis; muscle tissue below hypodermis is not shown for convenience. Intact scales stain bright red because of the strongly mineralized collagen layers. 14 days-regenerated scales are still poorly mineralized when compared to the intact scales and are anchored inside the scale pocket. The non-mineralized external layer of the scale can be observed in both intact and regenerated scales; in the intact scales some zones are partially mineralized. *Circulli* were observed at the posterior margin of intact and regenerated scales. anchor.bdl: anchoring bundle, bv: blood vessels, ep: epidermis, ext lr: external layer, dm: dermis, hypdm: hypodermis, hyp ostb: hyposquamal osteoblasts, minrl col lr: mineralized collagen layers, sc: scale, scp: scale pocket. Scale bars: 200 μm.

3.3.3 Collagen fibers birefringence

The natural birefringence of collagen fibers was enhanced by the sirius red staining in both the intact and regenerated scales of the three experimental groups. Representative images of these tissue conditions are shown in figure 3.5 where stained tissue sections were observed under polarized light to observe the organization of the collagen fibers in skin and scales. All pictures were taken at the longitudinal central axis of the scale, where the scale is thicker, except for the intact scale of the Placebo group, where the picture was taken close to one margin.

All scales appeared bright yellow under polarized light, demonstrating that they are mainly composed of large fibers of collagen type I. The darker layers observed in the scales correspond to the different orientation of the collagen fibers. As expected, more layers forming the typical plywood-like structure of the scales could be observed in intact scales compared to the regenerated scales.

Thin green or bluish collagen fibers were observed associated with both the superior and inferior layer of the scales. In figure 3.5 A, these fibers can be observed in the external layer of the intact scale from the Control group, lining the *circulli*. The fibres observed had the characteristics of thin reticular collagen type I fibers recently secreted or thin fibers of the minor collagen type V or type II which have also been described in teleost skin and scales. This layer of thin collagen fibers was more evident in the regenerated scales (figure 3.5 B, D and E) than in the intact scales independent of experimental groups. Similar thin bluish/green collagen fibers were also observed in the well defined basement membrane that separates and attaches the epidermis to the dermis (figures 3.5 C-F). The basement membrane from the AKG treated group seemed thicker, in both tissue conditions (e.g. intact and regenerated, figure 3.5 C and D) than the basement membrane from the other groups. In figures 3.5 C and D, a strong yellowish layer of presumptive collagen type I can be observed along at the basal side of the basal layer of cells along the basement membrane. The intensity of this was stronger in the AKG than in the Control and Placebo groups, but it is important not to forget that the intensity of a reaction is a very subjective character.

Independent of the experimental group, numerous yellow large fibers of collagen type I were observed in the dermis. The thickness of the dermis was not measured, and after a visual evaluation it did not seem different between experimental groups and tissue conditions.

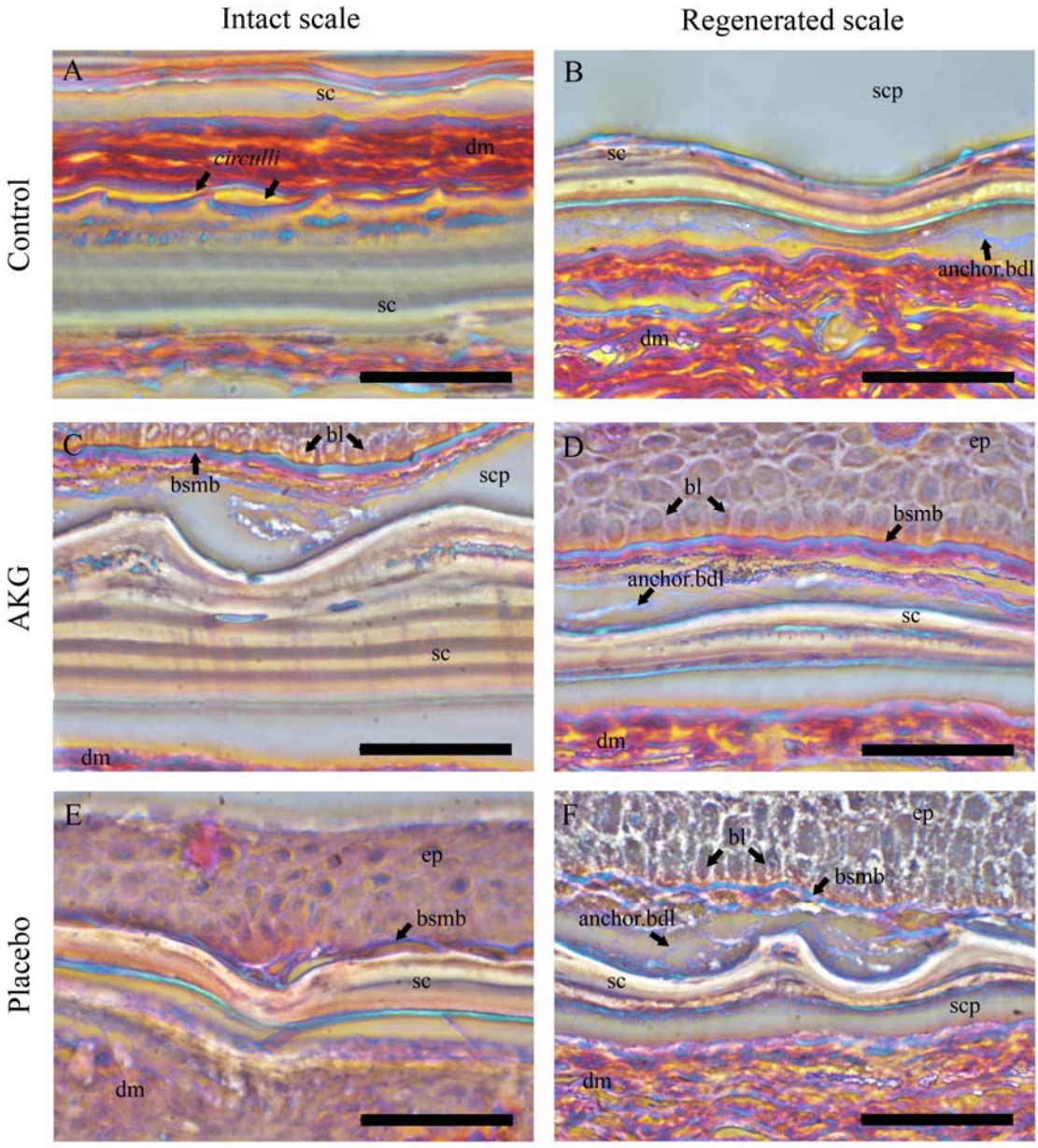

Figure 3. 5 – Transversal sections of the regenerated sea bream skin from the Control (**A** and **B**), AKG (**C** and **D**) and Placebo (**E** and **F**) groups stained with sirius red and observed under polarized light. The posterior part of the scale is orientated to the left. Thick collagen type I fibers appear yellow/orange and thinner collagen fibers, like collagen type V appear green/blue. anchor.bdl: anchoring bundles, bl: basal layer, bsmb: basement membrane, dm: dermis, ep: epidermis, sc: scale, scp: scale pocket. Scale bars: 50 µm

3.3.4 Aorta Elastic Recoil

The analysis of the aorta elastic recoil from the experimental groups is represented in figure 3.6. The elastic recoil of the Placebo group was higher than that of the Control but not statistically different (One-way ANOVA P>0.01). In the AKG treated group, the elastic recoil of the aorta was statistically different (One-way ANOVA P<0.01) and higher than that of the Control group but not the Placebo group.

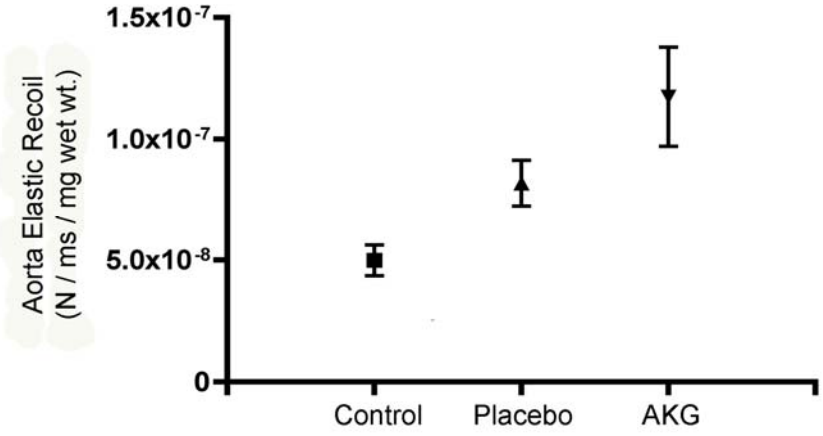

Figure 3. 6 – Aorta elastic recoil. Control (*n* = 6), AKG (*n* = 5) and Placebo (*n* = 5). Results are presented as mean ± SEM.

3.4 DISCUSSION

The influence of the oral administration of alpha-ketoglutarate was studied in adult sea bream. The composition of the treatment pills was 1000 mg AKG and 280 mg calcium. Considering that the AKG pill also had calcium, it became evident the need for a placebo group, where a similar amount of calcium was administered (1 pill = 600 mg calcium – tribasic calcium phosphate), through which the possible effects of AKG could be distinguished from the calcium effects. This separation is relevant when considering the hormonal regulation of calcium uptake and the regeneration of a mineralized tissue such as the scales. The commercial calcium pills given to the placebo group had 125 IU cholecalciferol, which promotes the uptake of calcium in the intestinal wall and could again mask the effects of the treatment with AKG. To ensure that all fish in the experiment received adequate levels of cholecalciferol, the food from the AKG treated group and control group were treated with a

few drops of cod liver oil which did not significantly alter the proximate composition of the diet but ensured a similar concentration of cholecalciferol.

3.4.1 Plasma parameters

The levels of the two hormones, cortisol and estradiol and the two ions, calcium and phosphorus were between the normal ranges for this species, and were not altered by experimental treatments. This demonstrates that oral administration of alpha-ketoglutarate and calcium is not affecting the levels of circulating cortisol, estradiol, calcium and phosphorus in adult sea bream blood. Moreover, the use of cortisol which is a common marker of stress made it possible to assess if the differences observed between experimental groups was a stress response. Plasmatic levels of cortisol have been linked to modulation of PTHrP levels in sea bream plasma (Abbink *et al.* 2004) and their regulation is calcium dependent: both cortisol and PTHrP plasma levels are higher when calcium is limited in the water or in the diet. The fact that no variation was observed in cortisol and calcium in the sea bream used in the experiment suggests their physiology was not modified by stress and the additional calcium supplied by the treatment had no significant effect on calcium homeostasis and that the differences observed in regeneration most likely resulted from AKG treatment.

In order to understand whether or not the mineralization process is influenced directly by AKG or via other factors it would be interesting to determine plasma PTHrP, the hypercalcaemic factor in teleosts (Flanagan *et al.* 2000). PTHrP is important in bone development in mammals (Miao *et al.* 2005) via its interaction with the PTH1 receptor. This receptor has been identified in scales and appears to be important in calcium turnover (Rotllant *et al.* 2005) but if it is also involved in scale regeneration remains to be established.

In teleosts, estradiol stimulates calcium resorption from scales (Persson *et al.* 1999; Persson *et al.* 1995) and this action is mediated by three different estrogen receptors (Pinto *et al.* 2009; Yoshikubo *et al.* 2005). The fact that estradiol and calcium levels were not altered after the oral administration of AKG demonstrated that apparently calcium metabolism is not altered. Recently, it was demonstrated that 17β-oestradiol significantly raised the expression of IGF-1 in the scales of the goldfish (Suzukia *et al.* 2009). It was not mentioned if IGF-1 plasma levels were also affected. Levels of IGF-1, an important factor for bone growth and remodelling in higher vertebrates, were also not determined in this study. While investigating the long-term influence of oral administration of AKG on the skeleton of lambs at slaughter, Harrison *et al.*

(2004) demonstrated that AKG increased the trabecullar and cortical bone density of the femur as well has its strength, but this positive influence seemed to be independent of the plasma concentration of IGF-1 in growing lambs. Enterally fed trauma patients with OKG revealed significant increases in circulating plasma levels of insulin, GH and IGF-1 after 4 days of continuous OKG administration (Jeevanandam & Petersen 1999). While studying the effect of OKG in reversing abnormal growth in prepubertal children receiving total parenteral nutrition (TPN), Moukarzel *et al.* (1994) reported increased concentrations of plasma IGF-1. In teleosts and higher vertebrates, estradiol and IGF-1 have the opposite effect: while in the former they stimulate mineral mobilization, in the later they stimulate mineral deposition. Despite this difference, determination of plasma IGF-1 would in the present experiment have provided important insights into another potential way in which AKG might act in sea bream.

It has recently been demonstrated that GH, when at the concentration of 100 ng/ml, stimulates osteoblastic activity in goldfish scales *in vitro* as revealed by the ~30% increase in alkaline phosphatase activity (Takahashi *et al.* 2008). The same amount of GH stimulated by ~10% the activity of osteoclasts measured by the activity of TRAP. Considering that AKG positively impacts collagen synthesis, that collagen is synthesised by osteoblasts and that GH can stimulate the activity of these cells, a similar effect of AKG on GH can not be excluded in the present study. Determination of plasma GH in the experimental fish could provide clues for this relation.

Plasmatic AST and ALT are commonly used as indicators of tissue injury. Ibarz *et al.* (2005) showed a three-fold increase in the levels of plasmatic AST in sea bream associated to cold-induced alterations in the liver and Gallardo *et al.* (2003) reported pathological levels over 600 mIU on steatotic livers. Thus, from a pathological point of view, dietary AKG did not affect significantly plasma activities of both enzymes. Transamination is the process by which the synthesis of the 10 non-essential amino acids occurs. The final products of transamination reactions are alanine, aspartate and glutamate, whose alpha-keto acids are produced by the conversion of metabolic fluids (Berg *et al.* 2002). AKG is converted to glutamate *via* either abundant amino-transaminases (alanine or aspartate) or glutamate dehydrogenase (GDH), all of which are present in the intestinal wall (Lambert *et al.* 2006). During transamination by branched-chain amino acids transferase (BCAT) glutamate donates an amino moiety to a branched-chain alpha-keto acid, forming alpha-ketoglutarate (Berg *et al.* 2002). Considering that plasmatic levels of both transaminases are normal, that AKG is mainly converted in the enterocytes to glutamate and glutamine, that dietary AKG disappeared from the lumen of the

intestinal wall but is not absorbed into the portal blood stream in young pigs and that a 60% increase in net portal proline was detected (Lambert *et al.* 2006), it seems likely that the slightly increase of AST in the present study is a response to increased concentrations of AKG in the body and its transamination into glutamate. According to Harrison and Pierzynowski (2008) there is still a mystery surrounding the origin of plasma AKG.

3.4.2 Morphology of sea bream skin

As reviewed by Bereiter-Hahn and Zylberberg (1993), when a scale is removed from its scale pocket this becomes exposed to the ambient water. Scales osteoblasts are removed along with the scale and the scale pocket appears as a long flat space lined by fibroblasts which form an endothelium-like layer, the scale pocket lining (SPL), and is filled with a gelatinous material, probably mucus. In the present work, this SPL was not observed in sea bream skin samples after scale removal probably because of the tissue manipulation. According to Sire and Akimenko (2004), undifferentiated fibroblasts initiate the formation of the papilla that will originate a new scale. These fibroblasts are recruited from the dermis to form the SPL and consequently the new scale. This is true for both, the ontogenetic and the regenerated scale. The observed pieces of epidermis attached to the underlying loose dermis had also been described after scale removal. According to Sire *et al.* (1990), they are involved in the wound-healing process that starts a few minutes after scale removal. If they are removed, re-epithelialization takes place more slowly. Since the epidermis recovery is the first step to wound healing, it should be expected that after 14 days of regeneration the epidermis was fully recovered, covering the newly enclosed scale pocket and forming a continuum with the remaining tissue.

At the papilla that will form the new scale three layers of cells start to form: a narrow space develops between the two upper cell layers and are involved in the formation of the new scale, and the inner layer remains close to the underlying *stractum compactum* and re-establishes the SPL. This differentiation is synchronous over the whole surface in contact with the regenerated epidermis ensuring that only one scale forms inside each scale pocket (reviewed by Bereiter-Hahn & Zylberberg 1993; Huysseune & Sire 1998; Sire & Akimenko 2004). The SPL do not participate in the formation of the regenerating scale. However, they are able to ensure the regeneration of a new scale if the regenerated scale is removed.

The external layer is the first to be deposited, both in the regenerated as well as in the ontogenetic scale. In some areas of the scale it becomes mineralized with scale development but it is always present and its thickness does not increase (Bereiter-Hahn & Zylberberg 1993). The process of scale mineralization starts with the production of thick collagen fibrils by the hyposquamal osteoblasts and occurs from days 4 to 9 after the beginning of regeneration and always after the formation of the external layer: the mineral deposit appears in the focus of the scale, and then extends to the peripheral areas, where *circulli* are the first loci to be mineralized. Mineral deposits of calcium phosphate salts then start to deposit above the collagen fibers, forming the calcified collagen sheets. The deposition of calcium phosphate is orientated by the collagen fibrils (Onozato & Watanabe 1979). Each sheet is oriented at a different angle from the sheet below, forming the plywood-like structure typical of elasmoid scales (Guellec & Zylberberg 1998). The angle that subsequent mineralized collagen layers form is species-specific, and information about this was not found for sea bream scales.

In the present work, the intact scales were thicker than the 14 days regenerated ones. In the regenerated scales not enough collagen sheets have been accumulated on the basal plate 14 days after scale removal to allow a clear visualization of the plywood-like structure. Two weeks after scale removal, collagen synthesis starts to decrease and the hyposquamal osteoblasts which are tall and prismatic in the early regenerated scale became thinner and similar to the ones from the ontogenetically developed scale (Sire & Akimenko 2004). In the present study, both elongated and cuboidal hyposquamal osteoblasts were observed in the regenerated scales, which suggest that the active phase of collagen production was already slowing down, hence the velocity of calcium deposition to mineralize the different layers. Previous work on European seabass (*Dicentrarchus labrax*) scale regeneration revealed a regenerated scale similar to but thinner (1-3 mineralized collagen sheets) than the ontogenetic one 15 days after scale removal (personal communication Guerreiro). Fully developed regenerated scales similar to the ontogenetic ones (5-6 mineralized collagen sheets) were observed by day 30 after scale removal (unpublished results). Considering these observations on sea bass scale regeneration and that the process of mineralization of the elasmoid scale is similar between species, it should be expected that a regenerated scale similar, both in thickness and in shape, to the ontogenetic one should be observed in sea bream skin samples from the present experiment 30 days after scale removal. Reinforcing this idea is the fact that

calcification occurs by the deposition of successive layers with progressively more layers of the fibrillary plate towards the scale center (Olson & Watanabe 1980).

3.4.3 Collagen fibers birefringence

The organization of the collagen fibers in the intact and regenerated skin and scales of sea bream was demonstrated under polarized light. In this case the intensity of the colour reflects the way in which the fibers are diffracting the rays of incident light, and this can vary according to the plan in which the light reaches the tissue. The use of circularly polarized light diminishes this variation (Whittaker *et al.* 1994). When studying skin repair in male Wistar rats in response to red polarized-laser therapy Silva *et al.* (2006) reported that changes in the collagen fibrils or in the extrafibrillar matrix can alter birefringence. If the AKG treatment had had an effect on collagen synthesis, then a higher birefringence in the treated skin and scales might be expected. The quantification of the optical path difference (OPD), a ratio between the incident/emergent light would help quantifying the real birefringence of the tissue, since it measures the retardation of the two rays of polarized light when it reaches an object (Silva *et al.* 2006).

The stronger basement membrane in the AKG treated group needs further evaluation. In what respects the role of AKG in collagen production, more information is needed in order to demonstrate that it has a positive impact on skin tissue. It would be worth quantifying the protein collagen type I in the experimental sea bream skin samples in order to evaluate the protein content of the tissue. The evaluation of the number of collagen fibers in the dermis could also help demonstrate whether or not there are more fibers in the AKG treated skin and scales.

3.4.4 Sea bream aorta elastic recoil

The present study is the first time that the elastic recoil in sea bream tissues has been quantified after alpha-ketoglutarate supplementation. The aorta is an elastic artery with a high stretching potential that helps maintain blood pressure. In fish, it is responsible for pumping the blood through a single loop throughout the body (Roberts 2001). The blood goes from the heart to gills and then to the rest of the body and back at the heart again. In blood vessels, collagen confers resistance and structure but elastin, a vital component of major blood vessels

(Rosenbloom & Cywinski 1976) has a major role in resistance to deformity and compliance. Compliance is the ability of the vessel to expand and/or contract in order to accommodate a particular volume of blood and a particular hydrostatic pressure and depends on its collagen, elastin and smooth muscle composition (http://medical-dictionary.thefreedictionary.com /blood+vessel+compliance). The hydroxylation of proline residues by P4H has been shown to play an important role not only on the stability of the collagen molecule (Son *et al.* 2007) but also of elastin (Rosenbloom & Cywinski 1976; Siddiq *et al.* 2008). Using cell cultures from chick aorta, Rosenbloom and Cywinski (1976) demonstrated that the inhibition of P4H partially inhibit procollagen but not tropoelastin secretion. It has been described that alpha-ketoglutarate increases the pool of proline residues *via* glutamate (Filip & Pierzynowski 2007) and it is also a co-factor for P4H (Son *et al.* 2007). Considering these facts, it seems reasonable to attribute the higher elastic recoil of AKG treated aortas to the stimulation of P4H, which consequently implied a higher collagen and elastin production by the tissue cells. This hypothesis needs confirmation such as histological and molecular characterization of control and AKG treated aortas and the determination of their collagen and elastin content to assess the influence of AKG.

Chapter 4

Molecular Characterization of sea bream skin and scales after oral administration of alpha-ketoglutarate (AKG)

4.1 INTRODUCTION

Alpha-ketoglutarate (AKG) participates in the tricarboxylic acid cycle. It is converted into succinate with the loss of CO_2 and formation of NADH and is a key intermediate in oxidative metabolism (Filip & Pierzynowski 2007). AKG administered as a nutritional supplement positively influences energy metabolism in the enterocytes, sparing glutamate and glutamine carbon and reducing nitrogen excretion (Lambert *et al.* 2006). AKG supplementation also leads to stronger bones in turkeys, piglets and lambs by the reinforcement of collagen deposition in trabecullar and cortical bone (Harrison *et al.* 2004; Kowalik *et al.* 2005; Tatara *et al.* 2004) but its influence on teleost mineralization processes has not been studied so far.

Scales in fish skin do not only contribute to the protective function of the integument but are also an important calcium and phosphorus reservoir which is readily available in periods of high calcium demand, such as vitellogenesis (Mugiya 1980; Persson *et al.* 1995). Recent studies on calcium mobilization from sea bream scales demonstrated that this is accomplished *via* PTH1R (Rotlland *et al.* 2005) and three estrogen receptors ERα, ERβa and ERβb (Pinto *et al.* 2009; Yoshikubo *et al.* 2005), revealing a role for PTHrP and estradiol on calcium homeostasis in teleosts. Treatment of rainbow trout *Oncorhynchus mykiss* with 17β-oestradiol raised circulating calcium levels through calcium mobilization from the scales which had a higher TRAP activity and reduced staining for calcium (Persson *et al.* 1995). Almost all fish lose their scales during their life time and the shed scales are immediately replaced by regenerating ones. Ontogenetic scales have their own dynamics of formation and grow and mineralize very fast, which means that they need a larger quantity of calcium than the ontogenetically developing ones. Remodelling of scales is carried out by osteoblasts and osteoclasts, the same cells that intervene in bone formation and resorption/remodelling in higher vertebrates. In all species the number of regenerated scales increases with age (Bereiter-Hahn & Zylberberg 1993). Extracellular matrix proteins, like collagen type I, osteonectin and osteopontin are essential in the mineralization process.

The present work is focused on the regenerated skin and scales of adult sea bream after oral administration of AKG. Proliferation processes in the skin and scales was evaluated by immunohistochemistry using antisera specific for proliferating cell nuclear antigene (PCNA) and p63, a keratinocyte stem cell marker important in stratified epithelia. The abundance of osteoclasts and osteoblasts was determined respectively by the detection of tartrate-resistant alkaline phosphatase and osteonectin. The influence of AKG on the transcription of key

matrix proteins in skin and scales, collagen type I and osteopontin were determined by qPCR and was complemented by evaluation of the pattern of expression of collagen type I and osteonectin by *in situ* hybridization. This histological and molecular approach is discussed in the context of the effects of AKG.

4.2 MATERIALS AND METHODS

4.2.1 Experimental animals and set up

Twenty adult sea bream (*Sparus aurata* L.) acquired from Viveiros Vila Nova (Vila Nova de Milfontes, Portugal) were divided and maintained in three 500 L conic tanks and acclimated to fresh food (commercial frozen clams) during one week (section 2.1). During this period fish were fed every morning 2% of their body weight in clams, coated with a few drops of cod liver oil to avoid rejection. Once adapted to the fresh food, the clams were used as the vehicle to apply the desired treatments. Three experimental groups were considered, corresponding to each tank: the AKG treated group, the Placebo and the Control group – section 2.1 for details. Experiments took place over 14 days: on day 0, fish were anesthetised not only to confirm their weight (kg) and standard length (cm) but also for scale removal from the left side of the body. All fish were sampled by the end of the experiment.

4.2.2 Tissue sampling and processing

At day 14 post start of experiment, the sea bream from the 3 experimental groups were killed with an overdose of 2-phenoxy-ethanol and skin samples (with regenerated scales, intact and no scales) were collected for both histology and RNA extraction. These skin samples were fixed in 4% PFA and liquid nitrogen, respectively. A blood vessel, the aorta, was also collected and fixed in a saline solution for elasticity analysis (section 2.2).

4.2.3 Immunohistochemical study on sea bream skin

A 3-step indirect method was used to visualize the presence of the Proliferating Cell Nuclear Antigene (PCNA), Osteonectin and p63 (keratinocyte stem cell marker) in sea bream skin (with regenerated, intact and no scales) histological sections. Three individuals from the

Control and AKG groups and two individuals from the Placebo group were used. The protocol indicated in section 2.4 was followed. Dewaxed and rehydrated sea bream skin samples were incubated overnight at 4 ºC with a dilution in TCT (appendix II) of the primary antibodies indicated in table 4.1. For some of them, it was necessary to apply heat induced epitope retrieval with 0.1M Sodium Citrate pH 6.

Table 4. 1 – Primary antibodies used in immunohistochemical study. Their origin, dilution and secondary antibody used are indicated. HIER: heat induced epitope retrieval. PCNA: Monoclonal Mouse Anti-Proliferating Cell Nuclear Antigen Clone PC10, Nº M 0879.

Antibody	Origin	HIER	Dilution	2 ^{ary} Ab
p63 (4A4): sc-8431	Santa Cruz Biotechnology Inc.	yes	1:50	Anti-mouse Ig, biotinylated species specific whole antibody (from sheep; GE Healthcare UK Limited)
Osteonectin OS-03 (A270)		no	1:3000	Anti-rabbit Ig, biotinylated species specific whole antibody (from donkey ; GE Healthcare UK Limited)
PCNA	DakoCytomation	yes	1:350	Anti-mouse Ig, biotinylated species specific whole antibody (from sheep; GE Healthcare UK Limited)

The sections were then incubated in a 1/200 dilution in PBST of the respective secondary antibody (table 4.1) for 1 h at room temperature and then with a 1/400 dilution in 0.15M PBS pH 7.2 of the complex Streptavidin – horseradish peroxidase conjugate (GE Healthcare UK Limited) for 45 minutes at room temperature. Colour was developed using diaminobenzidine tetrahydrochloride (appendix II) as the chromogen in a solution containing 0.05% DAB, 0.015% H_2O_2 in 0.15M PBS pH 7.2 for 10 minutes at room temperature. The reaction was stopped by washing sections 5 minutes in the same buffer and then dehydrated, cleared in xylene and mounted in DPX. Control reactions in which the primary antisera were omitted from the staining procedure were negative. Stained sections were analyzed using a microscope (Leica DM2000) coupled to a digital camera (Leica DFC480) and linked to a computer for digital image analyses.

4.2.4 Demonstration of TRAP activity

The presence of the Tartrate-resistant acid phosphatase (TRAP) was demonstrated according to Witten *et al.* (2001). For TRAP determination, three tissue sections from the Control and AKG groups and two tissue sections from the Placebo group were pre-incubated for 30

minutes at 20 ºC in 0.1 M acetate buffer, plus 100 mmol di-sodium tartrate, pH 5.5. TRAP was demonstrated with naphtol AS-TR phosphate (N-AS-TR-P) as substrate and hexazotized pararosaniline (PRS) (section 2.3.4). Tissue sections were counterstained with Haematoxylin and mounted with DPX. Stained sections were analyzed using a microscope (Leica DM2000) coupled to a digital camera (Leica DFC480) and linked to a computer for digital image analyses.

4.2.5 Expression of ColIα1 and SPP1 in sea bream skin and scales by qPCR

The expression of collagen type I (ColIα1) and osteopontin (SPP1) on sea bream skin with intact and regenerated scales (n = 19 for both skin/scale conditions) was studied by quantitative real-time PCR in all experimental groups: Control, AKG and Placebo. RNA was extracted from sea bream skin, DNAse treated (Ambion DNA-*free*™ kit) and 500 ng used for cDNA synthesis with 200 ng of p(dN)6 random hexamers (GE Healthcare, UK), 100 U of MMLV-RT and 20 U of RNAsin® Plus RNase Inhibitor (Promega) in a final volume of 20 µl. cDNA was synthesized in a Robocycler Gradient 40 well Hot Top thermocycler (Stratagene) for 10 minutes at 20 ºC followed by 50 minutes at 42 ºC and 5 minutes at 72 ºC. To confirm the quality and quantity of the cDNA produced, the 18S ribosomal RNA was amplified and used as an internal standard. A 25 µl reaction containing 1 µl of cDNA (diluted 1/10), 1.5 mM $MgCl_2$, 0.1 mM dNTPs, 2.5 pmol/µl forward primer (5'-TCAAGAACGAAAGTCGGAGG-3'), 2.5 pmol/µl reverse primer (5'-GGACATCTAAGGGCATCACA-3'), 0.5 U EuroTaq Taq DNA polimerase (EuroCLone, Italy) was run on a MyCycler thermocycler (BioRad Laboratories) with the following program: 2 minutes at 95 ºC, 25 cycles of 45 seconds at 95 ºC, 30 seconds at 59 ºC and 45 seconds at 72 ºC, followed by a final step of 5 minutes at 72 ºC to inactivate the enzyme. The reaction products were fractioned on a 1.5% agarose gel stained with ethidium bromide to determine its quality. DNA contamination was excluded by running a –RT reaction which came out negative, where the reverse transcriptase was excluded from the PCR.

Specific primers for sea bream ColIα1 and SPP1 were designed based on the available cDNA sequences (table 2.1) using the Beacon Designer software (Premier Biosoft, Palo Alto, California): ColIα1_Fw AGACCTGCGTATCCCCAACTC and ColIα1_Rv GCCACCGTTCATAGCCTCTCC which amplified a 110 bp amplicon and SPP1_Fw AGGTTGCTGACAGTTCTGAGAG and SPP1_Rv GCGGCTGCTGCTACAATG which

amplified a 130 bp amplicons. Both qPCRs were run on an optimized annealing temperature of 57 ºC. Quantification was performed in duplicate reactions using the SYBR Green chemistry and the relative standard curve method. qPCR reaction was performed in a final volume of 20 µl containing 1x *Power* SYBR®Green PCR master mix (Applied Biosystems, UK), 2 µl of sample cDNA and 0.1 pmol/µl of forward and reverse primers in a StepOnePlus thermocycler from Applied Biosystems (software StepOne™ Real-Time PCR Software v2.0) with the following programme: 10 minutes at 95 ºC to activate the Taq DNA polymerase, 55 cycles of 30 seconds at 95 ºC, 20 seconds at 57 ºC and 30 seconds at 72 ºC for elongation. A standard curve relating initial template quantity to amplification cycle was produced using serial dilutions of linearized plasmidic DNA containing the gene of interest (section 2.8.7 and 2.8.8). For ColIα1 qPCR, the efficiency was 89.58 %, the slope was –3.6 and the R^2 was 0.999. The melt curve performed showed single product dissociation at 79.33 ºC. For SPP1 qPCR the efficiency was 104%, the slope was –3.2 and the R^2 was 0.977. The melt curve performed showed single product dissociation at 82.81 ºC. The gene ribosomal 18S was used as the reference gene. The primers were 18S_Fw CGATCAGATACCGTCGTAGTTC and 18S_Rv CCCTTCCGTCAATTCCTTTA which amplified an 86 bp amplicons at 60 ºC in the same PCR conditions described earlier. The relative expression of both genes was established by the ratio quantity of target gene/quantity of reference gene. A difference of $P<0.05$ between means was considered to be significant when using One-way ANOVA or students t-tests.

4.2.6 *In situ* hybridization for collagen type I and osteonectin

The pattern of expression of alpha 1 - collagen type I (ColIα1) and osteonectin (OSN) in sea bream skin (with regenerated scales, intact scales and no scales) was investigated by *in situ* hybridization**.** A cDNA encoding for part of ColIα1 was ligated into the pGem-T Easy vector (Promega, VWR, Portugal; appendix IV, figure 1) and a cDNA encoding part of osteonectin was ligated in pBluescript SK(-) (Stratagene; appendix IV, figure 2). Both clones were generously conceded by Doctor Dulce Estêvão, Centre of Marine Sciences (CCMAR), Comparative and Molecular Endocrinology Group, University of Algarve, Portugal.

Digoxygenin – labelled riboprobes (section 2.5.1) were prepared by *in vitro* transcription of plasmid DNA containing full length cDNAs encoding the complete sequence of sea bream ColIα1 and osteonectin (table 2.1). The DNA was linearized at 37 ºC for 2 h and then purified

and resuspended in 20 µl of MilliQ water. The riboprobes were synthesised using this linearized DNA, 1 U/µl of the adequate RNA polimerase in 1x transcription buffer with 1 µl of Digoxigenin – RNA labelling mix (Roche Diagnostics, Mannheim, Germany), for 2 h at 37º C. Table 4.2 shows the restriction enzymes and RNA polimerases used for this synthesis. The reactions were stopped with 2 µl of 0.2M EDTA pH 8. The riboprobes were purified by lithium precipitation, resuspended in 25 µl of MilliQ water and its purity and concentration was determined by fractioning the reaction products on a 1% agarose gel stained with ethidium bromide.

Table 4. 2 – Cloning vectors, restriction enzymes, RNA polimerase and size of both probes to be analysed: *Sparus aurata* alpha 1 – collagen type I and *Sparus aurata* osteonectin.

Gene	Cloning vector	Restriction enzyme	RNA polimerase	Probe size (bp)
ColIα1	pGem-T Easy	*Nco*I	SP6	811
Osteonectin	pBluescript SK(-)	*Bgl*II	T7	400

In situ hybridization was applied to three individuals of the Control and AKG groups and to two individuals from the Placebo group. Longitudinal sections perpendicular to the surface of sea bream skin (with regenerated, intact and no scales) were pre-hybridized at 56 ºC for 2 h with hybridization solution (section 2.5.2). *In situ* hybridization (section 2.5.2) was performed overnight at 56 ºC with the same solution containing the riboprobe (2 µl probe/100 µl of hybridization solution). To remove non-specifically bound probes, high stringency washes were done at 56 ºC with 2× SSC and 1× SSC. Detection of hybridized probes was carried out with 1/600 anti-digoxigenin-AP Fab fragments (Roche Diagnostics, Mannheim, Germany), overnight at 4 ºC, and colour developed at 37 ºC for 6 h using the chromogens NBT and BCIP as enzymatic substrates. The staining reaction was stopped with 1× PBS and the sections were fixed for 15 minutes in 4% PFA at room temperature, rinsed and mounted in glycerol gelatine. Negative controls were the hybridization probe was excluded from the hybridization and hybridization solution was used instead were negative. Stained sections were analyzed using a microscope (Leica DM2000) coupled to a digital camera (Leica DFC480) and linked to a computer for digital image analyses.

4.3 RESULTS

4.3.1 Immunohistochemical characterization of sea bream skin

4.3.1.2 Proliferating Cell Nuclear Antigene (PCNA)

The PCNA antibody reacts with the nucleus of any proliferating cell. Cells from sea bream skin stained positive for the PCNA antibody in skin samples with intact and regenerated scales, independent of experimental treatment. A very high activity of PCNA was observed in all experimental groups, for this reason only the images of the regenerated scales are shown in figure 4.1. PCNA positive staining was observed in scattered cells along the epidermis; some cells surrounding the posterior margin of the scales also reacted with this antibody, suggesting they are involved in scale formation and growth. Cells from skin samples with removed scales also reacted with this antibody, but the reaction was not as strong as in the intact and regenerated scales since the epidermis was disrupted because of scale removal.

4.3.1.3 p63

Strong positive staining for p63 was observed in a linear pattern along the supra basal cells of the epidermis. Some cells located in different layers of the epidermis also reacted with this antibody. In mammals p63 is a reliable keratinocyte stem cell marker and its localisation in the supra basal layer in fish skin appears to indicate it may have a similar role in fish. No differences were observed between experimental groups or skin conditions, for this reason only the images of the regenerated skin and scales are shown in figure 4.1. p63 was not observed in the most superficial layers of the epidermis nor in any of the cell types present in the dermis.

4.3.1.4 Osteonectin

Osteonectin is a matricellular glycoprotein involved in the structural integrity of the tissues. Positive staining for osteonectin was observed in sea bream skin samples but very differently from the previous antibodies since it showed a homogeneous presence along the tissue. Osteonectin reacted strongly not only in the epidermis, in the basal layer cells along the tissue

section, but also in the dermis, in fibroblasts and osteoblasts, as shown in figures 4.1 and 4.2. Fibroblasts were scattered in the connective tissue and showed an irregular and branched cytoplasm. A very strong signal in the posterior margin of the scale pocket as well as in the blood vessels was observed. An observation common to all experimental groups was that there seemed to be more osteonectin in the intact skin/scale than in the regenerated scales.

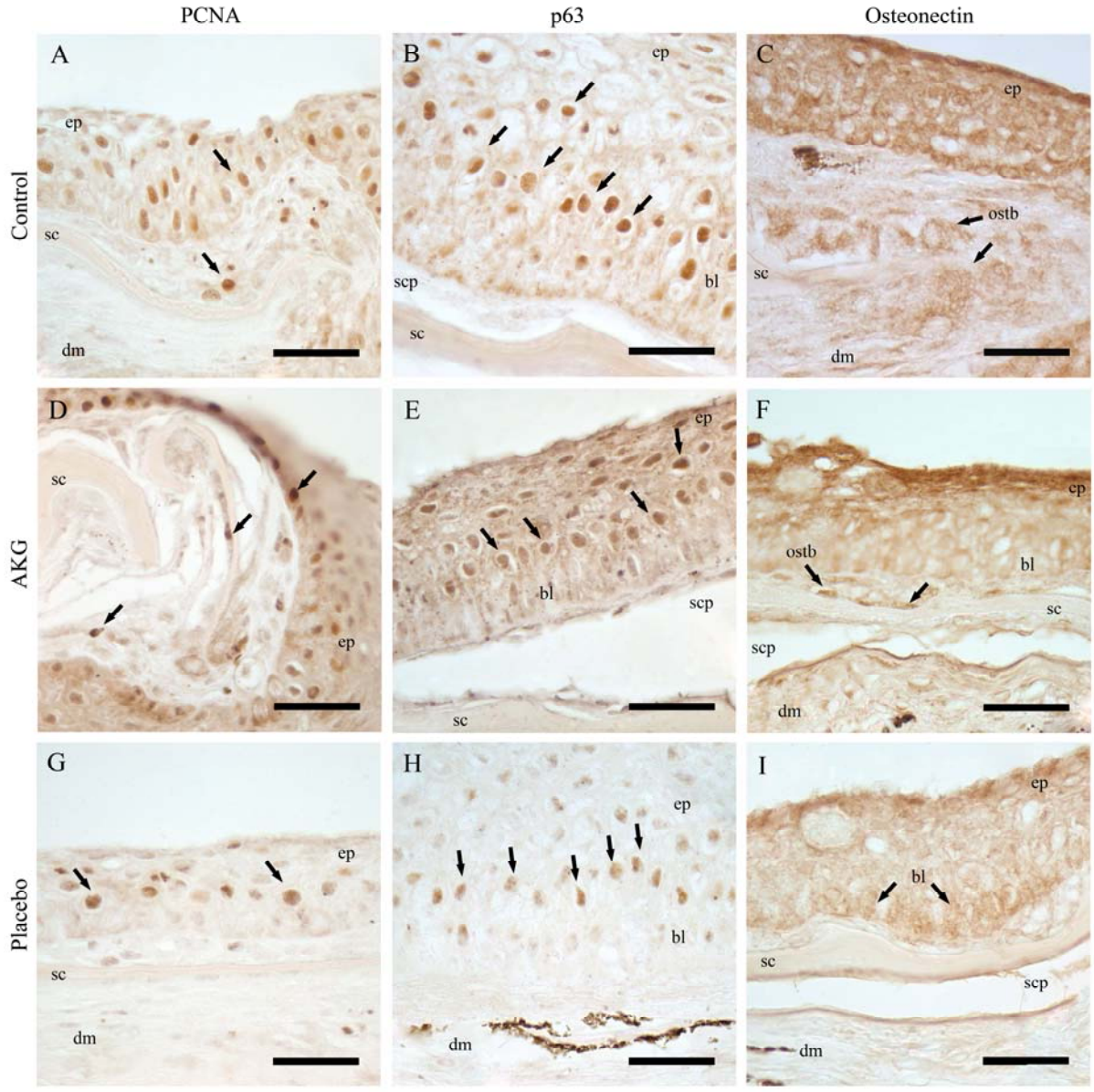

Figure 4. 1 – IHC for PCNA, p63 and osteonectin in the regenerated skin/scale of sea bream from the Control (**A-C**), AKG (**D-F**) and Placebo (**G-I**) groups. The posterior scale is orientated to the left. Clear and strong positive staining was observed for PCNA in several scattered cells along the epidermis, some cells associated to the scale, the osteoblasts also stained positive revealing their importance in scale growth and formation. p63 staining appeared in a linear pattern along the epidermis, close to the basal layer. Osteonectin was present in a homogeneous staining along the tissue; strong positive reaction was observed not only along the basal layer but also in osteoblasts. ep: epidermis, sc: scale, dm: dermis, scp: scale pocket, bl: basal layer, ostb: osteoblast. Arrows indicate cells with positive staining for the antibodies. Scale bars: 25 µm.

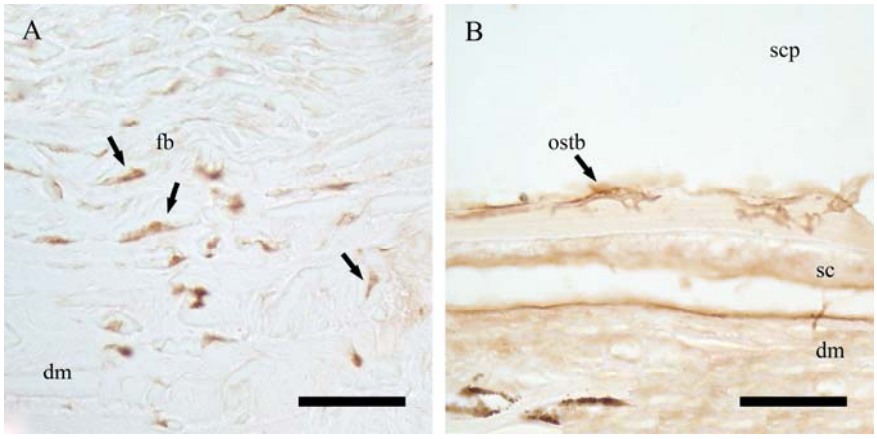

Figure 4. 2 – IHC for osteonectin in the regenerated skin/scale of sea bream from the Placebo group. **A**: Spindle and irregularly shaped fibroblasts in the dermis of sea bream skin reacted strongly with the anti-osteonectin antibody, which demonstrates that they are producing this proteoglycan. **B**: Episquamal osteoblast associated to the scale. dm: dermis, fb: fibroblasts, ostb: osteoblast, sc: scale, scp: scale pocket. Arrows indicate cells with positive staining for the antibody. Scale bar: 25 µm.

4.3.2 Expression of ColIα1 and SPP1 in sea bream skin and scales by qPCR

Two separate assays were performed with all experimental samples in order to validate the 18S as the reference gene: the differences in the threshold cycle (C_T) in the two assays were inferior to 0.5 meaning that the assays could be compared (Nolan *et al.* 2006). The first assay had a better efficiency (95%) than the second assay (87%) and its results were chosen to determine the relative expression of ColIα1. An efficiency between 90–110% is considered acceptable (Applyed-Biosystems 2008). One major drawback encountered in the validation of the qPCR assays in present work was the reference gene, ribosomal 18S. For collagen I, after log transforming the data, the relative expression of ColIα1 was higher in the intact scales of the Control and Placebo groups than in the regenerated scales and in the AKG group regenerated and intact scales showed the same level of expression of ColIα1, still no differences between groups. For SPP1, the relative expression of SPP1 was higher in the intact than in the regenerated scales of experimental groups. According to Bustin *et al.* (2009), the reference genes should be validated for each tissue or cell types and specific experimental designs. Other putative reference genes like the β-actin GAPDH will be evaluated in the near future. Despite the problems encountered the relative quantification of both genes is presented below.

4.3.2.1 Collagen type I (ColIα1)

The threshold cycle (C_T) and the quantities obtained from the qPCR assay are represented in table 4.3. The mean, standard error of the mean, maximum and minimum C_T and starting quantity values for each tissue condition and experimental group are presented. When comparing similar tissues (e.g. intact and regenerated) between experimental groups, no differences were observed for either the C_T (P = 0.656 and P = 0.153 for the intact and regenerated scales, respectively) or the amplicon quantity (P = 0.448 and P = 0.235 for the intact and regenerated scales, respectively).

Table 4. 3 – Raw data from the qPCR for collagen type I. The mean threshold cycles (C_T) and quantities (ng/µl) for the experimental groups and tissue condition are shown, along with the maximum and minimum values and SEM. C: Control, AKG: treatment with alpha-ketoglutarate and Pcb: Placebo groups. Osc: original scale, Rg: regenerated scale.

	C_T				Quantity (ng/µl)			
Group / Tissue	**Maximum**	**Minimum**	**Mean**	**SEM**	**Maximum**	**Minimum**	**Mean**	**SEM**
C Osc	20.94	18.84	19.77	0.238	0.0271	0.00705	0.0159	0.00226
C Rg	20.67	19.43	20.08	0.179	0.0186	0.00839	0.0127	0.00151
AKG Osc	20.88	18.69	19.44	0.354	0.0298	0.00752	0.0209	0.00351
AKG Rg	22.09	19.60	20.68	0.328	0.0166	0.00336	0.0094	0.00185
Pcb Osc	20.63	18.99	19.42	0.308	0.0245	0.00859	0.0199	0.00295
Pcb Rg	20.82	19.47	19.99	0.236	0.0180	0.00762	0.0135	0.00180

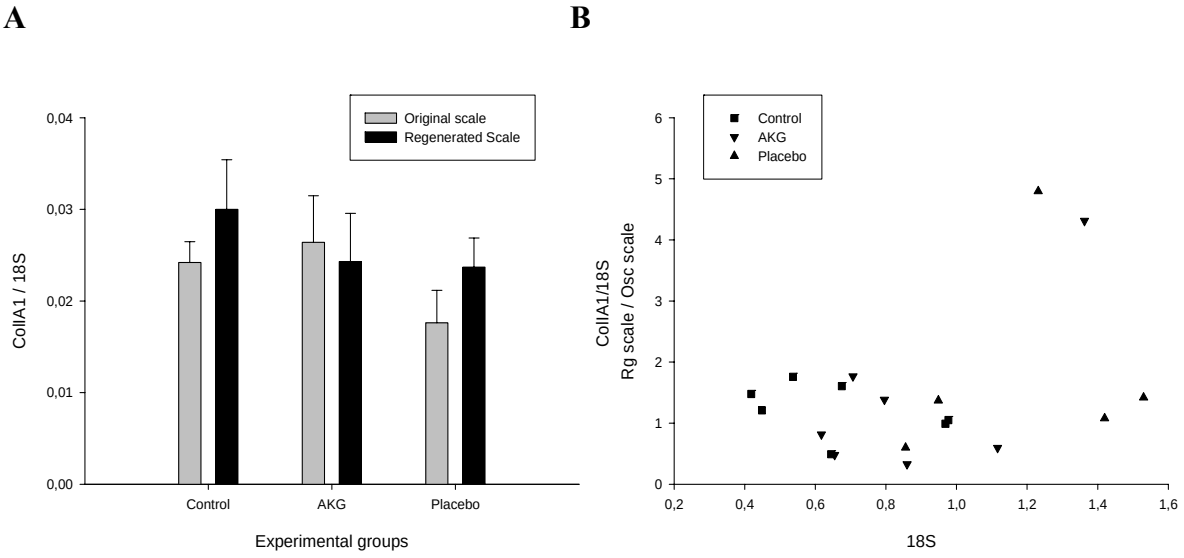

Figure 4. 3 – Expression of sbColIα1 in sea bream skin and scales (intact and 14 days regenerated) from the Control (n = 7), AKG (n = 7) and Placebo (n = 5) groups. **A**: Relative expression of ColIα1 in the intact (grey) and regenerated (black) scales of the three experimental groups. Results are presented as group mean + SEM. **B**: Individual variation represented by the ratio regenerated scale/intact scale based on the relative expression of ColIα1.

When comparing different tissues (e.g. intact and regenerated) in the same experimental treatment, no differences were observed for both the C_T and the amplicon quantity in the Control (P = 0.324 and P = 0.261, respectively) and the Placebo (P = 0.181 and P = 0.101, respectively) groups. The differences in the C_T`s and the quantities from the intact and regenerated scales were statistically different (P = 0.024 and P = 0.013, respectively) in the AKG treated group.

The relative expression of sea bream collagen type I in sea bream skin and scales is represented in figure 4.3 A. The levels of relative expression were not log transformed. When comparing ColIα1 expression in the intact scale between groups, the AKG group showed the higher level of relative expression (group mean = 0.0264±0.00509), but this was not different from the Control and Placebo groups (group mean = 0.0242±0.00226 and 0.0176±0.00355, respectively, P = 0.327). Considering the relative expression of ColIα1 in the regenerated scales between groups, the Control group showed the highest relative expression (group mean = 0.030±0.00541) but it was not statistically different from the AKG and Placebo groups (group mean = 0.0243±0.00526 and 0.0237±0.00318, respectively, with P = 0.625). When comparing the ColIα1 relative expression between intact and regenerated scales inside each group it can be observed that in the Control and Placebo groups the expression of ColIα1 was higher in the skin with regenerated scales than in the skin with intact scales, but this apparent difference was not statistically significant (P = 0.344 and P = 0,236, respectively). In the AKG group, the expression of ColIα1 was lower in the regenerated than in the intact skin, but this difference was not significant (P = 0.782).

The same fish in the experiments was the source of regenerated scales and intact scales and so analysis could be carried out on an individual by individual analysis. The individual variation in relative ColIα1 expression in each group is represented in figure 4.3 B. The ratio between ColIα1 relative expression in the regenerated and intact scales in the same fish varied between 0.490 – 1.759 in the Control group with a mean value of 1.226±0.163. In the AKG group the variation ranged from 0.327 – 4.313 with a mean value of 1.383±0.526 and in the Placebo group the range was 0.599 – 4.796 with a mean value of 1.853±0.750. In the Placebo group the individual variation was higher than in the other two groups, as revealed by the wider dispersion of the values meaning that there is a higher individual variation after oral administration of calcium. The Control and AKG group tended to cluster close to each other. Despite these differences, no statistical differences (P = 0.678) between the experimental groups were observed.

4.3.2.2 Osteopontin (SPP1)

The threshold cycle (C_T) and the quantities obtained from the qPCR assay are represented in table 4.4. The mean, standard error of the mean, maximum and minimum C_T and starting quantity values for each tissue condition and experimental group are presented.

Table 4. 4 – Raw data from the qPCR for osteopontin (SPP1). The mean threshold cycles (C_T) and quantities (ng/µl) for the experimental groups and tissue condition are shown, along with the maximum and minimum values and SEM. C: Control, AKG: treatment with alpha-ketoglutarate and Pcb: Placebo groups. Osc: original scale, Rg: regenerated scale.

	C_T				Quantity (ng/µl)			
Group / Tissue	**Maximum**	**Minimum**	**Mean**	**SEM**	**Maximum**	**Minimum**	**Mean**	**SEM**
C Osc	30.69	26.74	27.99	0.586	0.000104	0.00000622	0.0000571	0.0000146
C Rg	28.09	26.25	27.14	0.274	0.000147	0.0000393	0.0000870	0.0000163
AKG Osc	30.03	25.45	27.09	0.580	0.000260	0.00000996	0.000115	0.0000311
AKG Rg	29.79	25.88	27.88	0.502	0.000192	0.0000117	0.0000667	0.0000237
Pcb Osc	28.13	25.85	27.16	0.525	0.000196	0.0000383	0.000102	0.0000368
Pcb Rg	27.25	26.60	26.91	0.130	0.000114	0.0000720	0.0000935	0.00000864

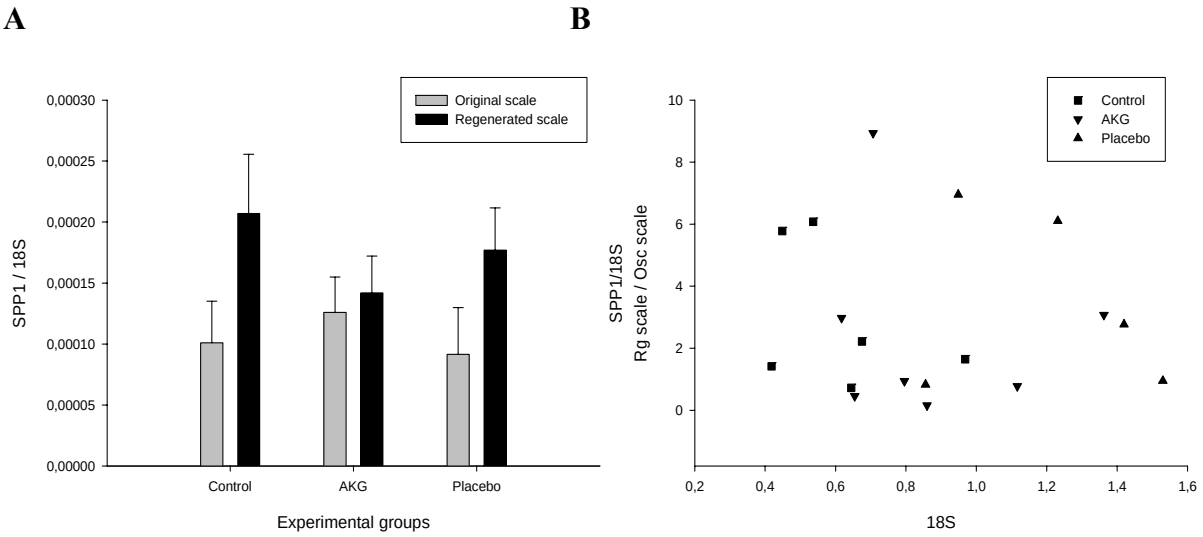

Figure 4. 4 – Relative expression of sbSPP1 in sea bream skin and scales (intact and 14 days regenerated) from the Control (n = 6), AKG (n = 7) and Placebo (n = 5) groups. A: Relative expression of SPP1 in the intact (grey) and regenerated (black) scales of the three experimental groups. Results are presented as group mean + SEM. B: Individual variation represented by the ratio regenerated scale/intact scale based on the relative expression of SPP1.

When comparing the same tissue condition between experimental groups, no differences were observed for both parameters the C_T (P = 0.482 and P = 0.192 for the intact and regenerated scales, respectively) and the amplicon quantity (P = 0.337 and P = 0.592 for the intact and

regenerated scales, respectively). When comparing the two tissue conditions inside each experimental group, no differences were observed for both the C_T and the amplicon quantity. This was true for all experimental groups: Control (P = 0.192 and P = 0.207, respectively), AKG (P = 0.327 and P = 0.238, respectively) and Placebo (P = 0.657 and P = 0.829, respectively).

The relative expression of sea bream osteopontin in sea bream skin and scales is represented in figure 4.4 A. The levels of relative expression were not log transformed. When comparing SPP1 expression in the intact scale between groups it can be observed that the AKG treated group showed a higher level of expression (group mean = 0.000126±0.0000289) than the Control (group mean = 0.000101±0.0000341) and Placebo (group mean = 0.0000916±0.0000383) groups, but this difference was not statistically significant (P = 0.742). When comparing SPP1 relative expression in the regenerated scales between groups, the Control group demonstrated the highest expression of SPP1 (group mean = 0.000207±0.0000486). In the AKG group SPP1 expression in the regenerated scales was the lowest observed (group mean = 0.000142±0.0000301). Despite the differences in the group mean values, no statistically significant differences were observed between the regenerated scales of the experimental groups (P = 0.494). When comparing SPP1 relative expression between intact and regenerated scales inside each group it can be observed that in all experimental groups SPP1 expression was higher in the regenerated than in the intact scales. Despite this, no statistical differences were observed inside the groups: Control with P = 0.112, AKG with P = 0.720 and Placebo with P = 0.137.

The individual variation in relative SPP1 expression in each group is represented in figure 4.4 B. The ratio between SPP1 relative expression in the regenerated and intact scales varied between 0.720 – 6.079 in the Control group with a mean value of 2.975±0.955. In the AKG group the variation ranged from 0.158 – 8.937 with a mean value of 2.475±1.166 and in the Placebo group the range was 0.828 – 6.949 with a mean value of 3.518±1.282. In the Placebo group the individual variation was higher than in the other two groups, as revealed by the wider dispersion of the values. The Control and AKG group tended to cluster close to each other. Despite these differences, no statistical differences (P = 0.817) between the experimental groups were observed.

4.3.3 Cells involved in mineral turnover in sea bream scales

The pattern of expression of ColIα1 and Osteonectin was studied by *in situ* hybridization and the results are shown in figure 4.5. For convenience, only the results from the regenerated scales are shown, but the same was observed for the intact scale independent of experimental treatment. A strong positive reaction for ColIα1 probe was observed in the anterior and posterior margins of the scale pockets in the cells associated to the scales as well as to the cells located above and below the scales (figure 4.5 A, D and G). These observations were true for the intact and regenerated scales of all experimental groups but were not observed in the samples with no scales (images not shown), probably because they were removed along with the scale. Osteonectin was also present in the same cells as ColIα1 (figure 4.5 B, E and H). It was observed in the anterior and posterior margins of the scale pocket and in the cells above and along the scale in all experimental groups. Osteonectin and ColIα1 are commonly used as markers of osteoblastic activity. In some tissue sections osteonectin was observed in the cells below to and associated to the intact scales, these were cuboidal in the Placebo group and more elongated in the Control group. The same was not observed in the AKG group for osteonectin. Osteonectin was also observed in the basal side of basal layer cells from the epidermis. Positive cells for osteonectin in the basal layer were observed along the epidermis, immediately above the scale pockets. This reaction was stronger in the regenerated than in the intact scales independent of experimental group. Basal layer cells in the reminiscent epidermis from the samples with no scales also stained positive for osteonectin, but this reaction was less intense than in the other skin conditions and was independent of experimental treatment (images not shown).

TRAP was demonstrated in sea bream skin/scales sections and images of the regenerated scales for all experimental groups are shown in figure 4.5 C, F and I. TRAP is demonstrated by the typical red precipitate that forms in the presence of naphtol and was observed in mononuleated cells associated to the scale suggesting that these might be osteoclasts. TRAP was not present in all stained tissue sections, it was observed in some cells of some sections which revealed that their presence is not homogeneous along the scale. Osteoclasts were observed at the posterior margin of the scale pocket, above and below the scale, and also at the posterior margin of the scale. These cells were not observed in the anterior margin of the scale pocket in any section analysed. No differences were observed between groups in what respects the demonstration of TRAP activity in intact and regenerated scales.

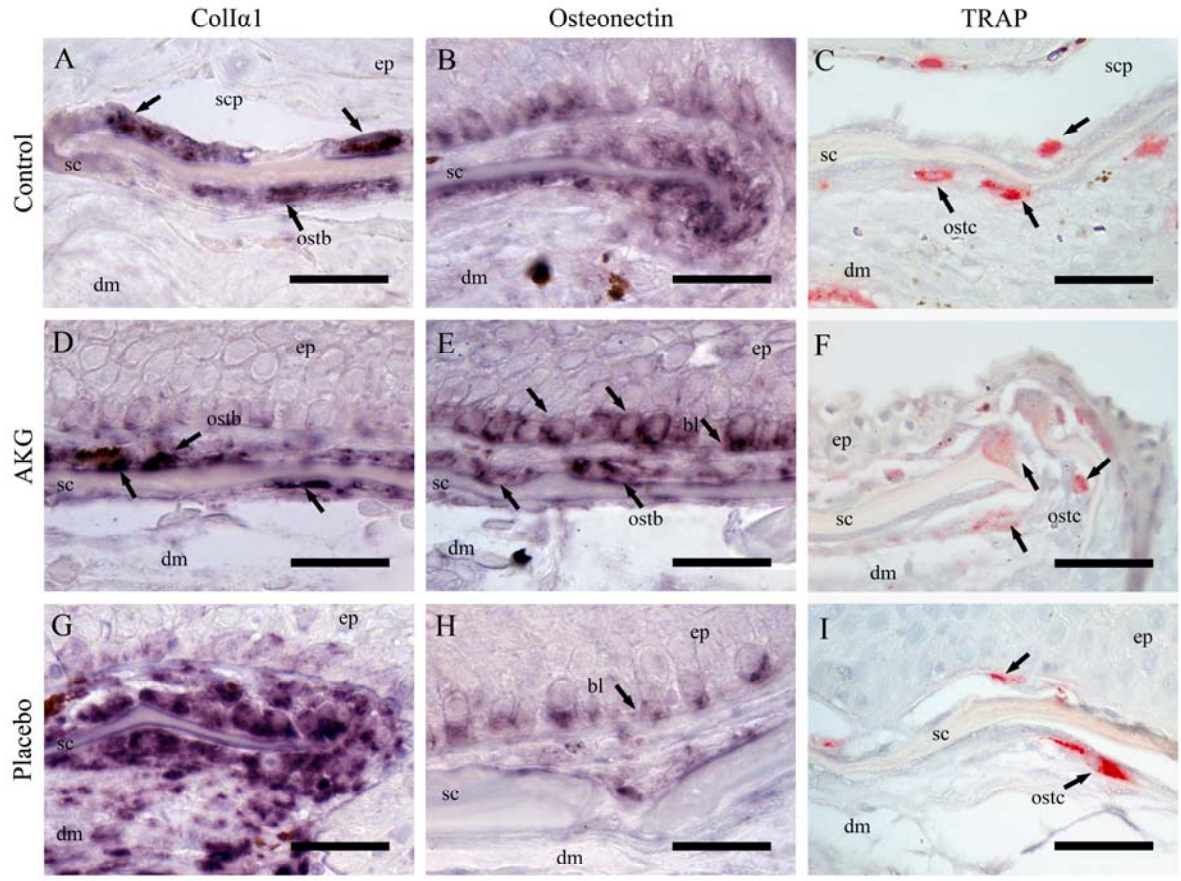

Figure 4. 5 – ISH with DIG-labelled riboprobes for sbColIα1and sbOSN and demonstration of TRAP in the regenerated skin/scale of sea bream from the Control (**A-C**), AKG (**D-F**) and Placebo (**G-I**) groups. Posterior scale is orientated to the right. bl: basal layer, dm: dermis, ep: epidermis, ostc: osteoclast, ostb: osteoblast, sc: scale, scp: scale pocket. Arrows indicate cells with positive staining with the probes and TRAP coloration. Scale bars: 25 μm.

4.4 DISCUSSION

The influence of the oral administration of AKG was studied in adult sea bream. The composition of the treatment pills was 1000 mg AKG and 280 mg calcium. Considering that the AKG pill also had calcium, it became evident the need for a placebo group, where a similar amount of calcium was administered (1 pill = 600 mg calcium – tribasic calcium phosphate), through which the possible effects of AKG could be distinguished from the calcium effects. This separation is relevant when considering the hormonal regulation of calcium uptake and the regeneration of mineralized tissues, such as the scales. The commercial calcium pills had 125 IU cholecalciferol, which promotes the uptake of calcium in the intestinal wall and could again mask the effects of the treatment with AKG. To

minimize this hypothesis, the food from the AKG treated group was pulverised with a few drops of cod liver oil. The same was true for the Control group.

4.4.1 Immunohistochemical characterization of sea bream skin

Proliferating cell nuclear antigene (PCNA, DakoCytomation) is a multifunctional 36kDa protein essential for the progression through the cell cycle, especially for the transitions from the G1 to the S phase. In teleosts, the intermediate stratum of the epidermis is composed of cells that remain mostly undifferentiated, serving as a reservoir to replace dead cells in each of the epidermis regions and can divide rapidly when necessary, like wound healing for instance (Guellec *et al.* 2004; Quilhac & Sire 1999). The presence of PCNA in scattered cells of different layers of the epidermis reflects the normal functioning of this skin layer in the experimental groups independent of experimental treatment at 14 days after scale removal. At the posterior margin of the scales, the few PCNA positive cells associated to the scale indicate the presence of proliferating cells. These marginal cells have been described as being responsible for the enlargement of the ontogenetically and regenerated scales (Bereiter-Hahn & Zylberberg 1993) and the presence of actively dividing cells in this region confirms this idea.

p63 is a p53 homologue, whose gene product act as a negative regulator of cell growth in response to DNA damage (Santa Cruz Biotechnology, Inc.). p63 is essential for several aspects of ectodermal differentiation during mice embryogenesis, but the same is not true for p53: mice lacking p53 are developmentally normal, suggesting that p53 homologues might compensate for its function during embryogenesis (Mills *et al.* 1999). Knock out mice for p63 are born alive but with severe developmental defects that causes extreme water loss and death after a few hours: the apical ectoderm ridge does not differentiate which causes the limbs to be truncated or absent, the skin is not stratified and does not express markers of differentiation like keratin 1 and 14, and structures dependent upon epidermal-mesenchymal interactions (like hair follicles, teeth and mammary glands) are also absent. Given the importance of p63 in stratified epithelia, its presence in the skin of sea bream might be related to the lack of differentiation reported for the cells in teleosts epidermis (Guellec *et al.* 2004): undifferentiated cells serve as a reservoir to replace dead cells in each of the epidermis region. The maintenance of this undifferentiated state could be attributed to the presence of p63, has it has been described for normal human skin (Reis-Filho *et al.* 2002). A progressive reduction

of p63 levels from basal to supra-epidermal cells was observed in the present experiment independent of experimental treatment or tissue condition and is in accordance to what was previously reported for normal human and rat skin (Mills *et al.* 1999; Reis-Filho *et al.* 2002). The pattern of expression of osteonectin was the same in the intact and 14 days regenerated scales, being the signal stronger in the intact scales independent of experimental treatment. Despite the fact that earlier stages during scale regeneration were not studied, the results obtained suggest that osteonectin might be more important for the structural integrity of the adult skin and scale than during the process of scale regeneration, where a weaker reaction with the antibody was observed. The role of osteonectin as an important matricellular protein in several tissues has been described.

4.4.2 Cells involved in mineral turnover in sea bream scales

The presence of collagen type I and osteonectin in the same cell type associated to the sea bream scales makes it possible to identify putative osteoblasts. Several studies on elasmoid scale growth and regeneration have shown that the same cells involved in tetrapodes bone deposition and remodelling are also present in fish scales. The episquamal osteoblasts in sea bream scales 14 days after scale removal were thin and flattened cells observed mainly at the anterior and posterior margins of the scale. At the posterior margins, episquamal osteoblasts were aligned along the *circulli* and these observations had already been described for other teleost species (Bereiter-Hahn & Zylberberg 1993). The morphology of episquamal osteoblasts might reflect their function: they are more involved in extracellular matrix deposition than in the mineralization process, so they continuously produce proteins and glycoproteins that are deposited in the scale external layer. In figure 4.2 B, an image of an episquamal osteoblast reacting with the osteonectin antibody is shown. Its morphology can be clearly observed and is similar to the thin and elongated fibroblast from which it originated. Several rounded osteoblasts observed at the posterior margin of the scales (figures 4.5 B and G) reacted strongly with the sbOSN and sbColIα1 riboprobes but the reaction with the sbOSN antibody was not so strong (figure 4.1 C, F and I). These osteoblasts form a rim enclosing the scale edge and ensure the increase in diameter of the scale, which helps explaining why they are producing ColIα1 and OSN that are then secreted to the external layer. Some of these cells had the apico-basal axes obliquely orientated towards the growing edge of the scale. According to Bereiter-Hahn & Zylberberg (1993), the morphology of these marginal

osteoblasts in the regenerated scales differs from the ontogenetic ones. In the present work, differences in morphology between the marginal osteoblasts from the regenerated and ontogenetic scale were not observed. The presence of ColIα1 and ColVα1 in episquamal and hyposquamal osteoblasts was demonstrated by Guellec and Zylberberg (1998) in the scales of the goldfish. The episquamal osteoblasts showed a higher synthetic activity only in the first stages of regeneration.

The hyposquamal osteoblasts were thin and flattened cells observed along the scale but not always forming a continuum on the inner surface. Taking into account the morphology of the cells, these hyposquamal osteoblasts were, at 14 days after scale removal, similar to the hyposquamal osteoblasts from the ontogenetic scales, since according to Bereiter-Hahn and Zylberberg (1993) the hyposquamal osteoblasts from the early regenerating scale and during ontogeny are tall and prismatic and actively producing the collagen that will form the plywood-like structure. The strongest phase of mineralization of the regenerated scale occurs during the first two weeks after scale removal, which explains why hyposquamal osteoblasts are tall and prismatic during this phase and then become more flattened as collagen synthesis diminishes. Hyposquamal osteoblasts are unable to change their position and arrangement as isolated cells do.

It has been shown that TRAP activity can be used as a marker for osteoclastic activity in fish scale tissue, as reported for mammalian bone (Persson *et al.* 1995; Suzuki *et al.* 2000; Witten 1997). In the present study, the TRAP activity was located in distinct intracellular granules in some cells, which is consistent with what has been previously described for *Oreochromis niloticus* bone (Witten 1997). Teleosts osteoclasts have been described as being mainly mononucleated cells and this is the case in sea bream, although multinucleated cells have been observed associated with the bone in some species. Osteoclasts are involved in scale mineral turnover and the observed scattered presence along the scale suggests that they are only present in places where mineral turnover is necessary. This turnover might be important in controlling the scale shape as it is being formed (Pinto *et al.* 2009; Yoshikubo *et al.* 2005) not only in the intact but also in the regenerated scales. Despite the dynamics of the regeneration process, the ontogenetic scale has its own dynamics, as it is being re-shaped or maintained in the integument which is constantly exposed to the environmental water. In their studies with electron microscopy, Sire *et al.* (1990) demonstrated that in several species of teleosts fish bone osteoclasts under normal and experimental conditions were morphologically similar to those of higher vertebrate's: a ruffled border was present, along with numerous

vacuoles, lysosomes and mitochondria, extensive Golgi zones and numerous vacuoles located near the resorption area. With standard histological techniques such as those used in the present study it is very difficult to observe if the osteoclasts in sea bream scales have a ruffled border as the one in higher vertebrate's osteoclasts. Large globular multinucleated osteoclasts located in both sides of the scale have been described for *Eigenmannia virescens* under light-microscopical observations (Sire *et al.* 1990). The fact that small rounded mononucleated osteoclasts were observed on both surfaces of intact and regenerated scales reinforces the idea that scale reshaping or remodelling can occur both in the external layer and in the lamellar collagenous plates. In *O. niloticus* bones considerable evidence exists that TRAP is released into the subosteoclastic resorption zone in spite of the lack of a ruffled border, since this cell structure was not observed with transmission electron microscopy (Witten 1997).

4.4.2.1 Interaction between epidermis and dermis

The basal layer cells of the epidermis reacted strongly with the sbOSN riboprobe and the anti-sbOSN antibody (figures 4.5 B, E, H and figure 4.1 I, respectively), meaning that they are actively synthesizing and secreting osteonectin. Basal epidermal cells have been shown to be actively involved in protein synthesis and morphological data on zebrafish suggests that the skin is already pre-patterned at the onset of scale initiation: *sonic hedgehog* starts to be expressed in the basal epidermal cells immediately after the formation of the papilla, above the developing scale, and is continuously expressed in a crescent population of cells at the posterior margin of the scale since then (Sire & Akimenko 2004). The preceding study demonstrated that the basal epidermal cells use the signalling molecule *shh* to regulate scale forming cells in the regions that are in close relationship with the epidermal cover. In *Hemichromis bimaculatus* and in the zebrafish the developmental sequences strongly suggest that the cells of the basal layer of the epidermis are involved in the deposition of the limiting layer, meaning that this tissue could contain epidermal products (elasmodin) (Huysseune & Sire 1998; Sire & Akimenko 2004). A slight reaction with the sbColIα1 riboprobe was also observed in the basal cell layer of the epidermis in all experimental groups (figure 4.5 D and G), in the regenerated and ontogenetically developed scales. Considering that OSN and ColIα1 are observed in the basal cell layer of the epidermis and that the scale limiting layer is not yet present in the 14 days regenerated scale, it wouldn't be surprising that these cells could be contributing to the reinforcement of the basement membrane that separates the

epidermis from the dermis in adult sea bream, assuring the resistance and integrity of the skin. It is true that the limiting layer of the scale is only observed in the matured scales and forms late in the process of scale regeneration, but that the basal layer of cells from the epidermis is involved in this process seems unlikely since at 14 days of regeneration the scale is already enclosed in the scale pocket and covered by the vascularised connective tissue of the upper dermis. One of the main functions of this single cell layer it to keep the epidermis attached to the underlying dermis by means of anchoring structures (hemidesmosomes) attached to the basement membrane (Guellec *et al.* 2004). The contribution of the epidermal basal layer of cells to the production and reinforcement of the basement membrane was clearly demonstrated by Guellec *et al.* (2004) while studying the pattern of expression of ColIα2 during the ontogeny of zebrafish skin. Basal layer cells start producing the first collagen that is deposited in the dermis and, as skin gets thicker and scales start to develop, they stop contributing to the dermal stroma and become more involved in the deposition of the basement membrane. The pattern of expression of ColIα1 in the skin of metamorphosing Atlantic halibut was demonstrated by Campinho *et al.* (2007): it is expressed in the epidermal basal cells and dermal fibroblasts until metamorphic climax; after metamorphosis it is only expressed in the dermal endothelial cells. This description matches the results obtained in the present experiment for adult sea bream skin, where expression of ColIα1 was observed in the dermis, associated to the scale forming cells.

4.4.3 Expression of collagen I and osteopontin in sea bream skin and scales

In the present work, no differences in the level of expression of ColIα1 between the intact and 14 days regenerated skin and scales were observed inside and between experimental groups. According to Zylberberg *et al.* (1992), regenerating scales are more active at collagen production than the ontogenetic ones but collagen synthesis starts to decrease 2 or 3 weeks after scale removal, depending on the species (Zylberberg *et al.* 1992). This could help explain the similarity between tissue conditions and experimental groups since the active phases of collagen synthesis had already happened in the earlier days of regeneration and if it was different at some point in the regeneration process, then at 14 days of regeneration, when the scale is already morphologically similar to the adult scale, the differences probably disappeared.

The RNA extracts contained skin with scales, either intact or 14 days regenerated, so it is not possible to distinguish the amount of collagen type I in the skin from the one in the scales. Elasmoid scales are relatively large mineralized structures imbricated in the dermis, but when considering the cells that are actively involved in their formation and reshaping, the number of these cells that are contributing to the final RNA pool is very limited, and is easily overcome by all the cells in the epidermis and dermis which could also be synthesising collagen. When studying differences in the expression of normally highly expressed genes as the collagen type I, it is important to bear this in mind since it is not clear what differences in copy number are necessary to lead to a detectable up regulation in the assays available. Furthermore, the *in situ* hybridizations with sbColIα1 probe demonstrated that a minor population of cells in the skin is actively synthesising collagen I. This population of cells is concentrated in the posterior margin and upper and lower surfaces of the scale and is not scattered throughout the dermis, as might be expected when the importance of collagen I as the major constituent of the dermis connective tissue is considered. This situation clearly reflects that the analysis of the transcriptome might not match the protein content of the different layers of the tissue. Nevertheless, collagen type I expression in the intact scales of the AKG treated group showed a tendency to be higher than in the Control and Placebo groups, revealing that the stimulation of collagen synthesis by AKG in sea bream scales can not be excluded yet.

In teleosts, osteopontin (SPP1) is expressed in mineralized and partially mineralized tissues like the branchial arches, operculum and teeth and cartilage, respectively (Fonseca *et al.* 2007). SPP1 is up-regulated during *in vitro* mineralization of VSa16 (osteoblast-like) and VSa13 (chondrocyte-like) ECM, demonstrating its importance in teleosts mineralization processes. Considering the above mentioned tissue distribution of SPP1 in sea bream and that, with the exception of scales, teleosts skin is not mineralized, the measured SPP1 may be attributed mainly to the scale forming cells. The production of osteopontin by osteoblasts, osteoclasts and fibroblasts has been demonstrated in other species (Sodek *et al.* 2000) and considering that the *in situ* results in the present study associate these same types of cells to the scale, it seems likely that scale osteoblasts and osteoclasts are the cells responsible for SPP1 production in sea bream scales. Osteopontin is a non-collagenous protein associated to collagen fibers in bone (Sodek *et al.* 2000) and its involvement, as an ECM protein, in the orientation of the hydroxyapatite crystals has been suggested (Zhang *et al.* 1990). In order to

evaluate if SPP1 is also associated with fibrillary collagen in sea bream scales an immunohistochemical study would have to be performed with a specific antibody. Similarly, *in situ* hybridization with a sbSPP1 probe would provide insight into the cells involved in osteopontin production in sea bream skin and scales. The tendency for a higher expression of SPP1 in the regenerated scales coincides with the tendency for a higher ColIα1 expression in the same tissue, and this is in accordance with what has been previously described for regenerating scales (Zylberberg *et al.* 1992). Also, considering the tendency for a higher SPP1 expression in the intact scales of the AKG treated group, and that the same was observed for collagen I, the influence of AKG in stimulating sea bream scale mineralization needs further evaluation.

Chapter 5

General discussion and future perspectives

5. GENERAL DISCUSSION AND FUTURE PERSPECTIVES

Once the skin is disrupted, its vital functioning has to be restored rapidly as a defence against the external environment. The first event in skin wound repair is the re-establishment of the epidermis continuity which follows an orderly sequence of cellular and biochemical events. The bundles of epidermis that remains attached to the dermis after scale removal represents a crucial source of cells to be recruited for the tissue recovery. The epidermal basal layer of cells differentiate rapidly and this step has been interpreted by some authors as the first stage of epithelial-mesenchymal interactions that will lead to scale regeneration (Quilhac & Sire 1999). The present study in sea bream reinforced the idea that the basic organization and structure of the regenerating scales resembles that of the ontogenetic ones. It is generally assumed that development is a highly conservative process. Despite showing an approximately sequence of events by which a scale is achieved, regeneration process can not be an exact recapitulation of the ontogenetic development (Guellec *et al.* 2004). The major differences between scale formation and regeneration are in the first stages, and are probably related to the rapid formation of the new scale. During ontogenesis, the cells which aggregate migrate from the deep to the superficial dermis whereas in regeneration the cells which accumulate to form the pappila are mobilized from the vicinity of the old scale pocket in the superficial dermis (Sire & Akimenko 2004). The correspondence of 1 papilla: 1 scale, observed in both ontogenetic and regeneration processes is considered to reflect epidermal-mesenchymal interactions.

In this study, plasma levels of cortisol, estradiol, calcium and phosphorus were not significantly altered by alpha-ketoglutarate administration, demonstrating that the physiological state of the experimental animals was not affected by the treatment. It would be interesting to analyse the calcium and phosphate content of the scales, to see whether or not it is altered after oral administration of AKG or calcium supplement. It would also be interesting to determine the plasmatic levels of growth hormone and IGF-I in sea bream plasma from the present experiment, to see if AKG induces any alteration in hormonal balance. Determination of plasma AKG and plasma amino acids proline and glutamate after AKG administration is a key step to verify if the pool of proline and hydroxyproline is higher as it has been described for turkeys (Tatara *et al.* 2005) and humans (Jeevanandam & Petersen 1999). Seemingly, quantification of P4H by qPCR or by an enzymatic assay could help demonstrating if AKG is influencing collagen synthesis, and this information could then be

related to what was observed in the treated sea bream aortas, the ones that had higher elastic recoil.

Skin and scales are tissues rich in collagen. The presence and molecular characterization of the cells involved in scale formation, the osteoblasts, and resorption and remodelling, the osteoclasts were demonstrated in sea bream skin. Their shape and localization were coincident to what had been previously described for elasmoid scales. The arrangement of the densely packed collagen from the scales basal plate, characterized by a plywood-like structure (Guellec & Zylberberg 1998; Mugiya 1980; Witten & Huysseune 2007; Zylberberg *et al.* 1992) was evidenced by the picro sirius red staining through which, under polarized light, large collagen fibers appear bright yellow. In sea bream skin after oral administration of alpha-ketoglutarate, the basement membrane that links the epidermis to the dermis seemed thicker, both in intact and regenerated tissue, as revealed by collagen birefringence. The intensity of collagen birefringence under polarized light can be a subjective character for evaluation and measure of the exact protein content in the different layers of the tissue would give an idea on whether or not AKG, if influencing this process, is stimulating collagen production. The collagen I and SPP1 content, as revealed by quantification with qPCR, was not different between experimental groups and tissue conditions. Despite the fact that skin and scales are extremely rich in collagen type I protein, the amount of transcripts present in the tissue may not reflect the protein content. Therefore, in order to study the influence of AKG through the analysis of the transcriptome other factors have to be considered.

The influence of alpha-ketoglutarate in extracellular matrix proteins of sea bream skin remains to be elucidated and a qPCR for osteonectin would provide more information on matricellular proteins in the process of scale mineralization, once chosen the right reference gene.

The set of information gather with this preliminary work on the influence of alpha-ketoglutarate in sea bream provides promising clues to the role of AKG in collagen synthesis.

References:

Abbink, W.,Bevelander, G. S.,Rotllant, J.,Canario, A. V. M.Flik1, G. (2004). "Calcium handling in Sparus auratus: effects of water and dietary calcium levels on mineral composition, cortisol and PTHrP levels." The Journal of Experimental Biology 207: 4077-4084.

Applyed-Biosystems (2008). "Real-time PCR: Understanding C_T."

Bereiter-Hahn, J. & Zylberberg, L. (1993). "Regeneration of Teleost Fish Scales." Comparative Biochemistry and Physiology 105A(4): 625-641.

Berg, J. M.,Tymoczko, J. L.Stryer, L. (2002). Biochemistry - 5th edition, W.H. Freeman and Company.

Bienko, M.,Radzki, R. P.,Puzio, I.,Filip, R.,Pierzynowski, S. G.Studzinski, T. (2002). "The influence of alpha-ketoglutarate (AKG) on mineralization of femur in rats with established osteopenia." Acta Orthopaedica Scandinavica 73: 52.

Bustin, S. A.,Benes, V.,Garson, J. A.,Hellemans, J.,Huggett, J.,Kubista, M.,Mueller, R.,Nolan, T.,Pfaffl, M. W.,Shipley, G. L.,Vandesompele, J.Wittwer, C. T. (2009). "The *MIQE* Guidelines: Minimum Information for Publication of Quantitative Real-Time PCR Experiments." Clinical Chemistry 55(4): 611-622.

Campinho, M. A.,Silva, N.,Sweeney, G. E.Power, D. M. (2007). "Molecular, cellular and histological changes in skin from a larval to an adult phenotype during bony fish metamorphosis." Cell & Tissue Research 327: 267-284.

Canario, A. V. M.,Rotllant, J.,Fuentes, J.,Guerreiro, P. M.,Teodósio, H. R.,Power, D. M.Clark, M. S. (2006). "Novel bioactive parathyroid hormone and related peptides in teleost fish." FEBS Letters 580(1): 291-299.

Chard, T. (1973). "The radioimmunoassay of oxytocin and vasopressin." Journal of Endocrinology 58: 143-160.

Chard, T. (1990). An introduction to radioimmunoassay and related techniques. Amsterdam, Elsevier.

Colgravea, M. L.,Allinghama, P. G.Jones, A. (2008). "Hydroxyproline quantification for the estimation of collagen in tissue using multiple reaction monitoring mass spectrometry." Journal of Chromatography A 1212: 150-153.

Darby, I. A. & Hewitson, T. D. (2006). Methods in Molecular Biology. *In Situ* Hybridization Protocols. H. P. Inc. Totowa, New Jersey. **326**.

Donohue, J. & Sgoutas, D. (1975). "Improved radioimmunoassay of plasma cortisol." Clinical Chemistry 21(6): 770-773.

Filip, R. & Pierzynowski, S. G. (2007). "The role of glutamine and α-ketoglutarate in gut metabolism and the potential application in medicine and nutrition." Journal of Pre-Clinical and Clinical Research 1(1): 009-015.

Flanagan, J. A.,Power, D. M.,Bendell, L. A.,Guerreiro, P. M.,Fuentes, J.,Clark, M. S.,Canario, A. V. M.,Danks, J. A.,Brown, B. L.Ingleton, P. M. (2000). "Cloning of the cDNA for Sea Bream (*Sparus aurata*) Parathyroid Hormone-Related Protein." General and Comparative Endocrinology 118: 373-382.

Fonseca, V.,Laizé, V.,Valente, M. S.Cancela, M. L. (2007). "Identification of an osteopontin-like protein in fish associated with mineral formation." FEBS Journal 274: 4428-4439.

Foster, L. B. & Dunn, R. T. (1974). "Single-Antibody Technique for Radioimmunoassay of Cortisol in Unextracted Serum or Plasma." Clinical Chemistry 20(3): 365-368.

Fuentes, J.,Figueiredo, J.,Power, D. M.Canario, A. V. M. (2005). "Parathyroid hormone-related protein regulates intestinal calcium transport in sea bream (Sparus auratus)." American Journal of Physiology: Regulatory, Integrative and Comparative Physiology 291: R1499-R1506.

Gallardo, M. A.,Sala-Rabanal, M.,Ibarz, A.,Padrós, F.,Blasco, J.,Fernández, J.Sánchez, J. (2003). "Functional alterations associated with the 'winter syndrome' in gilthead sea bream (*Sparus aurata*)." Aquaculture 223: 15-27.

Guellec, D. L.,Morvan-Dubois, G.Sire, J.-Y. (2004). "Skin development in bony fish with particular emphasis on collagen deposition in the dermis of the zebrafish (*Danio rerio*)." International Journal of Developmental Biology 48: 217-231.

Guellec, D. L. & Zylberberg, L. (1998). "Expression of Type I and Type V Collagen mRNAs in the Elasmoid Scales of a Teleost Fish as Revealed by In Situ Hybridization." Connective Tissue Research 39(4): 257-267.

Guerreiro, P. M.,Fuentes, J.,Power, D. M.,Ingleton, P. M.,Flik, G.Canario, A. V. M. (2001). "Parathyroid hormone-related protein: a calcium regulatory factor in sea bream (Sparus aurata L.) larvae." American Journal of Physiology: Regulatory, Integrative and Comparative Physiology 281: R855-R860.

Guyton & Hall (2006). Textbook of Medical Physiology, Elsevier Saunders.

Hall, B. K. & Witten, P. E. (2007). Plasticity of and Transitions between Skeletal Tissues in Vertebrate Evolution and Development., Indiana University Press.

Hall, T. A. (1999). "BioEdit: a user-friendly biological sequence alignment editor and analysis program for Windows 95/98/NT." Nucleic Acids Symp. Ser 41: 95-98.

Harada, S.-i. & Rodan, G. A. (2003). "Control of osteoblast function and regulation of bone mass." Nature 423: 349-355.

Harrison, A. P. & Flatman, J. A. (1999). "Measurement of force and both surface and deep M wave properties in isolated rat soleus muscles." American Journal of Physiology: Regulatory, Integrative and Comparative Physiology 277: R1646-R1653.

Harrison, A. P.,Nielsen, O. B.Clausen, T. (1997). "Role of Na^+-K^+ pump and Na^+ channel concentrations in the contractility of rat soleus muscle." American Journal of Physiology: Regulatory, Integrative and Comparative Physiology 41: R1402-R1408.

Harrison, A. P. & Pierzynowski, S. G. (2008). "Biological effects of 2-oxoglutarate with particular emphasis on the regulation of protein, mineral and lipid absorption/metabolism, muscle performance, kidney function, bone formation and cancerogenesis, all viewed from a healthy ageing perspective state of the art - review article." Journal of Physiology and Pharmacology 59(Suppl 1): 91-106.

Harrison, A. P.,Tygesen, M. P.,Sawa-Wojtanowicz, B.,Husted, S.Tatara, M. R. (2004). "α-Ketoglutarate treatment early in postnatal life improves bone density in lambs at slaughter." Bone 35: 204-209.

Hartl, D. L. & Jones, E. W. (1999). Essential Genetics. Sudbury, Massachusetts, Jones and Bartlett Publishers.

Higuchi, R.,Dollinger, G.,Walsh, P. S.Griffith, R. (1992). "Simultaneous amplification and detection of specific DNA-sequences." BioTechnology 10(4): 413-417.

Huysseune, A. & Sire, J.-Y. (1998). "Evolution of patterns and processes in teeth and tooth-related tissues in non-mammalian vertebrates." European Journal of Oral Sciences 106(Suppl 1): 437-481.

Ibarz, A.,Blasco, J.,Beltrán, M.,Gallardo, M. A.,Sánchez, J.,Sala, R.Fernández-Borràs, J. (2005). "Cold-induced alterations on proximate composition and fatty acid profiles of several tissues in gilthead sea bream (*Sparus aurata*)." Aquaculture 249: 477-486.

Ishibashi, K. & Imai, M. (2002). "Prospect of a stanniocalcin endocrine/paracrine system in mammals." The American Journal of Physiology - Renal Physiology 282: 367-375.

Jeevanandam, M. & Petersen, S. R. (1999). "Substrate fuel kinetics in enterally fed trauma patients supplemented with ornithine alpha ketoglutarate." Clinical Nutrition 18(4): 209-217.

Jundt, G.,Berghãuser, K.-H.,Termine, J. D.Schulz, A. (1987). "Osteonectin- a differentiation marker of bone cells." Cell & Tissue Research 248: 409-415.

Junqueira, L. C. & Carneiro, J. (2005). Basic Histology - text and atlas, McGraw-Hill.

Kerr, J. M.,Fisher, L. W.,Termine, J. D.Young, M. F. (1991). The cDNA cloning and RNA distribution of bovine osteopontin. Gene. **108:** 237-243.

Kowalik, S.,Filip, R. S.,Śliwa, E.,Tatara, M. R.,Pierzynowski, S.Studzinski, T. (2005). "Influence of alpha-ketoglutarate on bone mineral density of the femur in piglets." Bull. Vet. Inst. Pulawy 49: 343-348.

Kranenbarg, S.,Cleynenbreugel, T. v.,Schipper, H.Leeuwen, J. v. (2005). "Adaptive bone formation in acellular vertebrae of sea bass (*Dicentrarchus labrax* L.)." The Journal Of Experimental Biology 208: 3493-3502.

Kubista, M.,Andrade, J. M.,Bengtsson, M.,Forootan, A.,Jonák, J.,Lind, K.,Sindelka, R.,Sjöback, R.,Sjögreen, B.,Strömbom, L.,Ståhlberg, A.Zoric, N. (2006). "The real-time polymerase chain reaction." Molecular Aspects of Medicine 27(2-3): 95-125.

Lambert, B. D.,Filip, R.,Stoll, B.,Junghans, P.,Derno, M.,Hennig, U.,Souffrant, W. B.,Pierzynowski, S.Burrin, D. G. (2006). "First-Pass Metabolism Limits the Intestinal Absorption of Enteral a-Ketoglutarate in Young Pigs." The Journal of Nutrition - Nutrient Physiology, Metabolism, and Nutrient-Nutrient Interactions: 2779-2784.

Lee, N. K.,Sowa, H.,Hinoi, E.,Ferron, M.,Ahn, J. D.,Confavreux, C.,Dacquin, R.,Mee, P. J.,McKee, M. D.,Jung, D. Y.,Zhang, Z.,Kim, J. K.,Mauvais-Jarvis, F.,Ducy, P.Karsenty, G. (2007). "Endocrine regulation of energy metabolism by the skeleton." Cell 130(3): 456-469.

Miao, D.,He, B.,Jiang, Y.,Kobayashi, T.,Sorocéanu, M. A.,Zhao, J.,Su, H.,Tong, X.,Amizuka, N.,Gupta, A.,Genant, H. K.,Kronenberg, H. M.,Goltzman, D.Karaplis, A. C. (2005). "Osteoblast-derived PTHrP is a potent endogenous bone anabolic agent that modifies the therapeutic efficacy of administered PTH 1–34." The Journal of Clinical Investigation 115(9): 2402-2411.

Mills, A. A.,Zheng, B.,Wang, X.-J.,Vogelk, H.,Roop, D. R.Bradley, A. (1999). "p63 is a p53 homologue required for limb and epidermal morphogenesis." Nature 398(22 April): 708-713.

Monnot, M.-J.,Babin, P. J.,Poleo, G.,Andre, M.,Laforest, L.,Ballagny, C.Akimenko, M.-A. (1999). "Epidermal Expression of Apolipoprotein E Gene During Fin and Scale Development and Fin Regeneration in Zebrafish." Developmental Dynamics 214: 207-215.

Moukarzel, A. A.,Goulet, O. i.,Solos, J. S.,Marri-Henneberg, C.,Buchman, A. L.,Cynober, L.,Rappaport, R.Ricour, C. (1994). "Growth retardation in children receiving long-term total parenteral nutrition: effects of ornithine a-ketoglutarate." The American Journal of Clinical Nutrition 60: 408-413.

Mugiya, Y. (1980). "The source of calcium in the regenerating scales of the goldfish, *Carasius auratus*." 66A: 521-524.

Mukherjee, D.,Sen, U.,Bhattacharyya, S. P.Mukherjee, D. (2004). "The effects of calcitonin on plasma calcium levels and bone metabolism in the fresh water teleost *Channa punctatus*." Comparative Biochemistry and Physiology Part A 138: 417-426.

Nakamura, A.,Dohi, Y.,Akahane, M.,Ohgushi, H.,Nakajima, H.,Funaoka, H.Takakura, Y. (2009). "Osteocalcin Secretion as an Early Marker of In Vitro Osteogenic Differentiation of Rat Mesenchymal Stem Cells." Tissue Engineering: Part C 15(2): 169-180.

Nolan, T.,Hands, R. E.Austin, S. A. (2006). "Quantification of mRNA using real-time RT-PCR." Nature Protocols 1(3): 1559-1582.

Olin, T.,Bergstrom, E.,Jungvid, H.Decken, A. v. d. (1992). "Effect of dietary acids (AKG) on intermediary metabolism of nutrients in Atlantic salmon (*Salmo salar*) during 17-b-estradiol induced vitellogenin synthesis." Acta Agric. Scand. 42: 246-253.

Olson, O. P. & Watanabe, N. (1980). "Studies on Formation and Resorption of Fish Scales: IV. Ultrastrucutre of Developing Scales in Newly Hatched Fry of the Sheepshead Minnow, *Cyprinodon variegatus* (Atheriniformes: Cyprinodontidae)." Cell & Tissue Research 211: 303-316.

Onozato, H. & Watanabe, N. (1979). "Studies on Fish Scale Formation and Resorption: III. Fine Structure and Calcification of the Fibrillary Plates of the Scales in *Carassius auratus* (Cypriniformes: Cyprinidae)." Cell & Tissue Research 201: 409-422.

Pacifici, M.,Oshima, s.,Fisher, L. W.,Young, M. F.,Shapiro, I. M.Leboy, P. S. (1990). "Changes in Osteonectin Distribution and Levels are Associated with Mineralization of the Chicken Tibial Growth Cartilage." Calcified Tissue International 47: 51-61.

Pearse, A. G. E. (1985). Histochemistry - Theoretical and Applied, Churchill Livingstone.

Persson, P.,Björnsson, B. T.Takagi, Y. (1999). "Characterization of morphology and physiological actions of scale osteoclasts in the rainbow trout." Journal of Fish Biology 54: 669-684.

Persson, P.,Takagi, Y.Bjornsson, B. T. (1995). "Tartrate resistant acid phosphatase as a marker for scale resorption in rainbow trout, *Oncorhynchus mykiss:* effects of estradiol-17β treatment and refeeding." Fish Physiology and Biochemistry 14(4): 329-339.

Pinto, P. I. S.,Estêvão, M. D.,Redruello, B.,Socorro, S. M.,Canário, A. V. M.Power, D. M. (2009). "Immunohistochemical detection of estrogen receptors in fish scales." General and Comparative Endocrinology 160(1): 19-29.

Quilhac, A. & Sire, J.-Y. (1999). "Spreading, Proliferation, and Differentiation of the Epidermis After Wounding a Cichlid Fish, *Hemichromis bimaculatus*." The Anatomical Record 254: 435-451.

Redruello, B.,Estêvão, M. D.,Rotllant, J.,Guerreiro, P. M.,Anjos, L. I.,Canário, A. V.Power, D. M. (2005). "Isolation and Characterization of Piscine Osteonectin and Downregulation of Its Expression by PTH-Related Protein." Journal of Bone and Mineral Research 20(4): 682-692.

Reis-Filho, J. S.,Torio, B.,Albergaria, A.Schmitt, F. C. (2002). "p63 expression in normal skin and usual cutaneous carcinomas." Journal of Cutaneous Pathology 29: 517-523.

Roberts, R. J. (2001). The Anatomy and Physiology of Teleosts. In: Fish Patology, W.B. Saunders.

Rosenbloom, J. & Cywinski, A. (1976). "Inhibition of proline hydroxylation does not inhibit secretion of tropoelastin by chick aorta cells." FEBS Letters 65(2).

Rotlland, J.,Redruello, B.,Guerreiro, P. M.,Fernandes, H.,Canario, A. V. M.Power, D. M. (2005). "Calcium mobilization from fish scales is mediated by parathyroid hormone related protein via the parathyroid hormone type 1 receptor." Regulatory Peptides 132: 33-40.

Rotllant, J.,Redruello, B.,Guerreiro, P. M.,Fernandes, H.,Canario, A. V. M.Power, D. M. (2005). "Calcium mobilization from fish scales is mediated by parathyroid hormone related protein via the parathyroid hormone type 1 receptor." Regulatory Peptides 132: 33-40.

Rotllant, J.,Worthington, G. P.,Fuentes, J.,Guerreiro, P. M.,Teitsma, C. A.,Ingleton, P. M.,Balment, R. J.,Canario, A. V. M.Power, D. M. (2003). "Determination of tissue and plasma concentrations of PTHrP in fish: development and validation of a radioimmunoassay using a teleost 1–34 N-terminal peptide." General and Comparative Endocrinology 133: 146-153.

Rutten, E. P.,Engelen, M. P.,Schols, A. M.Deutz, N. E. (2005). "Skeletal muscle glutamate metabolism in health and disease: state of the art." Current Opinion in Clinical Nutrition & Metabolic Care 8: 41-51.

Science, R. A. (1996). Non radioactive *In Situ* Hybridization Application Manual, Roche Applied Sciences.

Seeley, R.,Stephens, T.Tate, P. (2001). Anatomia e Fisiologia, Lusodidacta.

Siddiq, A.,Aminova, L. R.Ratan, R. R. (2008). "Prolyl 4-hydroxylase activity-responsive transcription factors: From hydroxylation to gene expression and neuroprotection." Front Biosci. 13: 2875–2887.

Sigma-Aldrich (2008). qPCR Technical Guide. St. Louis, MO, USA, Sigma-Aldrich.

Silva, D. d. F. T. d.,Vidal, B. d. C.,Zezell, D. M.,Zorn, T. M. T.,Núñez, S. C.Ribeiro, M. S. (2006). "Collagen birefringence in skin repair in response to red polarized-laser therapy." Journal of Biomedical Optics 11(2): 024002-024006.

Sire, J.-Y. & Akimenko, M.-A. (2004). "Scale development in fish: a review, with description of sonic hedgehog (shh) expression in the zebrafish (*Danio rerio*)." International Journal of Developmental Biology 48: 233-247.

Sire, J.-Y.,Huysseune, A.Meunie, F. J. (1990). "Osteoclasts in teleost fish: Light- and electron-microscopical observations." Cell & Tissue Research 260: 85-94.

Sodek, J.,Ganss, B.McKee, M. D. (2000). "Osteopontin." Critical Reviews in Oral Biology & Medicine 11: 279-303.

Son, E. D.,Choi, G. H.,Kim, H.,Lee, B.,Chang, I. S.Hwang, J. S. (2007). "Alpha-Ketoglutarate Stimulates Procollagen Production in Cultured Human Dermal

Fibroblasts, and Decreases UVB-Induced Wrinkle Formation Following Topical Application on the Dorsal Skin of Hairless Mice." Biol. Pharm. Bull. 30(8): 1395-1399.

Suzuki, N.,Suzuki, T.Kurokawa, T. (2000). "Suppression of osteoclastic activities by calcitonin in the scales of goldfish (freshwater teleost) and nibbler fish (seawater teleost)." Peptides 21(1): 115-124.

Suzukia, N.,Hayakawab, K.,Kamedab, T.,Tribab, A.,Tangb, N.,Tabatac, M. J.,Takadad, K.,Wadae, S.,Omorif, K.,Srivastavg, A. K.,Mishimah, H.Hattorii, A. (2009). "Monohydroxylated polycyclic aromatic hydrocarbons inhibit both osteoclastic and osteoblastic activities in teleost scales." Life Sciences 84(13-14): 482-488.

Takahashi, H.,Suzuki, N.,Takagi, C.,Ikegame, M.,Yamamoto, T.,Takahashi, A.,Moriyama, S.,Hattori, A.Sakamoto, a. (2008). "Prolactin Inhibits Osteoclastic Activity in the Goldfish Scale: A Novel Direct Action of Prolactin in Teleosts-." Zoological Science 25: 739-745.

Taşkiran, D.,Taşkiran, E.,Yercan, H.Kutay, F. Z. (1999). "Quantification of Total Collagen in Rabbit Tendon by the Sirius Red Method." Tr. J. of Medical Sciences 29: 7-9.

Tatara, M. R.,Brodzki, A.,Krupski, W.,Sliwa, E.,Silmanowictz, P.,Majcher, P.,Pierzynowski, S. G.Studzinski, T. (2005). "Effects of α-ketoglutarate on bone homeostasis and plasma amino acids in turkeys." Poultry Science Association 84: 1604-1609.

Tatara, M. R.,Krupski, W.,Sliwa, E.,Maciejewski, R.Dabrowski, A. (2007). "Fundectomy-Evoked Osteopenia in Pigs Is Mediated by the Gastric-Hypothalamic-Pituitary Axis." Experimental Biology and Medicine 232: 1449-1457.

Tatara, M. R.,Majcher, P.,Krupski, W.,Pierzynowski, S. G.Studzinski, T. (2004). "Influence of alpha-ketoglutarate on cortical bone density, geometrical properties and mechanical endurance of the humerus in turkeys." Bull. Vet. Ins. Pulawy 48: 461-465.

Tatara, R. M.,Pierzynowski, S.,Majcher, P.,Krupski, W.,Brodki, A.Studzinski, T. (2004). "Effect of alpha-ketoglutarate (AKG) on mineralisation, morphology and mechanical endurance of femur and tibia in turkey." Bull. Vet. Ins. Pulawy 48: 305-309.

Termine, J. D.,Kleinman, H. K.,Whitson, S. W.,ConnMary, K. M.,McGarvey, L.Martin, G. R. (1981). "Osteonectin, a bone-specific protein linking mineral to collagen." Cell 26(1): 99-105.

Whittaker, P.,Kloner, R. A.,Boughner, D. R.Pickering, J. G. (1994). "Quantitative assessment of myocardial collagen with picrosirius red staining and circularly polarized light." Basic Research in Cardiology 89: 397-410.

Witten, P. E. (1997). "Enzyme histochemical characteristics of osteoblasts and mononucleated osteoclasts in a teleost fish with acellular bone (*Oreochromis niloticus*, Cichlidae)." Cell & Tissue Research 287(3): 591-599.

Witten, P. E. & Hall, B. K. (2003). "Seasonal changes in the lower jaw skeleton in male Atlantic salmon (*Salmo salar* L.): remodelling and regression of the kype after spawning." Journal of Anatomy 203(3): 435-450.

Witten, P. E.,Hansen, A.Hall, B. K. (2001). "Features of Mono- and Multinucleated Bone Resorbing Cells of the Zebrafish Danio rerio and Their Contribution to Skeletal Development, Remodeling, and Growth." Journal of Morphology 250: 197-207.

Witten, P. E. & Huysseune, A. (2007). Mechanisms of Chondrogenesis and Osteogenesis in Fins. In: Hall BK (ed.) Fins into Limbs: Evolution, Development, and Transformation. Chicago, The University of Chicago Press.

Wong, M. L. & Medrano, J. F. (2005). "Real-time PCR for mRNA quantitation." BioTechniques 39: 75-85.

Yata, M.,Yoshida, C.,Fujisawa, S.,Mizuta, S.Yoshinaka, R. (2001). "Identification and Characterization of Molecular Species of Collagen in Fish Skin." Food Chemistry and Toxicology 66(2): 247-251.

Yata, M.,Yoshida, C.,Fujisawa, S.Yoshinaka, R. (2001). "Identification and Characterization of Molecular Species of Collagen in Fish Skin." JFS: Food Chemistry and Toxicology 66(2): 247-251.

Yoshikubo, H.,Suzuki, N.,Takemura, K.,Hoso, M.,Yashima, S.,Iwamuro, S.,Takagi, Y.,Tabata, M. J.Hattori, A. (2005). "Osteoblastic activity and estrogenic response in the regenerating scale of goldfish, a good model of osteogenesis." Life Sciences 76: 2699-2709.

Zhang, Q.,Domenicucci, C.,Goldberg, H. A.,Wrana, J. L.Sodek, J. (1990). "Characterization of Fetal Porcine Bone Sialoproteins, Secreted Phosphoprotein I (SPPI, Osteopontin), Bone Sialoprotein, and a 23-kDa Glycoprotein." The Journal of Biological Chemistry 265(13): 7583-7589.

Zylberberg, L.,Bonaventrure, J.,Cohen-Solal, L.,Hartmann, D. J.Bereiter-Hahn, J. (1992). "Organization and characterization of fibrillar collagens in fish scales *in situ* and *in vitro*." Journal of Cell Science 103: 273-285.

Zylberberg, L.,Bonaventure, J.,Cohen-Solal, L.,Hartmann, D. J.Bereiter-Hahn, J. (1992). "Organization and characterization of fibrillar collagens in fish scales *in situ* and *in vitro*." Journal of Cell Science 103: 273-285.

Biological parameters of experimental fish

Table 1 – Biological parameters of experimental fish at the end of the experimental trial. SL: Standard length.

Treatment	Nº	Weight (g)	SL (cm)	Observations:
AKG	1	448	27.6	female 100%
	2	342	26.5	female 85%
	3	444	28.5	female 99%, male 1%
	4	438	28.0	female 95%, male 5%
	5	310	25.1	no gonad; 2nd vessel close o the vertebrae
	6	528	29.4	little gonad
	7	386	27.2	no vessel from the heart (first vessel)
Placebo	8	444	28.5	male
	9	380	27.1	male male; lordosis in the tail region
	10	398	26.3	male
	11	511	29.1	little gonad
	12	282	24.1	
Control	13	824	34.2	
	14	738	33.2	
	15	772	32.8	
	16	786	33.2	
	17	780	33.2	femal 100%; eroded operculum
	18	954	36.6	female 98%, male 2%
	19	821	33.0	

Solutions used in the protocols described in the previous chapters are presented in alphabetical order in the present appendix. Solutions required for the preparation of working solutions are also described herein. TRAP staining solutions are indicated in a separate section at the end of the chapter.

3% Acetic acid

Preparation of 100 ml solution:

Dissolve 3 ml of Glacial acetic acid (Merck) in 97 ml of distilled water and store in the dark at room temperature.

1% Acid – alcohol

Preparation of 100 ml solution:

Dissolve 1 ml of concentrated Hydrochloric acid (Merck) in 100 ml of 70 % ethanol and store at room temperature.

Acidified water

Preparation of 100 ml solution:

To 100 ml of distilled water add 0.5 ml of glacial acetic acid (Merck) and store in the dark at room temperature.

Activated charcoal

Preparation of 100 ml solution:

0.075 mg Dextran (Sigma-Aldrich)

1.5 mg activated charcoal (C-5385, Sigma-Aldrich)

Dissolve both components in 100 ml of gelatine buffer (see below)

1% Alcian Blue 8GX solution

Preparation of 100 ml solution:

Dissolve 1 g of Alcian Blue 8GX (Sigma-Aldrich) in 100 ml of 3% aqueous acetic acid (see above). Store almost indefinitely in the dark at room temperature.

Blocking solution 2% and 1%

Preparation of 100 ml solution:

2 g or 1 g Blocking Reagent (Roche; for 2% and 1% solution respectively)

Dissolve in 100 ml of maleic acid buffer (MBA, see below) at 65 ºC and mix occasionally. Cool at room temperature, aliquot and store at – 20 ºC.

Cell lysis solution (0.2M NaOH + 1% SDS)

Preparation of 1 ml solution:

100 µl NaOH (see below)

800 µl Distilled water

100 µl SDS (see below)

Mix the three components in the established order and use immediately.

CHAPS 2% (3-[3-cholamidpropyl)dimethylammonio]-1-propanesulfonate)

Preparation of 100 ml solution:

Dissolve 2 g CHAPS in 100 ml of diethyl pyrocarbonate treated sterile water (see below) and store at room temperature.

To prepare 100 ml of **2xSSC/0.12% CHAPS**, dilute 6 ml of 2% CHAPS in 94 ml of 2x SSC (see below).

2M Citric Acid

Preparation of 100 ml solution:

Dissolve 42 g Citric acid (Sigma-Aldrich) in 100 ml of MilliQ water. Autoclave for 20 minutes at 121 ºC and store at room temperature.

1% DAB

Preparation of 10 ml solution:

Dissolve 0.1 g DAB (Sigma-Aldrich, Madrid, Spain) in 10 ml of bi-distilled water. Aliquot and store at -20 ºC.

DAB peroxidase substrate solution

Preparation of 5 ml solution:

To 5 ml of 0.15M PBS pH 7.2 (see below) add 200 µl of 1% DAB (see above) and mix well; add 200 µl of 0.3% H_2O_2 (see below), mix well and use immediately.

50x Denhardt`s solution

Preparation of 100 ml solution:

1 g Bovine serum albumin

1 g Phicoll (Sigma-Aldrich)

1 g Polyvinilpirrolidona (PVP, Sigma-Aldrich)

Dissolve overnight at 4 ºC, filter, aliquot and store at – 20 ºC.

Developing buffer (100 mM Tris-HCl, 100 mM NaCl, 50 mM $MgCl_2$, pH 9.5)

Preparation of 100 ml solution:

10 ml Tris-HCl solution pH 9.5 (see below)

2 ml 5M NaCl (see below)

5 ml 1M $MgCl_2$ (see below)

Mix the appropriate volume of the each solution, make the volume up to 100 ml with distilled water and use immediately.

Diethilpyrocarbonate (DEPC) treated water

Preparation of 100 ml solution:

Add 10 µL DEPC to 100 ml Ellix® or MilliQ® water in a Duran bottle and mix thoroughly. Wait approximately 2 h and autoclave for 20 minutes at 121 ºC. Store at room temperature.

Eosin Y 1% aqueous solution

Preparation of 100 ml solution:

Dissolve 1g Eosin Y (Sigma-Aldrich) in 100 ml of double-distilled water and store until use.

Ethylenediaminetetraacetic acid (EDTA) 0.5M and 0.2M pH 8

Preparation of 100 ml solution:

7.6 g (0.2M) $C_{10}H_{14}N_2Na_2O_8 \cdot 2H_2O$ (USB)

19 g (0.5M) $C_{10}H_{14}N_2Na_2O_8 \cdot 2H_2O$ (USB)

Dissolve the desired amount of EDTA in 90 ml of distilled water and adjust the pH to 8 with NaOH. Check the pH until complete dissolution and adjust the final volume to 100 ml. Autoclave for 20 minutes at 121 ºC. Store at room temperature.

Gelatine buffer

Preparation of 100 ml solution:

Dissolve 0.1 g Gelatine (G-9382 Sigma-Aldrich, Madrid, Spain) in 10 ml of 0.05M phosphate buffer pH 7.6 (see below), make the volume up to 100 ml with distilled water and add 0.01 g of sodium azide (Sigma-Aldrich, Madrid, Spain). Store at 4 ºC.

GTE

Preparation of 100 ml solution:

1.125 g Glucose (marca)

2.5 ml 1M Tris pH 8 (see below)

2 ml 0.5M EDTA pH 8 (see above)

Dissolve the three components in 100 ml of bi-distilled water and autoclave for 20 minutes at 121 ºC. Store at room temperature.

Harris haematoxylin solution

Preparation of 100 ml solution:

1 g Haematoxylin

10 g Aluminium potassium sulphate

0,25 g Mercury oxyde

4 ml Glacial acetic acid

5 ml Absolute ethanol

Dissolve the haematoxylin in absolute ethanol. Dissolve the aluminium sulphate in 100 ml of warm distilled water. Combine the solutions and boil for 4 minutes, remove from the heat and add the mercury oxide, mix well and boil until the dye becomes a dark purple colour. Cool the solution rapidly under running water, add the glacial acetic acid and filter the solution. Immediately before using dilute 50:50 in absolute ethanol and filter the resulting solution. Store the stock solution in the dark at room temperature.

Heparin (10 mg·ml^{-1})

Preparation of 10 ml solution:

Dissolve 100 mg Heparin ammonium salt (Sigma-Aldrich) in 10 ml of MilliQ water, aliquot and store at – 20 ºC.

0.3% Hydrogen peroxide

Preparation of 10 ml solution:

Add 100 µl of hydrogen peroxide 30% (Sigma-Aldrich, Madrid, Spain) to 10 ml of bi-distilled water and use immediately.

***In situ* hybridization solution**

Preparation of 100 ml solution:

50 ml Deionized formamide

20 ml sterile 20x SSC buffer (see below)

2 ml 50x Denhardt`s solution (see above)

2 ml Torula RNA yeast (50 $mg \cdot ml^{-1}$, see below)

2 ml 2% CHAPS (see above)

1 ml Heparin (10 $mg \cdot ml^{-1}$, see above)

Mix all the reagents together and adjust the pH to 6.0 with 2M citric acid solution (see above). Make the volume up to 100 ml with sterile DEPC treated Ellix® water (see above), aliquot ant store at – 20 ºC.

Light green dye solution

Preparation of 100 ml solution:

0.2 g Citric acid (Sigma-Aldrich)

10 ml distilled water

0.2 g Light green

Prepare a solution of 2% citric acid by dissolving it in 10 ml distilled water. Add the light green and mix until complete dissolution. Store the stock solution in the dark at room temperature. To obtain the working solution of 2% light green, dilute 1:10 in distilled water immediately before use.

4M Lithium Chloride

Preparation of 100 ml solution:

Dissolve 16.96 g Lithium Chloride (Sigma-Aldrich) in 100 ml of DEPC treated Ellix® water and store at room temperature.

Luria-Bertani broth (LB broth)

Preparation of 100 ml of culture medium:

Dissolve 2 LB-broth tablets (Sigma) in 100 ml of bi-distilled water and autoclave for 20 minutes at 121 ºC. Let it cool to room temperature and add 100 µl of Ampicilin 50 mg/ml. Use immediately or store at 4 ºC.

Luria-Bertani culture media (LB/Amp/X-gal/IPTG)

Preparation of 100 ml of culture medium:

2 tablets of LB-agar (Sigma)

150 µl Ampicilin 50 mg/ml

160 µl X-gal 50 mg/ml

100 µl 0.5M IPTG (Isopropyl β-D-1-thiogalactopyranoside)

Dissolve the 2 tablets of LB-agar in 100 ml of bi-distilled water and autoclave for 20 minutes at 121 ºC. Thaw the antibiotic, the X-gal and the sugar IPTG on ice. Let the culture media cool at room temperature and add the three components. Mix carefully to avoid many air bubbles and distribute the media on to the Petri dishes in a flow chamber (SterileGemini). Store at 4 ºC in a sealed plastic bag.

2% Magnesium Chloride

Preparation of 100 ml solution:

Dissolve 2 g of $MgCl_2$ in 100 ml distilled water.

1M Magnesium Chloride solution

Preparation of 100 ml solution:

0.95 g Magnesium Chloride (Sigma-Aldrich)

Dissolve in 100 ml of DEPC treated water (see above) and store at room temperature.

Maleic Acid Buffer (MAB; 100 mM maleic acid; 150 mM NaCl, 0.1 % tween-20, pH 7.5)

Preparation of 100 ml solution:

1.161 g Maleic Acid (Sigma-Aldrich)

0.8775 g Sodium chloride (Sigma-Aldrich)

Dissolve in 90 ml of distilled water and adjust the pH to 7.5. Complete the volume 100 ml and autoclave for 20 minutes at 121 ºC. Allow to cool and add 100 ul of Tween-20 (Sigma-Aldrich). Store at room temperature.

20 % Methanol in PBST with 3 % Hydrogen Peroxide

Preparation of 100 ml solution:

To 77 ml of PBST (see below) add 20 ml of methanol (Merck) and 3 ml of hydrogen peroxide 30v (commercial) and use immediately.

Orange G solution

Preparation of 100 ml solution:

2 g Orange G (C.I. 16230)

0.5 % Phosphotungstic acid

Dissolve the orange G in 100 ml of 0.5% phosphotungstic acid solution (see below). Stand for 24 h and use supernatant. Keep in the dark at room temperature.

Paraformaldehyde 4%, for *in situ* hybridization

Preparation of 100 ml solution:

Dilute 10.8 ml of 37 % paraformaldehyde (Sigma-Aldrich) with 89.2 ml of phosphate-tween buffer (PTW, see below) and use immediately.

Paraformaldehyde (PFA) 4% pH 7.4, for tissue fixation

Preparation of 1L solution:

40 g PFA (Sigma-Aldrich)

Sodium Hydroxide (NaOH)

1M PBS pH 7.4

Dissolve the PFA in 900 ml DEPC treated Ellix® water; add 100 µL of NaOH and heat at 65 ºC until complete dissolution. Let it cool to room temperature and add 100 ml of sterile 1M PBS pH 7.4. Keep at 4 ºC up to two weeks.

1% Periodic Acid

Preparation of 100 ml solution:

To 1 g of Periodic acid (Sigma-Aldrich, Madrid, Spain) add 100 ml of distilled water. Stir until complete dissolution and keep in the dark at room temperature.

0.01M Phosphate Buffer Saline (PBS) pH 7.6, for plasma dilutions

Preparation of 100 ml solution:

0.156 g Sodium hydrogen phosphate, dihydrated ($NaH_2PO_4.2H_2O$, Merk)

0.1770 g Disodium hydrogen phosphate, dihydrated ($Na_2HPO_4.2H_2O$, Merk)
Dissolve each reagent separately in 100 ml of bi-distilled water at room temperature. Adjust the pH of the disodium hydrogen phosphate solution with the sodium hydrogen phosphate solution until the final pH is 7.6. Store at 4 ºC.

0.05M Phosphate Buffer Saline (PBS) pH 7.6, for radioimmunoassays
Preparation of 100 ml solution:
0.78 g Sodium hydrogen phosphate, dihydrated ($NaH_2PO_4.2H_2O$, Merk)
0.89 g Disodium hydrogen phosphate, dihydrated ($Na_2HPO_4.2H_2O$, Merk)
Dissolve each reagent separately in 100 ml of bi-distilled water at room temperature. Adjust the pH of the disodium hydrogen phosphate solution with the sodium hydrogen phosphate solution until the final pH is 7.6. Store at – 20 ºC.

0.15M Phosphate Buffer Saline (PBS) pH 7.2, for IHC
Preparation of 100 ml solution:
2.34 g Sodium hydrogen phosphate, dihydrated ($NaH_2PO_4.2H_2O$, Merk)
2.67 g Disodium hydrogen phosphate, dihydrated ($Na_2HPO_4.2H_2O$, Merk)
Dissolve each reagent separately in 100 ml of bi-distilled water at room temperature. Adjust the pH of the disodium hydrogen phosphate solution with the sodium hydrogen phosphate solution until the final pH is 7.2. Store at room temperature and use in the following days.

1M Phosphate Buffer Saline (PBS) pH 7.4, for the preparation of PFA solutions
Preparation of 100 ml solution:
4.68 g Sodium hydrogen phosphate, dihydrated ($NaH_2PO_4.2H_2O$, Merk)
12.46 g Disodium hydrogen phosphate, dihydrated ($Na_2HPO_4.2H_2O$, Merk)
Dissolve in 90 ml of distilled water. Check the pH to 7.4 and make the volume up to 100 ml. Autoclave for 20 minutes at 121 ºC. Store at room temperature.

10x Phosphate Buffer Saline pH 7.0, for ISH and IHC
Preparation of 100 ml solution:
7.597 g Sodium Chloride
1.246 g Disodium hydrogen phosphate, dihydrated ($Na_2HPO_4.2H_2O$, Merk)
0.468 g Sodium hydrogen phosphate, dihydrated ($NaH_2PO_4.2H_2O$, Merk)

Dissolve the reagents in 60 ml of distilled water, adjust the pH to 7.0 and make the volume up to 100 ml. Autoclave the solution for 20 minutes at 121 ºC. Store the stock solution at room temperature.
To prepare 100 ml of **1x PBS** buffer dilute 10 ml of 10x PBS buffer with 90 ml of DEPC treated water.

Phosphate-Triton Buffer (PBST)
Preparation of 100 ml solution:
To 100 ml of 1x PBS (see above) add 100 µl of Triton-X (Sigma-Aldrich) and mix until complete dissolution.

Phosphate-Tween Buffer (PTW)
Preparation of 100 ml solution:
To 100 ml of 1x PBS (see above) add 100 µl of Tween-20 (Sigma-Aldrich) and mix until complete dissolution.
To prepare 100 ml of **2x SSC/PTW** (1:1, v/v) add 50 ml of PTW to 50 ml of 2x SSC (see below).

1% Phosphomolibdic acid
Preparation of 100 ml solution:
Dissolve 1 g of phosphomolibdic acid () in 100 ml of distilled water. Store at room temperature.

0.5% Phosphotungstic acid
Preparation of 100 ml solution:
Dissolve 0.5 g of phosphotungstic acid (Sigma-Aldrich) in 100 ml of distilled water and store in the dark at room temperature.

0.1% Picro-sirius Red solution
Preparation of 100 ml solution:
Dissolve 0.1 g of Direct Red 80 (Sigma-Aldrich 365548) in 100 ml of a saturated aqueous solution of picric acid (Merck). Keep in a ventilated place, in the dark at room temperature. This solution is stable for 3 years and can be used several times.

3M Potassium Acetate pH 5.2

Preparation of a 100 ml solution:

Dissolve 29.4 g KAc (Sigma-Aldrich) in 90 ml of distilled water. Adjust the pH to 5.2 with glacial acetic acid (Merck). Make the volume up to 100 ml with distilled water and store at room temperature.

Saline solution

Preparation of 100 ml solution:

Dissolve 0.9 g NaCl (Sigma-Aldrich) in 100 ml of distilled water and autoclave for 20 minutes at 121 ºC. Store at 4 ºC.

3M Sodium Acetate pH 5.2

Preparation of 100 ml solution:

Dissolve 24.6 g Sodium acetate (Merck) in 90 ml of DEPC treated Ellix® water and adjust the pH to 5.2 with acetic acid. Make the final volume up to 100 ml and store at room temperature.

0.1M Sodium Citrate pH 6

Preparation of 100 ml solution:

0.1 g Sodium Citrate (Merck, VWR, Portugal)

Dissolve the sodium salt in 90 ml of bi-distilled water. Adjust the pH to 6 with 0.1M Citric Acid. Make the final volume up to 100 ml and store at 4 ºC.

5M Sodium Chloride

Preparation of 100 ml solution:

Dissolve 29.25 g Sodium chloride (Sigma-Aldrich) in 100 ml of distilled water and autoclave for 20 minutes at 121 ºC. Store at room temperature.

20x Sodium chloride-sodium citrate buffer (20x SSC)

Preparation of 100 ml solution:

17.53 g Sodium chloride

8.82 g Sodium citrate

Dissolve the reagents in 60 ml of distilled water and adjust the pH to 7.0 with acetic acid. Complete the volume to 100 ml and autoclave the solution for 20 minutes at 121 ºC. Store the stock solution at room temperature.

To prepare 100 ml of **2x SSC** dilute 10 ml of 20x SSC in 90 ml of sterile Ellix® water. All other concentrations of SSC buffer should be prepared as described using the appropriate amount of concentrated solution.

0.1% Sodium Dodecyl Sulphate (SDS)

Preparation of 100 ml solution:

1 g Sodium Dodecyl Sulphate (USB)

Dissolve the powder in 100 ml of distilled water and shake vigorously until complete dissolution. Store at room temperature.

0.2M Sodium Hydroxide (NaOH)

Preparation of 100 ml solution:

0.8 g NaOH (Sigma-Aldrich)

Dissolve the sodium hydroxide tablets in 100 ml of distilled water and store at room temperature.

0.5% Sodium Methabisulphite

Preparation of 100 ml solution:

Dissolve 0.017 g of Sodium methabisulphite (Sigma-Aldrich) in 100 ml of distilled water and agitate until complete dissolution. Store at room temperature.

Torula RNA yeast (50 mg·ml^{-1})

Preparation of 10 ml solution:

0.5 g Torula RNA yeast powder (Roche)

Add 10 ml of distilled water to the RNA yeast powder and 50 µl of saturated sodium hydroxide and warm the solution up to 60 ºC until complete dissolution. Allow the solution to cool to room temperature, aliquot and store at – 20 ºC.

Tris-Carrageenan Triton X-100 (TCT)

Preparation of 100 ml solution:

0.70 g Carrageenan (Fluka Biochemika)

Dissolve the carrageenan in 100 ml of PBST (see above) and add 500 µl of Triton X-100 (Sigma-Aldrich). Store at 4 ºC.

10x Tris-borate-EDTA Buffer (10x TBE)

Preparation of 100 ml solution:

10.8 g Tris Base (Sigma-Aldrich)

5.5 g Boric Acid (Sigma-Aldrich)

10 ml EDTA 0.5M pH 8.0 (see above)

Dissolve the salts in 90 ml distilled water and make the volume up to 100 ml. Autoclave the solution for 20 minutes at 121 ºC. Store the stock solution at room temperature.

To prepare 100 ml of **1x TBE** buffer dilute 10 ml of 10x TBE buffer with 90 ml of distilled water (for gels to run DNA samples) or DEPC treated water (for gels to run RNA samples).

1M Tris-HCl solution pH 7.5, pH 8 or pH 9.5

Preparation of 100 ml solution:

12.114 g Tris (Tris(hydroxymethyl)-aminomethane, Sigma-Aldrich)

Dissolve in 90 ml of distilled water and adjust the pH to 7.5, 8 or 9.5 with concentrated hydrochloric acid and/or sodium hydroxide. Make the volume up to 100 ml with distilled water and store at room temperature.

Tris-NaCl solution (100 mM Tris-HCl, 150 mM NaCl, pH 7.5)

Preparation of 100 ml solution :

10 ml of 1M Tris-HCl solution, pH 7.5 (see above)

3 ml of 5M NaCl solution (see above)

Mix both solutions and complete the volume up to 100 ml with distilled water and ude immediately.

Xylidine Ponceau solution

Preparation of 100 ml solution:

0.25 g Xylidine ponceau 2R (Sigma-Aldrich)

0.25 g Acid Fucsin (Sigma-Aldrich)

100 ml 1% acetic acid (1ml Glacial acetic acid + 99 ml distilled water)

Dissolve the xylidine ponceau 2R in 50 ml of 1% acetic acid. Dissolve the acid fucsin in 50 ml of 1% acetic acid. Store the stock solution in the dark at room temperature. Just before use, mix the two solutions 1:1 to obtain the working solution for the stain.

TRAP STAINING SOLUTIONS:

0.1M Acetate buffer, pH 5.5

Preparation of 100 ml solution:

0.82 g Sodium acetate anhydrous

30 ul Acetic acid

Dilute the sodium salt in 100 ml of distilled water and add the acetic acid. Store at 4 ºC.

0.5M Di-sodium tartrate dehydrate

Preparation of 100 ml solution:

11.504 g di-sodium tartrate dehydrate

Dissolve the salt in the water and store at 4 ºC.

Pre-incubation solution for TRAP

Preparation of 100 ml solution:

To 90 ml of 0.1M Acetate buffer pH 5.5 add 10 ml of 0.5M di-sodium tartrate dehydrate and use immediately.

4% Sodium Nitrate

Preparation of 100 ml solution:

Dissolve 4 g of $NaNO_2$ in 100 ml of distilled water.

Pararosaniline solution (PRS), for TRAP staining

Preparation Pararosaniline solution:

1 g PRS (Sigma-Aldrich)

5.75 ml Hydrochloric acid 32%

Dissolve the PRS in 19.25 ml of demineralised water and the HCl by heating. Store in the dark at 4 ºC.

For hexazotiation, add 2ml of 4 % $NaNO_2$ at 20 ºC and use immediately.

Enzyme substrate solution N-AS-TR-P

Preparation of 2 ml solution:

2 mg Naphtol AS-TR Phosphate (Sigma-Aldrich)

2 ml N,N-dimethylformamide (Merck)

Dissolve the N-AS-TR-P in the dimethylformamide and store in the dark at -20 ºC.

Developing solution for TRAP staining

Preparation of 33 ml solution:

1 ml hexazotized PRS

600 µL 2% $MgCl_2$

2 ml enzyme substrate solution N-AS-TR-P

30 ml 0.1 M acetate buffer with 100 mM of 0.5M tartrate

Add all the components, mix gently and use immediately.

Paraffin embedding

Tissue samples were placed in appropriate histological cassettes and immersed in 70% DEPC ethanol in an automatic tissue processor (Leica TP 1020). The following program for automated dehydration, clearing and paraffin (Paraffin Low fusion solidification point 56-58ºC, Histosec, Merck, VWR, Portugal) embedding was set up following the instrument instructions and consisted of:

Solution	Treatment	Time (minutes)
70% Ethanol	Dehydration	10
95% Ethanol	Dehydration	30
95% Ethanol	Dehydration	30
100% Ethanol	Dehydration	60
100% Ethanol	Dehydration	60
100% Ethanol: Xylene (1:1)	Clear	60
Xylene	Clear	60
Xylene	Clear	90
Xylene: Paraffin (1:1)	Infiltration	120
Paraffin	Infiltration	120

Once the program finished paraffin blocks were prepared with the processed material using moulds of appropriate size.

Preparation of slides with APES (aminopropyltriethoxysilane, Sigma-Aldrich) for mounting paraffin sections

A batch of glass slides was treated each time using a glass slide rack that takes 25 slides.
Slides were washed by immersing in a 1% acid/alcohol solution (1% Hydrocloric acid, 70% ethanol, 29% distilled water, v/v) for 30 minutes. Slides were removed, the excess acid solution allowed to run off, and the slides were rinsed in running tap water for 1 – 2 minutes and then briefly immersed in distilled water. Slides were dried at room temperature overnight. Slides were coated with aminopropyltriethoxysilane (APES, Sigma-Aldrich, Madrid, Spain) by immersing in acetone for 10 minutes and then in a 2% (v/v) solution of APES in acetone for 5 minutes. The excess APES solution was allowed to run off and slides were rinsed in distilled water. After drying at room temperature, all slides were boxed and stores until required.

Tissue sections dehydration and clearing to obtain definitive preparations

The procedure for the preparation of definitive preparations is the same for histological stains, histochemistry, and immunohistochemistry. On completion of staining of sectioned material, definitive preparations were prepared by dehydration, clearing (see table below), mounting with DPX (BioChemika, Sigma-Aldrich, Madrid, Spain) and covering with a glass coverslip.

Solution	Treatment	Time (minutes)
70% Ethanol	Dehydration	5
95% Ethanol	Dehydration	5
100% Ethanol	Dehydration	5
Xylene I	Clearing	10
Xylene II	Clearing	10

Preparation of agarose gels

The preparation of agarose gels for electrophoresis was similar for all procedures. The volume of agarose solutions prepared was adjusted to be appropriate to the size of the gel mould utilized.

For a 1% agarose gel of 50 ml:

Agarose (0.5 g, Lonza) was weighted and added to 50 ml of 1x TBE buffer (appendix II). The mixture was microwaved until complete dissolution of the agarose. The solution was cooled for a few seconds with running tap water, 50 µl of ethidium bromide solution (0.5 $mg \cdot ml^{-1}$) were added and the gel was poured into the mould and allowed to solidify.

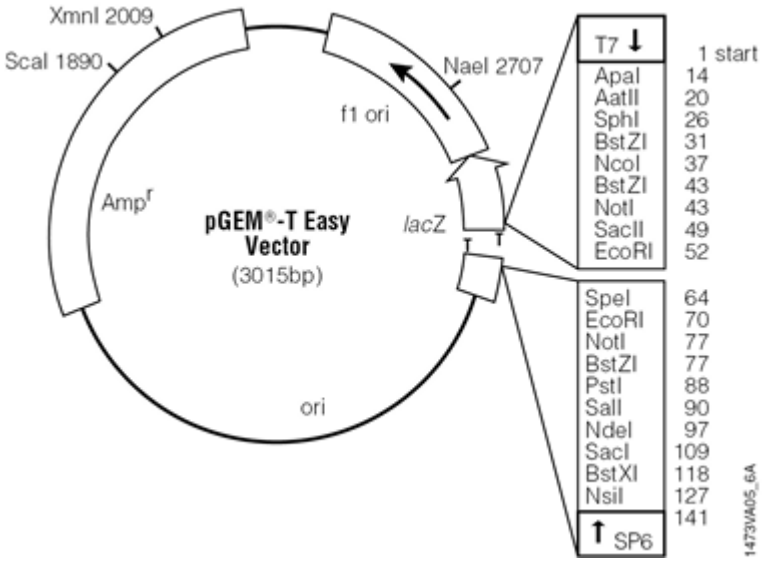

Figure 1 – Cloning vector pGEM®-T Easy from Promega.

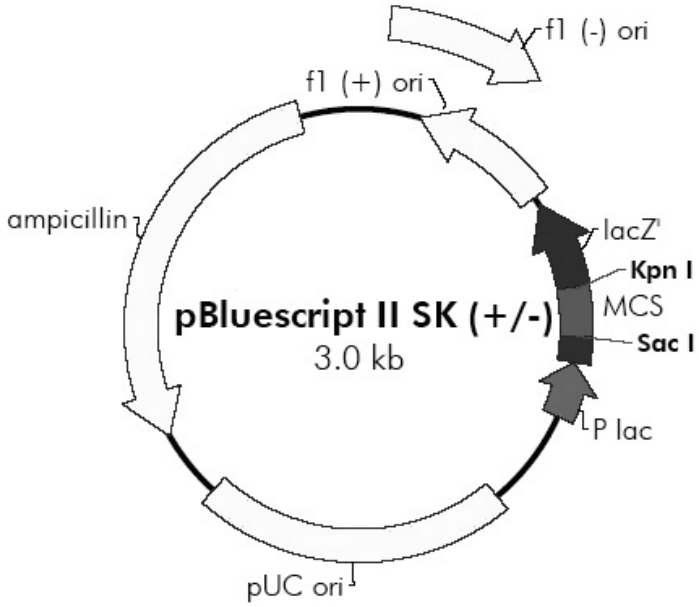

Figure 2 – Cloning vector p-Bluescript II S/K(+) from Stratagene.